Answers Research Journal 7 (2014):103–145.
www.answersingenesis.org/arj/v7/radioisotope-dating-meteorites-allende-cv3.pdf

Radioisotope Dating of Meteorites: I. The Allende CV3 Carbonaceous Chondrite

Andrew A. Snelling, Answers in Genesis, P.O. Box 510, Hebron, Kentucky 41048.

Abstract

Meteorites have been used to date the earth with a 4.55 ± 0.07 Ga Pb-Pb isochron called the geochron. They appear to consistently yield 4.56–4.57 Ga radioisotope ages, adding to the uniformitarians' confidence in the radioisotope dating methods. The Allende CV3 carbonaceous chondrite meteorite, which fell to earth in Mexico February 8, 1969, is one of the most-studied meteorites. Many radioisotope dating studies in the last 40 years have used the K-Ar, Ar-Ar, Rb-Sr, Sm-Nd, U-Th-Pb, Lu-Hf, Mn-Cr, W-Hf, Al-Mg, and I-Xe methods to yield an abundance of isochron and model ages for this meteorite from chondrules, Ca-Al inclusions, whole-rock samples, and matrix, mineral, and other fractions, all of which components are described. The age data were all tabulated and plotted on frequency versus age histogram diagrams, and strongly cluster at 4.56–4.57 Ga, dominated by Pb-Pb isochron and model ages. The earliest (1976) and the latest (2010) determined Pb-Pb isochron ages at 4.553±0.004 Ga and 4.56718±0.0002 Ga respectively are essentially the same, testimony to that technique's supremacy as the uniformitarians' ultimate, most reliable dating tool. Apart from scatter of the U-Pb, Th-Pb, Rb-Sr, and Ar-Ar ages, no systematic pattern was found in the Allende isochron and model ages similar to the systematic pattern of isochron ages found in Precambrian rock units during the RATE project. If such evidence in earth rocks is applied to meteorites, then Allende seems to have no apparent evidence in it of past accelerated radioisotope decay. However, if accelerated radioisotope decay did occur on the earth, then it could be argued every atom in the universe would be similarly affected at the same time. Furthermore, meteorites are regarded as primordial material left over from the formation of the solar system, which is compatible with the Hebrew text of Genesis that suggests God made primordial material on Day One of the Creation Week, from which He made the non-earth portion of the solar system on Day Four. Thus today's measured radioisotope composition of Allende may reflect a geochemical signature of that primordial material, which included atoms of all elemental isotopes. So if some of the daughter isotopes were already in the Allende meteorite when it was formed, and if the parent isotopes in the meteorite were also subject to subsequent accelerated radioisotope decay at the same time it occurred in earth rocks, then the 4.56718±0.0002 Ga Pb-Pb isochron "age" for the Allende cannot be its true real-time age, which according to the biblical paradigm is only about 6000 real-time years. The results of further studies of more radioisotope ages data for many more meteorites will confirm or adjust these tentative interim suggestions based on these Allende radioisotope ages data.

Keywords: radioisotope dating, meteorites, Allende, carbonaceous chondrite, matrix, chondrules, Ca-Al inclusions, organic carbon, K-Ar, Ar-Ar, Rb-Sr, Sm-Nd, U-Th-Pb, Lu-Hf, Mn-Cr, W-Hf, Al-Mg, I-Xe, isochron ages, model ages, discordant radioisotope ages, accelerated radioisotope decay, primordial material, geochemical signature.

Introduction

In 1956 Claire Patterson at the California Institute of Technology in Pasadena published his now famous paper entitled "Age of meteorites and the earth" (Patterson 1956). In it he reported lead (Pb) isotope analyses of three stony and two iron meteorites, and plotted the results on a Pb-Pb isochron diagram (fig. 1). The age obtained from the excellent isochron passing through these data points was 4.55±0.07 Ga. Patterson also found that the lead isotope analysis of a modern ocean sediment sample plotted on the same isochron. He thus argued that, because the lead in the modern ocean sediment sample was presumably an accumulation of leads mixed from many earth sources over the time since the earth formed, the modern ocean sediment's lead isotope composition represented an averaged and integrated lead isotopic composition for the earth itself. And therefore, because the lead isotope composition of the modern ocean sediment plotted on this meteorite Pb-Pb isochron, the earth must be the same age as the meteorites, namely, 4.55±0.07 billion years. Of course, implicit in this conclusion were the assumptions that the meteorites all formed at the same time and they represented primordial earth materials, because it was also assumed the meteorites are remnant materials from when the solar system formed.

Patterson's Pb-Pb isochron thus became known as the geochron, that is, the isochron that defined the age of the earth. And apart from some minor adjustments due to refinements in determinations of the U-Pb decay constants, this claimed age for the earth and this basis for it have stood unchallenged for more than five decades. Indeed, the continued radioisotope dating of meteorites, many meteorites analyzed many times by many different radioisotope methods, has only strengthened the claim that all

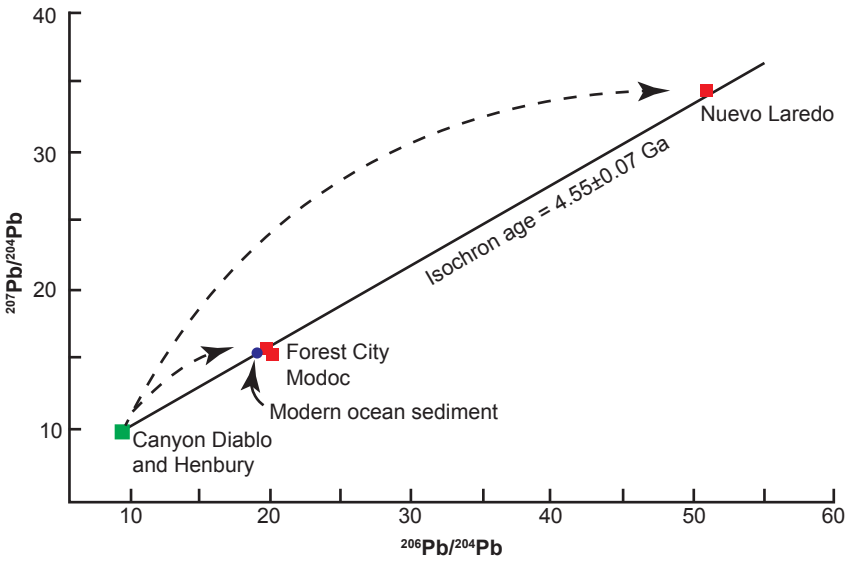

Fig. 1. The Pb-Pb isochron obtained by Patterson (1956) using three chondrite meteorites (red squares) and two iron meteorites (green square). The Pb isotopic composition of modern ocean sediment (blue circle) falls on the isochron, suggesting that meteorites and the earth are related and of the same age, which is why this isochron has been called the geochron. The dashed lines are growth by radioisotope decay curves (after Dalrymple 2004).

the meteorites are about 4.56–4.57 billion years old (Dalrymple 1991, 2004), which is thus argued to be the upper maximum for the earth's age, assuming all the meteorites represent primordial earth materials, "leftover" material from when the solar system formed. This has provided uniformitarians with apparently impregnable evidence for a 4.55 billion-year-old earth, and great confidence in the supposed reliability of their increasingly sophisticated radioisotope dating methods

Perhaps the most well-known meteorite is Allende, a carbonaceous chondrite (CV3) meteorite (Krot et al. 2005) which has often been described as the best and most-studied meteorite in history (Morris 2007; Norton 2002). Therefore, it is important to fully investigate just what ages, both isochron and model ages, the different radioisotope dating methods have yielded for this meteorite and its various components, and to explore what they might mean and their potential significance within the biblical framework for the history of the earth and the solar system. A further concerted effort still needs to be made towards understanding what these seemingly impregnable radioisotope "ages" mean within the biblical framework, so that these claimed vast ages and the radioisotope dating methods that supply them are no longer a stumbling-block to both Christians and non-Christians submitting to God's Word.

The Allende CV3 Carbonaceous Chondrite Meteorite

On Saturday, February 8, 1969, between 1:05 and 1:10 a.m. (U.S. Central Standard Time) a brilliant fireball was observed over much of northern Mexico and adjacent areas of Texas and New Mexico (Clarke et al. 1970). The most spectacular phenomena were centered around the city of Hidalgo del Parral in the south-central part of the state of Chihuahua, Mexico (fig. 2). The fireball approached from the south-southwest, moved across the sky, and as it neared its terminal point the brilliant light was accompanied by tremendous detonations and a strong air blast. In those five minutes the fireball broke up in the atmosphere, showering more than two tonnes (2.2 tons) of a rare carbonaceous chondrite meteorite, consisting of thousands of pieces with fusion crusts (a coating formed by their passage through the atmosphere), over an area of about 300 km^2 (115.8 mi^2) (Clarke et al. 1970; Norton 2002).

The original stone is believed to have been approximately the size of an automobile (at least 10 m^3 [13 yd^3]) traveling towards the earth at more than 15 km/sec (9.3 mi/sec). The roughly elliptical strewnfield extending in a southwest-northeast direction is estimated to have measured approximately 8 km (4.9 mi) by 50 km (31.6 mi) (fig. 3), making it the largest stony meteorite strewnfield that has been studied in any detail (Clarke et al. 1970). It is estimated that approximately 2–3 tonnes (2.2–3.3 tons) of specimens were collected from that strewnfield over the next 25 years, making it the greatest total weight ever recovered in a stony meteorite strewnfield up to that time (Norton 2002). The first specimen was recovered in the northern section of the field in the small town of Pueblito de Allende located in the obscure Valley of the Rio de Allende (fig. 3), so this meteorite became known as Allende. The largest fragment recovered was

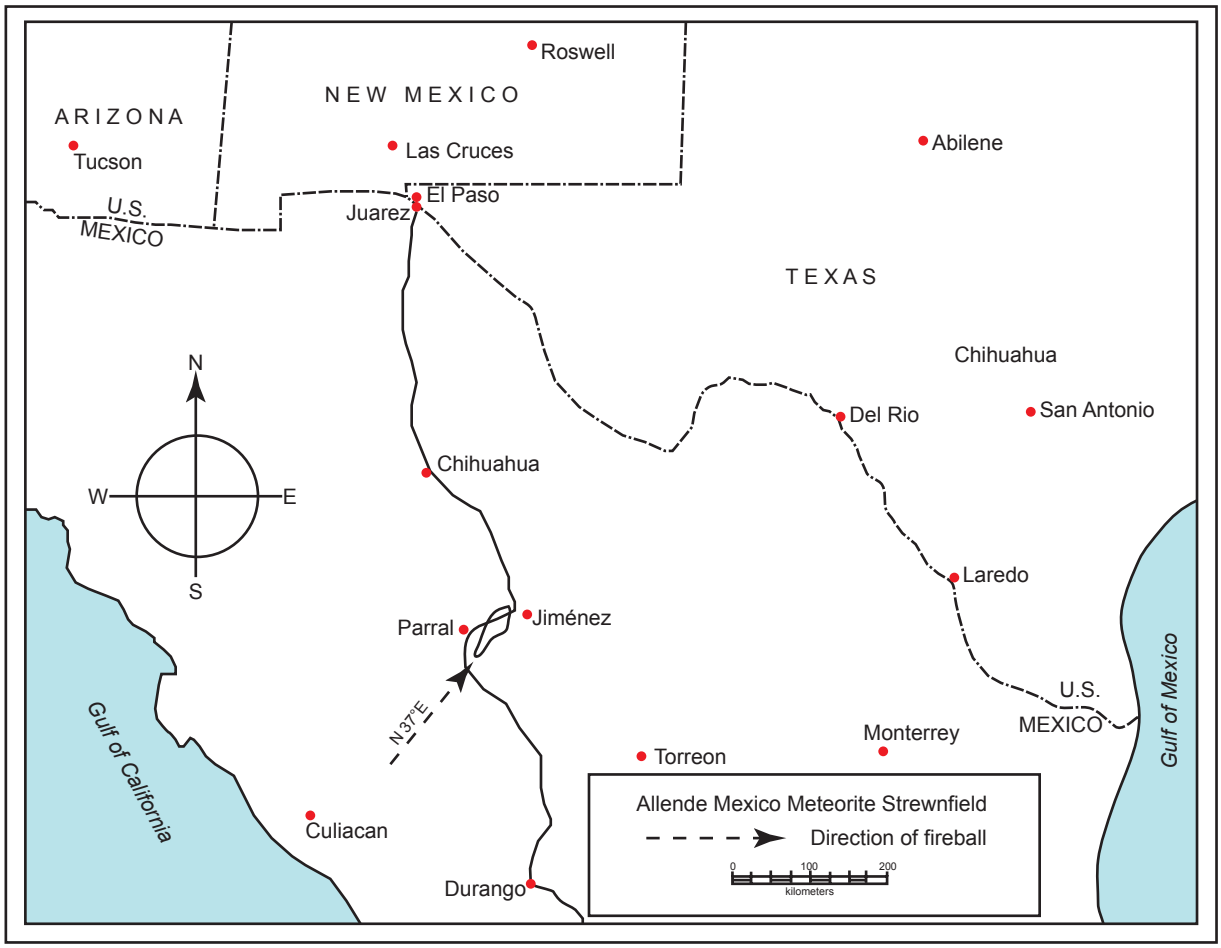

Fig. 2. Location in northern Mexico of the Allende meteorite strewnfield, with the direction of the fireball approach indicated (after Clarke et al. 1970).

discovered at the northern end of the strewnfield just to the east of Sierra de Almoloya (fig. 3) and weighed approximately 110 kg, (242 lb) but had been broken into many fragments on impact (Clarke et al. 1970).

Individual Allende specimens are fusion crusted (fig. 4). A view of a polished slab surface reveals that this meteorite consists of a jumble of refractory Ca-Al-rich inclusions and round objects called chondrules set in a dark, carbonaceous matrix (fig. 5). Chondrules are unique to stony meteorites which are thus called chondrites, so because of its carbonaceous matrix Allende is classified as a carbonaceous or C chondrite. Further classification involves typing according to where the first meteorite or prototype in the category was found and whose characteristics are used to define the group. Thus Allende is a CV chondrite, the V designating the town of Vigarano in Emilia, Italy, in which two stones weighing a total of 16 kg (35.2 lb) fell in 1910 whose characteristics are used to define this group (Norton 2002). Then the last parameter to group chondrites is a petrologic (petrographic)-chemical typing scheme that provides a guide to the degree of thermal and aqueous alteration (Van Schmus and Wood 1967). Chondrite types 3-6 show progressive stages of thermal metamorphism (Norton, 2002), with this sequence from type 3 (commonly called unequilibrated) to type 6 (commonly called equilibrated) representing an increasing degree of chemical equilibrium and textural recrystallization (Krot et al. 2005). Type 3 chondrites are widely considered the least modified by secondary processes, but even those cannot be considered truly pristine, as most show evidence of moderate amounts of hydrothermal alteration (Norton 2002). Nevertheless, of the Type 3 chondrites, the reduced CV3.0 chondrites, which are the least metamorphosed (Sears et al. 1991), come closest to being pristine. Therefore, Allende as a CV3 carbonaceous chondrite is regarded as close to pristine, and thus the intensive study of it has been warranted.

The Components of the Allende CV3 Carbonaceous Chondrite Meteorite

It is useful to have some knowledge of the constituent components and minerals within the Allende meteorite, because in dating studies radioisotope analyses have been made on whole

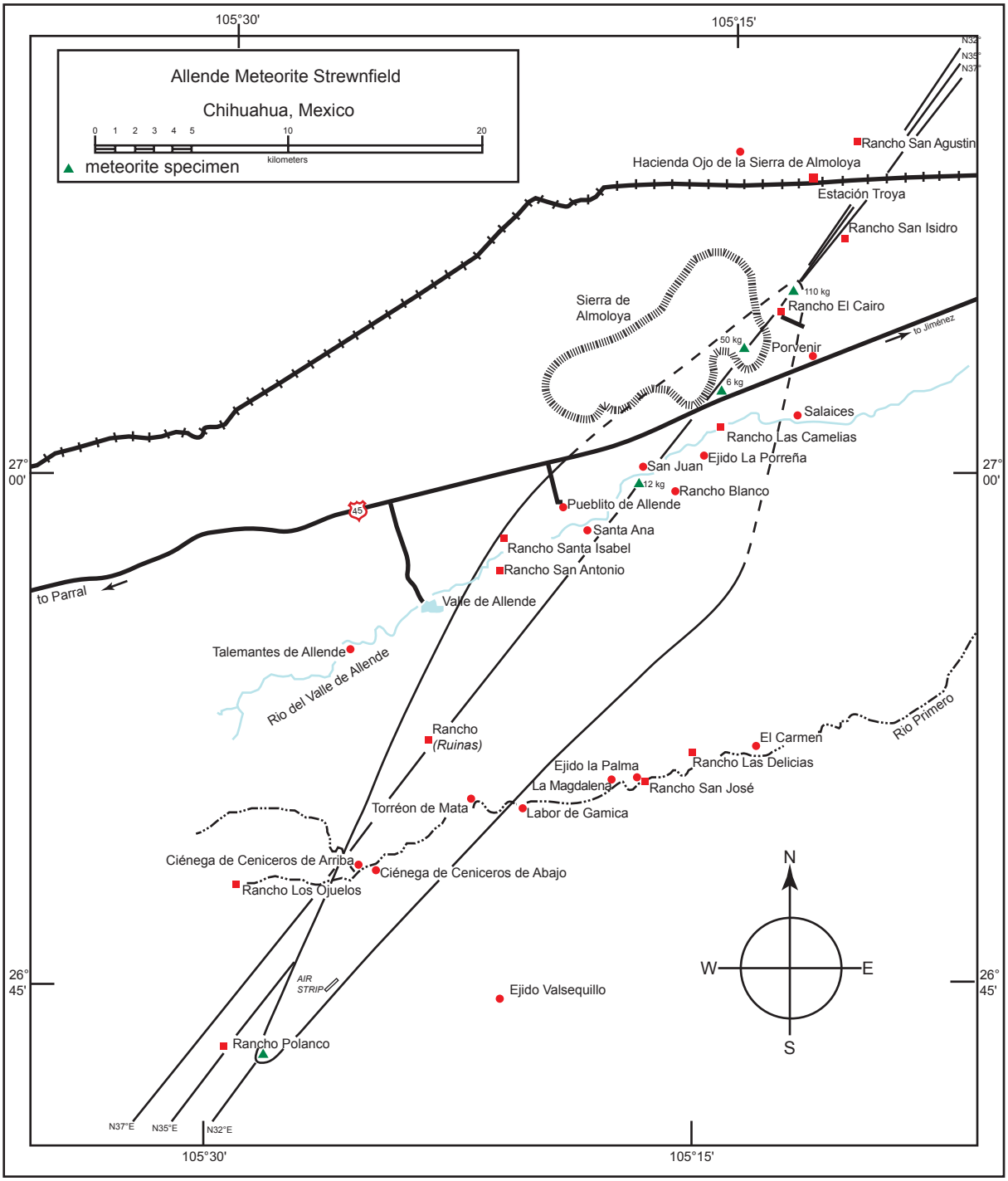

Fig. 3. Plan of the Allende meteorite strewnfield in the state of Chihuahua, Mexico, showing the locations where some of the larger meteorite specimens were recovered and their weights (green triangles) (after Clarke et al. 1970).

samples and separated components. The latter procedure is done because it is argued that some components may have formed earlier in the solar nebula. Regardless, the integrity of radioisotope dating results depend on the suitability and integrity of the samples, minerals, or components being analyzed, so a knowledge of the constituents in meteorites like Allende is vital when assessing the quality of radioisotope dates.

Krot et al. (2005) describe the CV chondrites as characterized by:

1. millimeter-sized chondrules with mostly porphyritic textures, most of which are Mg-rich and ~50% of which are surrounded by coarse-grained igneous rims;
2. high matrix / chondrule ratios (0.5-1.2);
3. unique presence of abundant salite-hedenbergite (pyroxene)±andradite (garnet) nodules in the matrix;

4. high abundance of millimeter-to-centimeter-sized refractory Ca-Al-rich inclusions (CAIs) and amoeboid olivine aggregates (AOAs); and
5. common occurrence of igneous melilite-spinel-pyroxene ± anorthite CAIs.

To this list of components could also be added Fe-Ni metal alloys and sulfides.

Fig. 4. A fragment of the Allende CV3 carbonaceous chondrite with a partial fusion crust and lead-gray interior. The white specks are Ca-Al inclusions (CAIs). This specimen measures about 12.7 cm (5 in) horizontally. Source: Norton (2002).

Matrix

Matrix material is best defined as the optically opaque mixture of grains 10 nm to 5 μm in size, and distinguishable by their shapes and textures, that rims chondrules, inclusions and other components, and fills in the interstices between them (Scott and Krot 2005). CV chondrites like Allende have much higher densities (~3.5 g/cm^3) than other carbonaceous chondrites, essentially the same densities as ordinary chondrites (Norton 2002). This is, in part, because the matrix is much more compact—there is less pore space—and the water content is less than 2 wt%. The interior is also different from other carbonaceous chondrites, the matrix being medium gray rather than black (fig. 5). CV chondrites contain on the average about 42 vol.% matrix, but Allende has a higher average value of about 60 vol.% matrix.

Examination of matrix material in thin section shows it to be black and opaque (fig. 6). High magnification of ultra-thin sections reveals the dominant mineral to be olivine, seen as a uniform distribution of tiny, euhedral crystals dispersed in opaque material (Norton 2002). Like the matrix in ordinary chondrites, the olivine is Fe-rich with an average fayalite content of 50% (Fa_{50}). In Allende the matrix olivine grains contain abundant inclusions of Ca-Fe-rich pyroxene, nepheline, and pentlandite [$(Fe,Ni)_9S_8$], with magnetite (Fe_3O_4) also present, and even at times some poorly graphitized carbon

Fig. 5. A polished surface of a slab of the Allende CV3 carbonaceous chondrite. The large circular inclusions, many of them rimmed, are chondrules, and the convoluted white inclusions are Ca-Al inclusions (CAIs), all set in a lead-gray matrix. Source: Wikipedia http://www.en.wikipedia.org.

(Scott and Krot 2005). The opaque components of the matrix itself consist of pentlandite [$(Fe,Ni)_9S_8$], troilite (FeS) and minor grains of Ni-rich metal alloy, awaruite (Ni_3Fe). Contributing to the opacity of the matrix is evenly distributed carbon-based material that thinly coats much of the olivine. CV3 chondrites are carbon-poor compared to the other water-bearing carbonaceous chondrites, averaging less than 1 wt% carbon. Allende contains only 0.29 wt% carbon.

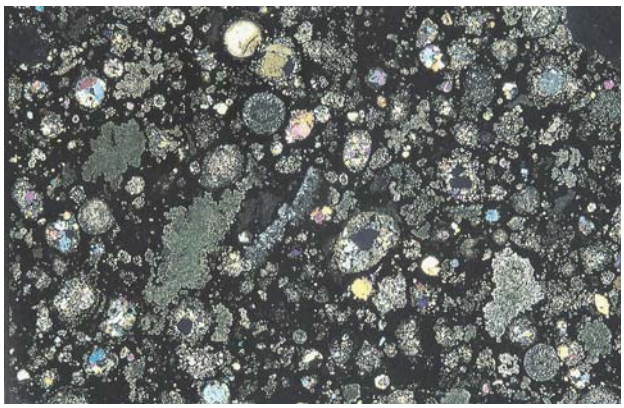

Fig. 6. A typical view of the Allende CV3 carbonaceous chondrite under crossed-polarized light in thin section under a petrological microscope showing the array of components. These include the rounded chondrules of many different structures and mineralogies, the amoeboid olivine aggregates (AOAs), dark inclusions, individual mineral grains and convoluted Ca-Al inclusions (CAIs), all set in a black matrix of tiny opaque mineral grains. The field is 22 mm (0.866 in) wide horizontally. The elliptical chondrule with the dark center just below center and right is 3 mm (0.118 in) in its longest dimension. Source: Norton (2002).

Chondrules

Chondrules are igneous-textured, rounded particles composed mainly of olivine and low-Ca pyroxene crystals with tiny grains of Fe-Ni metal and sulfides set in a feldspathic glass or microcrystalline matrix (Krot et al. 2009; Scott and Krot 2005). The most obvious distinction between CV3 chondrites and all other carbonaceous chondrite groups is the texture of the chondrule fields. Chondrules fill an average of 44 vol.%, whereas in Allende it is about 30 vol.% (Norton 2002). The chondrules are much larger on the average than those in the other groups, being typically between 0.5 and 2.0 mm (0.019 and 0.0787 in) or more. Occasionally, especially in Allende, much larger chondrules are found, some exceeding 4 or 5 mm (0.157 or 0.196 in) or diameter with a record being a whopping 25 mm (1 in)!

The most common, almost 94% of the chondrules in Allende (Scott and Krot 2005), are porphyritic olivine chondrules made up of small tightly packed euhedral and subhedral olivine grains remarkably uniform in size (>90 modal % olivine) (fig. 7) (Norton 2002; Scott and Krot 2005). Some contain elongated prisms of clinoenstatite showing polysynthetic twinning (fig. 8). Commonly seen within these chondrules are opaque grains of Fe-Ni metal alloys, iron sulfide, and magnetite. Surrounding the chondrules are halos of dark brown material composed of serpentinite, a product of aqueous alteration of olivine followed by dehydration (fig. 9). Mixed with the serpentinite is opaque FeS and $NiFe_2S$. The olivine within many of the chondrules is almost pure forsterite averaging (Fa_6), but larger crystals frequently show a zoning with increasing Fe content towards their edges and may be caused by reaction with the Fe-rich matrix (Norton 2002).

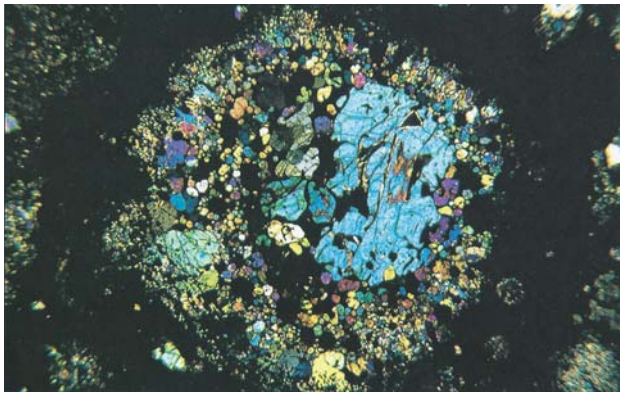

Fig. 7. A porphyritic olivine chondrule under crossed-polarized light in thin section under a petrological microscope with anhedral olivine grains showing bright interference colors. A large deeply embayed blue olivine grain occupies half of the interior of this exceptionally large chondrule, measuring 4 mm (0.157 in) in diameter, in the Allende CV3 carbonaceous chondrite. Source: Norton (2002).

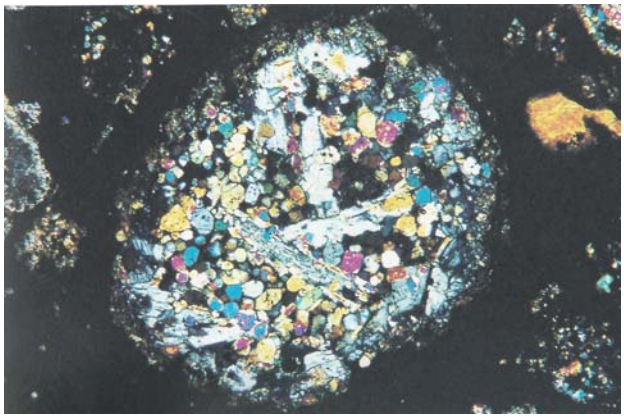

Fig. 8. A porphyritic olivine-pyroxene chondrule measuring 1.8 mm (0.070 in) across under crossed-polarized light in an Allende CV3 carbonaceous chondrite thin section under a petrological microscope. It contains small colorful equant crystals of olivine interspersed with large lath-shaped blades of white clinoenstatite (pyroxene). Source: Norton (2002).

Barred olivine chondrules are rarer in CV3 chondrites compared to the porphyritic chondrules, but still comprise up to 6% of the chondrules (Scott and Krot 2005). The bars may be contiguous with the rim material as one crystal (fig. 10) or several sets of parallel prisms with different orientations and thus different birefringent colors may compose the chondrule (fig. 11). All are set in a glassy mesostasis. Often surrounding the barred olivine chondrules is a "corona" of loosely packed tiny olivine crystals that is in optical continuity with the chondrule.

Porphyritic pyroxene chondrules are even rarer than barred olivine chondrules. Their individual crystals of low-Ca pyroxene are usually large, tightly grouped and lack rim material. These excentroradial pyroxene chondrules are very rare, amounting to less than 0.2 vol. % (Scott and Krot 2005).

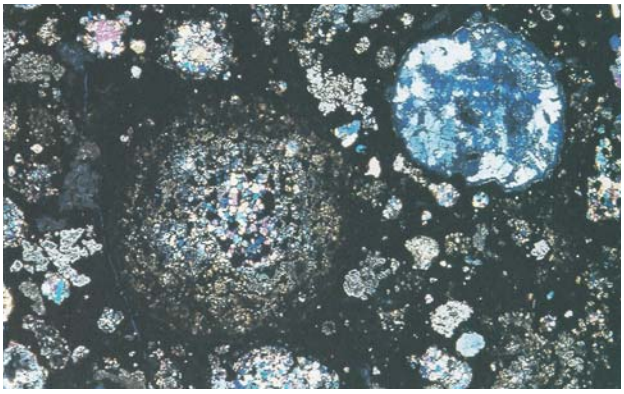

Fig. 9. A large granular olivine chondrule measuring 3.7 mm (0.14 in) across with tiny anhedral olivine crystals under crossed-polarized light in an Allende CV3 carbonaceous chondrite thin section under a petrological microscope. The entire chondrule is surrounded by brown serpentinite produced by hydrous alteration of olivine. The blue chondrule to the upper right is a porphyritic pyroxene chondrule. Source: Norton (2002).

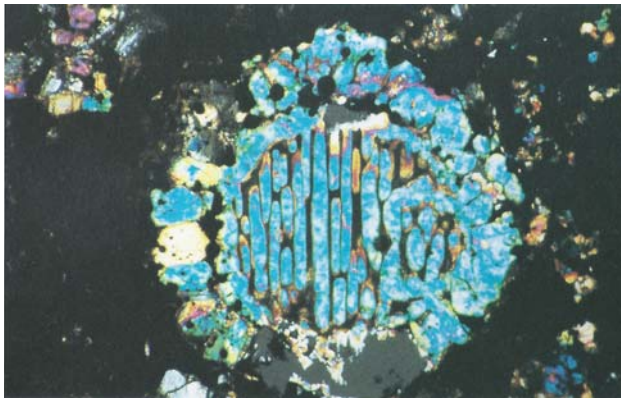

Fig. 10. A barred olivine chondrule from the Allende CV3 carbonaceous chondrite under crossed-polarized light in thin section under a petrological microscope. The olivine bars and double rim are in optical continuity, and the dark object below, interrupting the thick rim, is a missing section with the mounting glass in extinction. Several circular blebs of Fe-Ni metal appearing black are in the rim above. The field of view is 1.9 mm (0.074 in) in the longest dimension. Source: Norton (2002).

All of the chondrules so far described are textually similar to chondrules found in ordinary chondrites. There are chondrules in CV3 chondrites that are extremely rare in other chondrite groups but rather common in CV3 chondrites such as Allende (Norton 2002). In particular, in thin sections in transmitted light some remarkably round forms ranging in size from 0.1 mm to 2 mm (0.039 in to 0.078 in) stand out. They have an overall dark gray color with white needle-like crystals arranged around the perimeter roughly aligned radially with the center. These are anorthite-forsterite-spinel chondrules. The white crystals are Ca-rich plagioclase or anorthite prisms getting progressively smaller from edge to center (fig. 12).

Fig. 11. A polysomatic barred olivine chondrule under crossed-polarized light under a petrological microscope showing several sets of parallel olivine bars oriented at different angles to each other resulting in different interference colors and extinction points. A thick rim encloses the polysomatic bars except at the upper edge where the rim has been disrupted. The horizontal field of view in this Allende CV3 carbonaceous chondrite thin section is 2.1 mm (0.082 in). Source: Norton (2002).

Spinel ($MgAl_2O_4$) is found as tiny dark, opaque crystals throughout the chondrule and within the anorthite prisms, with forsterite (olivine) occurring between the prisms.

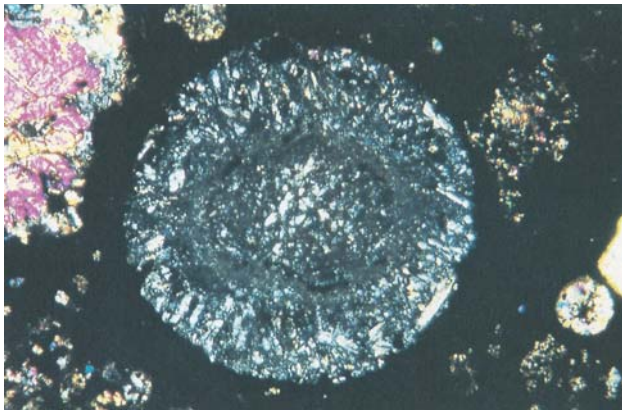

Fig. 12. An anorthite-forsterite-spinel chondrule from the Allende CV3 carbonaceous chondrite in thin section under a petrological microscope. The large white crystals along the edge are anorthite (plagioclase). Spinel is scattered through the chondrule as very small opaque crystals. The darker blades are forsterite (olivine). Note that the forsterite and plagioclase are radially arranged with respect to the center. A sparse olivine aggregate is in the lower left and upper right corners. Viewed in crossed-polarized light, the chondrule's diameter is 1.6 mm (0.062 in). Source: Norton (2002).

Amoeboid Olivine Aggregates

Amoeboid olivine aggregates (AOAs) are irregularly shaped objects with fine grain sizes (5–20 μm) that occupy up to a few percent of the carbonaceous chondrites (Scott and Krot 2005). Scattered more or less uniformly in the matrix, these are aggregates of micrometer-sized crystals composed primarily of olivine, with lesser amounts of pyroxene and feldspathoids (Norton 2002). In the least-metamorphosed carbonaceous chondrites such as Allende, the olivine aggregates consist of forsteritic olivine ($Fa_{<1-3}$) with minor diopside and anorthite, and in some cases spinel. With increasing alteration and metamorphism, the olivine and spinel (where present) become increasingly FeO-rich.

Olivine aggregates can be associated with olivine-rich chondrules, forming a surrounding halo, or they can appear amoeboid-like as singular, irregular crystalline olivine masses with projecting arms (Norton 2002) (fig. 13). Like the olivine chondrules, the olivine in aggregates is nearly pure forsterite. Often enclosed within the aggregates are spherical nodules of high temperature oxides and silicates (such as melilite). The aggregates do not show characteristics of having been melted but accreted around the nodules, consolidating into aggregates within the matrix.

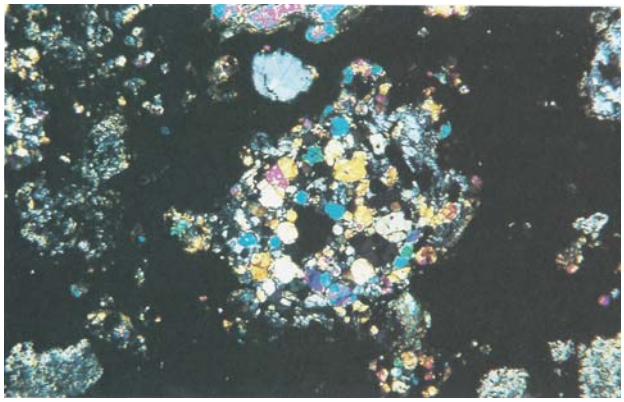

Fig. 13. An amoeboid olivine aggregate from the Allende CV3 carbonaceous chondrite in thin section under a petrological microscope viewed in crossed-polarized light. Note the "pseudo-pod-like" arms projecting into the matrix. The aggregate is 0.8 mm (0.314 in) at its narrowest. Source: Norton (2002).

Dark Inclusions

These are relatively common in CV3 chondrites and they remain perhaps the most enigmatic of the inclusions (Norton 2002). They are usually revealed in cut slabs as angular in shape and much larger than chondrules. To the eye, they appear fine-grained and featureless (fig. 14a), but under the microscope some show very small, roughly equant chondrules averaging about 0.1 mm (0.039 in) in diameter or less, superficially resembling a fragment of a CO3 chondrite (fig. 14b). The matrix around the fragments sometimes shows signs of alteration, and the composition is very close to that of the CV3 chondrite matrix.

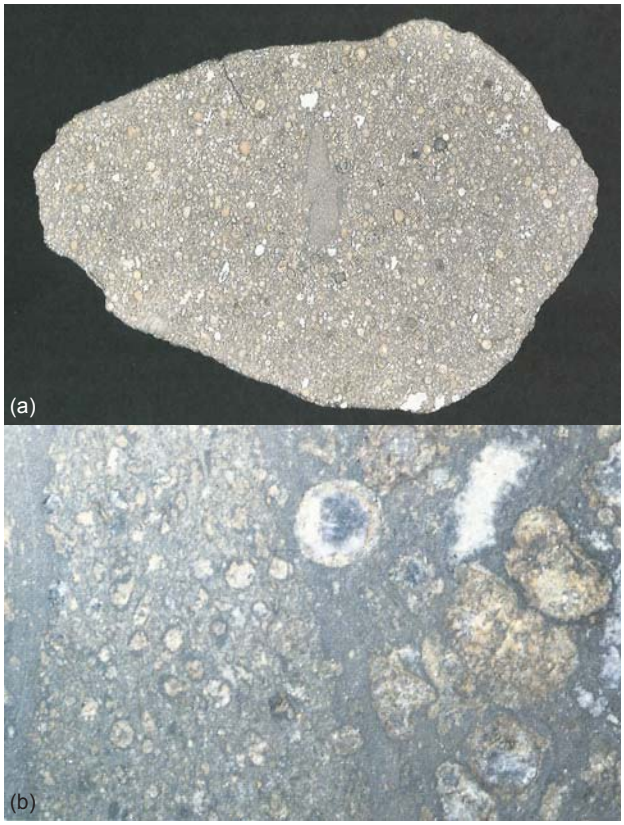

Fig. 14. (a) A xenolithic dark inclusion about 32 mm (1.25 in) long in an Allende CV3 carbonaceous chondrite slab. (b) Photomicrograph of the xenolithic inclusion in (a) in thin section under a petrological microscope showing tiny equant chondrules in a dark matrix. Around the edge of the inclusion is an altered zone that separates the CV3 texture from the inclusion texture. This mimics a fragment of a CO3 (carbonaceous Orgueil type 3) chondrite. Source: Norton (2002).

Calcium-Aluminum Inclusions (CAIs)

A very different inclusion is prominent in CV3 chondrites. They are non-igneous (interpreted as evaporative residues or gas-solid condensates by uniformitarians) or igneous (interpreted as possibly melted condensates by uniformitarians) objects rich in Ca, Al, and Ti giving their name Ca-Al inclusions, or CAIs (Krot et al. 2009; MacPherson 2005). They stand out conspicuously on broken surfaces of Allende and other CV3 chondrites, appearing as whitish or pinkish irregular masses contrasting against the black matrix. They are larger than most chondrules. Although they had been known for many years, they became the subject of intense research after the fall of Allende. While all CV3 chondrites contain these white inclusions, Allende seems to possess more than any other with about 5–10 vol.% (Norton 2002; Scott and Krot 2005). There are two types based on texture: fine-grained and coarse-grained. The fine-grained variety is composed of crystals less than 1 μm in size, too small to see clearly with a light microscope. Their irregular shapes terminate in lobate forms (fig. 15a). Under crossed-polarized light they have very low or no birefringence, remaining a gray-blue-silvery tone. The coarse-grained types have much larger crystals and some appear to have reaction rims (fig. 15b).

The mineralogy of these CAIs is complex, being composed in part of highly refractory oxides such as melilite ($Ca_2Al_2SiO_7$), spinel ($MgAl_2O_4$), and perovskite ($CaTiO_3$), and the silicates clinopyroxene and anorthite ($CaAl_2Si_2O_8$), giving CAIs a ceramic-like chemistry and mineralogy (MacPherson 2005). This mineralogy is comparable to that of the anorthite-forsterite-spinel chondrules. There is also a long list of unusual minerals found in CAIs that are rich in refractory elements, some of which are not otherwise seen in meteorites. The rims of some of the coarse-grained CAIs consist of two layers of olivine plates and laths ($Fa_{5\text{-}50}$ in Allende) and an outer layer of andradite (garnet) and hedenbergite (pyroxene), showing that they were involved in reactions with Mg-rich olivine that condensed on them while still in a molten state (Norton 2002; Scott and Krot 2005).

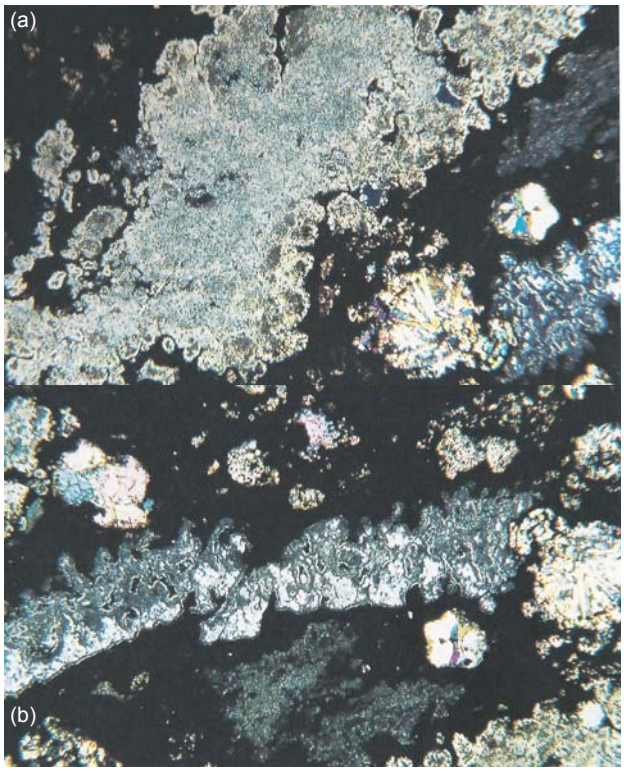

Fig. 15. (a) A large fine-grained Ca-Al-inclusion (CAI) 5.5 mm (0.216 in) long from an Allende CV3 carbonaceous chondrite specimen in thin section viewed in crossed-polarized light under a petrological microscope. It contains melilite (a silica-poor feldspathoid), spinel, and fassaite (a variety of the pyroxene augite). Melilite is the white bordering material. (b) A coarse-grained CAI in another Allende CV3 carbonaceous chondrite specimen viewed in thin section under crossed-polarized light under a petrological microscope. The white areas are melilite that has been partially altered to andradite (the Ca-Fe garnet) and grossular (the Ca-Al garnet), appearing dark gray to black. The faint rims around the andradite are diopside (pyroxene). The inclusion is 1.7 mm (0.066 in) long. Source: Norton (2002).

Radioisotope dating is claimed to show the CAIs to be the oldest of any solar system material (MacPherson 2005; Norton 2002; Scott and Krot 2005). The other significant feature of the CAIs is their isotopic composition. Generally, the elemental isotopic ratios of the elements in both the earth's crustal rocks and the meteorites are very nearly the same. However, a closer look at the chondrite meteorites, especially the carbonaceous C chondrites, shows the presence of isotopic anomalies, deviations in the isotopic ratios. For example, some of the apparently first-formed Al-rich minerals (the primary minerals found in CAIs) such as anorthite ($CaAl_2Si_2O_8$), melilite ($Ca_2Al_2SiO_7$), and spinel ($MgAl_2O_4$), contain excess ^{26}Mg in their crystal lattices, which suggests that probably the apparently extinct radioisotope ^{26}Al originally occupied those places.

The importance of such isotopic anomalies in meteorites is emphasized in the literature (MacPherson 2005; Norton 2002; Scot and Krot 2005). They are regarded as furnishing the best clues to conditions existing within the supposed solar nebula at the time the meteorite components were presumed to be forming.

The most important of these anomalies is that among the oxygen isotopes ^{16}O, ^{17}O, and ^{18}O. The relative abundances of the three oxygen isotopes in a sample are compared by calculating the difference between the $^{17}O/^{16}O$ ratio of the sample (referred to as $\delta^{17}O$) and a standard source, and then plotting this difference against the difference between the $^{18}O/^{16}O$ ratio ($\delta^{18}O$) and the standard. The reference standard for comparing oxygen isotope ratios is terrestrial ocean water, referred to as *standard mean ocean water* or SMOW.

There is a natural sorting process which causes the proportions of the three oxygen isotopes to change as a result of the differences in their masses. This occurs in many mass-dependent physical processes, such as chemical reactions, crystallization, vaporization and condensation, and diffusion. This *mass fractionation* (mass separation of the three oxygen isotopes) is proportional to their mass differences, so for any given process, the $^{18}O/^{16}O$ ratio changes twice as much as the $^{17}O/^{16}O$ ratio. Thus when the $\delta^{17}O$ deviations are plotted against the $\delta^{18}O$ deviations for terrestrial samples the values reflect this fractionation and plot along a line with a slope of ~0.5. This is the *terrestrial mass-fractionation* line from which all oxygen isotope ratios for different meteorite groups are compared. Any process that separates isotopes according to their masses will produce such a distribution line. The C chondrites show a large, widely-dispersed deviation off this terrestrial line. Most striking is the position of the CV3 chondrites, which plot along a line with a slope of ~1. These data come primarily from chondrules and high temperature (refractory) minerals found in Allende CAIs, which are enriched in ^{16}O relative to the other two heavier oxygen isotopes (MacPherson 2005; Norton 2002; Scott and Krot 2005). So another process apart from mass fractionation must be responsible, potentially suggesting that the oxygen isotopic compositions of Allende could have resulted from a mixture of two distinctly different materials.

Fe-Ni Metal Alloys and Sulfides

The form and occurrence of metallic grains in carbonaceous C chondrites are quite distinctive, tending to be rounded or ovoid in shape, and globules with somewhat roughened surfaces (Wood 1967). Two kinds of metallic grains are found in chondrites—grains composed of refractory elements

(Ir, Os, Ru, Mo, W, and Re) associated with CAIs, and grains composed predominantly of Fe, Co, and Ni associated with chondrules (Scott and Krot 2005). Most refractory nuggets have been studied in Allende CAIs. The metallic Fe-Ni grains found in chondrules in most type 3 chondrites such as Allende (CV3) typically contain concentrations of 0.1–1% Cr, Si, and P.

Most of the metallic grains in Allende (~0.5 wt %) are awaruite (Ni_3Fe), an Fe-Ni alloy similar to taenite (Norton 2002). Minor grains are found among the opaque components of the matrix itself, along with pentlandite [$(Fe,Ni)_9S_8$] and troilite (FeS). In Allende even the matrix olivine grains contain abundant inclusions of pentlandite, with magnetite (Fe_3O_4) also present (Scott and Krot 2005). Opaque grains of Fe-Ni metal alloys, iron sulfide, and magnetite are also commonly seen even distributed within the porphyritic olivine chondrules (Norton 2002; Wood 1967).

Organic Carbon

Some carbonaceous C chondrites are rich in carbon at 1.5–6 wt%, but others are not (Scott and Krot 2005). Allende in its matrix contains carbon, but only 0.29 wt% (Norton 2002). This is referred to as "organic carbon," a term that does not mean biogenic carbon, that is, carbon compounds made by living organisms. Instead, they are carbon compounds that have their counterparts in terrestrial organic carbon present in living organisms, but which can be formed by non-biogenic processes.

Many of the analyses to identify the carbon compounds in carbonaceous meteorites were performed on the Murchison CM chondrite, which like Allende fell in 1969. Of the total molecular carbon in Murchison, about 70% is in the form of insoluble molecular material not completely identified. The remaining 30% is soluble organic compounds. The list of these organic compounds identified includes non-volatile ($>C_{10}$) aliphatic hydrocarbons (saturated and unsaturated open long-chain hydrocarbons), amino acids, aromatic hydrocarbons, carboxylic acids, dicarboxylic and hydroxyl-carboxylic acids, nitrogen heterocycles, and aliphatic amines and amides (Cronin, Pizzarello, and Cruikshank 1988). Specific amino acids of identical composition and structure were found to be optically racemic, with equal numbers of left-handed and right-handed optical forms, which strongly suggested an extraterrestrial origin. Some 74 amino acids have been identified, of which eight are involved in protein synthesis in terrestrial life-forms. An additional 11 are also biogenic, though less commonly seen in biological systems. The majority of the 74 amino acids have no counterparts on earth and are thus truly extraterrestrial. Though none of these many organic compounds are now thought to be the result of life processes in space, they showed that complex organic molecules could apparently form beyond earth's environment.

Radioisotope Dating of the Allende CV3 Carbonaceous Chondrite Meteorite

The first radioisotope dating studies on Allende were published in 1973—a whole-rock Pb-Pb model age of 4.528 Ga (Huey and Kohman 1973); two whole-rock Pb-Pb model ages of 4.51 Ga and 4.52 Ga (Tilton 1973); Rb-Sr model ages for individual whole-rock samples, chondrules, and Ca-Al inclusions (CAIs) ranging from 3.59 Ga to 4.63 Ga (Gray, Papanastassiou, and Wasserburg 1973); and a Pb-Pb model age of 4.496 Ga (Tatsumoto, Knight, and Allègre 1973). Subsequently, the first statistically-significant isochron date was obtained by Tatsumoto, Unruh, and Desborough (1976) using some 20 isotopic analyses of the matrix, magnetic separates, aggregates, and chondrules that yielded a Pb-Pb isochron age of 4.553±0.004 Ga (fig. 16).

Numerous radioisotope dating studies of Allende have been undertaken in the ensuing decades, and many major studies have even been published in the last five or so years—Amelin et al. (2009), Amelin et al. (2010), Bouvier, Vervoort, and Patchett (2008), Burkhardt et al. (2008), Connelly et al. (2008), Connelly and Bizzarro (2009), Hans, Kleine, and Bourdon (2013), Jacobsen et al. (2008), Krot et al. (2009), and Trinquier et al. (2008)—indicating the scientific community still regards this meteorite as significant to their attempts to understand the origin and formation of the solar system and the earth by only natural processes. The currently accepted best estimate of the age of the Allende CV3 carbonaceous chondrite meteorite is 4.56718±0.0002 Ga based on a Pb-Pb isochron obtained from Pb isotopic analyses of fractions of an Allende CAI (fig. 17) (Amelin et al. 2010).

Creationists have commented little on the radioisotope dating of meteorites. Woodmorappe (1999) only very briefly discussed the claimed use of meteorites to date the earth's age via the Pb-Pb isochron method, but did not elaborate on what ages have been obtained on meteorites by all the various radioisotope methods and any significance or otherwise that can or should be attributed to those ages.

Similarly, Snelling (2005, 2009) only briefly touched on the meteorite Pb-Pb isochron used to date the age of the earth, the so-called geochron, and other radioisotope methods used to date meteorites, but he also mentioned the similar bulk geochemistry of meteorites to the earth's mantle in the context of crustal rocks potentially inheriting their isotopic ratios from mantle rocks. Snelling (2005) also suggested that future work should

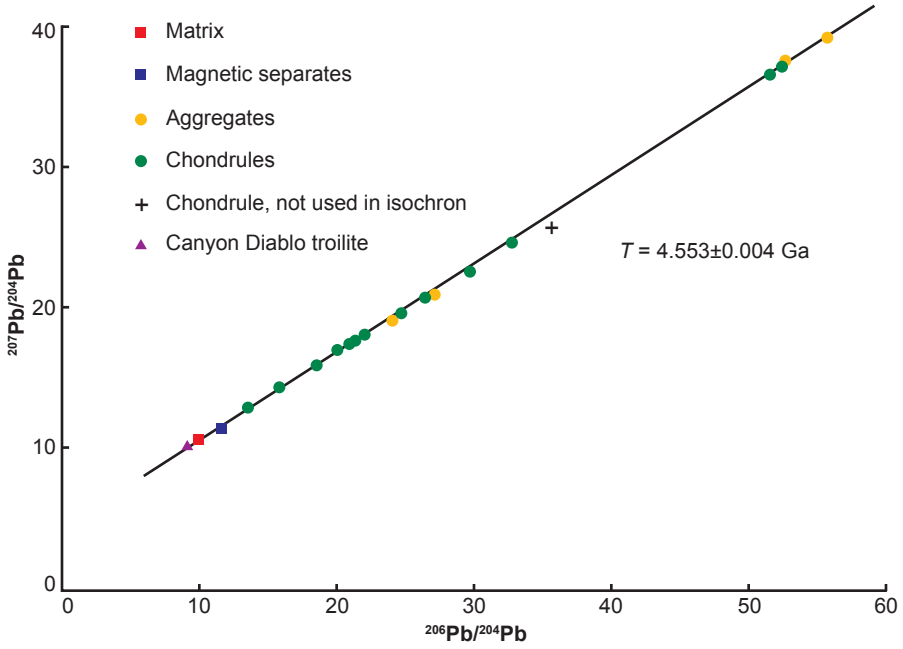

Fig. 16. The Pb-Pb isochron for the Allende CV3 carbonaceous chondrite obtained by Tatsumoto, Unruh, and Desborough (1976). This analysis used 28 mineral fractions and chondrules separated from the meteorite (green circles). The isochron passes through the composition of troilite from the Canyon Diablo iron meteorite (yellow circles). Where data are too tightly clustered to be shown individually, the number of data represented by a single symbol is indicated. The data for one chondrule was not used to calculate the isochron age, but the result is not significantly affected by its exclusion (after Dalrymple 2004).

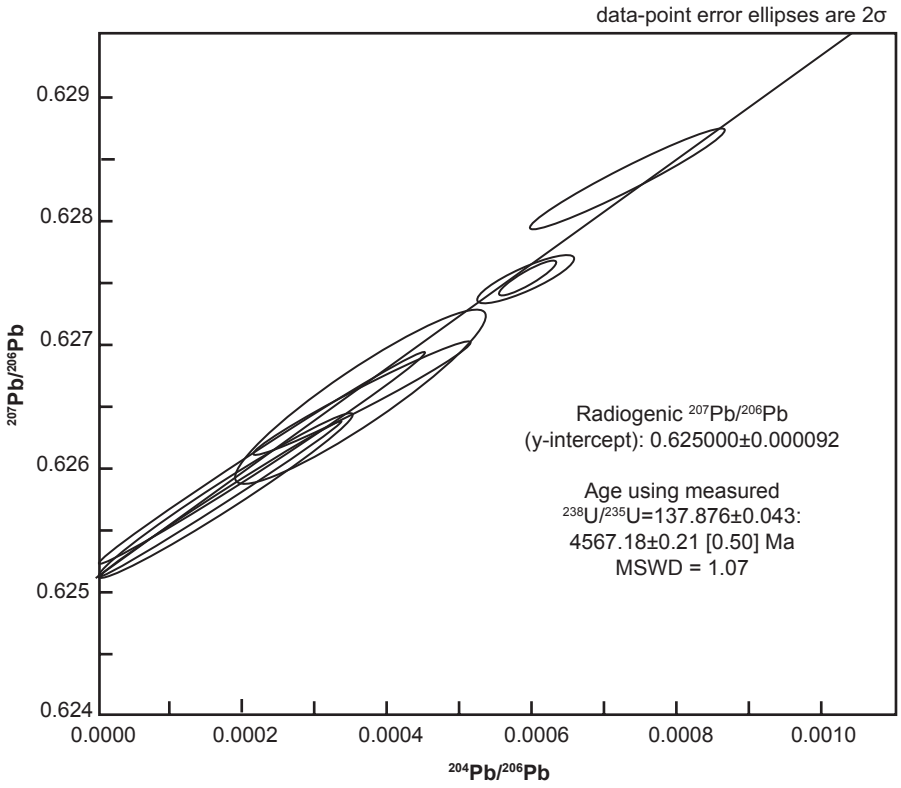

Fig. 17. Isochron plot of the Pb isotopic data for the Allende CAI SJ101 which yields the current best estimate for the age of the Allende CV3 carbonaceous chondrite meteorite at 4.56718±0.0002 Ga (after Amelin et al., 2010). The regression includes residues after acid washing of the fractions 1, 1+, 7, 8, and 9, and numerically recombined residues and third washes of the fractions 3, 4 and 5. The age uncertainty in brackets includes uncertainty of the $^{238}U/^{235}U$ ratio.

Table 1. Isochron ages for some or all components of the Allende CV3 carbonaceous chondrite meteorite, with the details and literature sources.

Sample	Method	Age	Error +/-	Notes	Source	Type
β-Decayers						
inclusions	K-Ar	4.82		Sample 12, White	Jessberger et al 1980	isochron age
chondrule(s)	Rb-Sr	4.38	0.08		Shimoda et al. 2005	isochron age
inclusions	Rb-Sr	4.56		Using D'Orbigny plagioclase Sr initial	Podosek et al. 1991, Hans, Kleine, and Bourdon 2013	isochron age
inclusions	Rb-Sr	4.63	0.23	Measured Data	Hans, Kleine, and Bourdon 2013	isochron age
inclusions	Rb-Sr	4.55	0.14	Corrected Data	Hans, Kleine, and Bourdon 2013	isochron age
whole-rock samples	Lu-Hf	4.78	0.62	Three samples plotted with 5 other samples from 5 other meteorites	Patchett et al 2004	isochron age
α-Decayers						
inclusions	Pb-Pb	4.553	0.004		Tatsumoto, Unruh, and Desborough 1976	isochron age
whole-rock samples	^{207}Pb-^{206}Pb	4.565	0.004		Chen and Tilton 1976	isochron age
inclusions	^{204}Pb-^{207}Pb	4.559	0.004		Chen and Wasserburg 1981	isochron age
inclusions (Ca-Al)	Pb-Pb	4.566	0.002		Manhes, Gopel, and Allègre 1988	isochron age
inclusions	^{207}Pb-^{206}Pb	4.566	0.002	Ca-Al	Allegre, Manhes, and Gopel 1995	isochron age
chondrules (9)	Pb-Pb	4.5668	0.0016		Amelin et al. 2002	isochron age
inclusions (Ca-Al)	Pb-Pb	4.567	0.006	3D linear regression, six samples with E	Amelin et al. 2002	isochron age
inclusions (Ca-Al)	Pb-Pb	4.5666	0.0017		Amelin et al. 2002	isochron age
inclusions (Ca-Al)	^{207}Pb-^{206}Pb	4.5685	0.0005	Three UCLA residues plotted with seven E6O inclusions (Amelin et al 2002)	Bouvier et al. 2007	isochron age
inclusions (Ca-Al)	^{207}Pb-^{206}Pb	4.568	0.0094	Three UCLA residues	Bouvier, Vervoort, and Patchett 2008	isochron age
inclusions (Ca-Al)	Pb-Pb	4.56759	0.0001	Acid-leached residues from a Ca-Al inclusion plus a leachate	Bouvier, Vervoort, and Patchett 2008	isochron age
chondrules	^{207}Pb-^{206}Pb	4.56545	0.00045		Connelly et al. 2008	isochron age
inclusions (Ca-Al)	^{207}Pb-^{206}Pb	4.56772	0.00093	Six points (px + melilite)	Connelly et al. 2008	isochron age
inclusion (Ca-Al)	^{207}Pb-^{206}Pb	4.56859	0.00061	F2 (px + mel + plag)	Connelly et al. 2008	isochron age
inclusion (Ca-Al)	^{207}Pb-^{206}Pb	4.56781	0.00079	TS32 (px + mel + plag)	Connelly et al. 2008	isochron age
inclusion (Ca-Al)	^{207}Pb-^{206}Pb	4.5707	0.00110	TS33 (px + mel + plag)	Connelly et al. 2008	isochron age
inclusions (Ca-Al)	^{207}Pb-^{206}Pb	4.56744	0.00034	CAIs AJEF & A43 residues & px second wash	Jacobsen et al. 2008	isochron age
inclusions (Ca-Al)	^{207}Pb-^{206}Pb	4.5676	0.00036	AJEF residues & px second wash	Jacobsen et al. 2008	isochron age
inclusions (Ca-Al)	^{207}Pb-^{206}Pb	4.5675	0.0014	A43 residues & px second wash	Jacobsen et al. 2008	isochron age
chondrules	Pb-Pb	4.56532	0.00081	Ten chondrules, plus Amelin & Krot (2007) chondrule data	Connelly and Bizzarro 2009	isochron age
chondrules	^{207}Pb-^{206}Pb	4.56537	0.00045	Combined Amelin et al 2002 and Connelly et al 2008 data	Krot et al 2009	isochron age
inclusions	Pb-Pb	4.56772	0.0007	Third washes of sample batch A004 in the data set	Amelin et al. 2010	isochron age
inclusions	Pb-Pb	4.56606	0.00063	Complementary residues of sample batch A004 in the data set	Amelin et al. 2010	isochron age
inclusions	Pb-Pb	4.56726	0.00019	Residues of sample batches A003 and A005 in the data set	Amelin et al. 2010	isochron age
inclusions	Pb-Pb	4.56709	0.00062	All data (washes and residues)	Amelin et al. 2010	isochron age
inclusions	Pb-Pb	4.56632	0.00076	All residues in the data set	Amelin et al. 2010	isochron age
inclusions	Pb-Pb	4.56726	0.00019	Sample batches A003 and A005 only, A005 #6 excluded	Amelin et al. 2010	isochron age
inclusions	Pb-Pb	4.56679	0.00022	All residues and second washes in the data set	Amelin et al. 2010	isochron age
inclusions	Pb-Pb	4.56718	0.00021	All residues in batches A003 and A005, and recombined residues and third washes in batch A004 (#2 ecluded)	Amelin et al. 2010	isochron age
inclusions and matrix	U-Pb	4.914	0.080		Tatsumoto, Unruh, and Desborough 1976	isochron age
inclusions and matrix	U-Pb	4.553	0.07		Tatsumoto, Unruh, and Desborough 1976	isochron age (concordia)
inclusions	U-Pb	4.548	0.025		Tatsumoto, Unruh, and Desborough 1976	isochron age (concordia)
inclusions (Ca-Al)	U-Pb	4.56805	0.00065	3D linear regression, six samples	Amelin et al. 2002	isochron age
inclusions (Ca-Al)	U-Pb	4.568	0.009	3D linear isochron, six samples with E	Amelin et al. 2002	isochron age
inclusions (Ca-Al)	U-Pb	4.568	0.015	3D linear planar, six samples with E	Amelin et al. 2002	isochron age
inclusions	U-Pb	4.56774	0.00033	Third washes and residues	Amelin et al. 2010	isochron age

inclusions	U-Pb	4.56704	0.0001	Residues--A003, A005 measured; A004 recombined--forced through O	Amelin et al. 2010	isochron age
inclusions	U-Pb	4.566	0.01	Residues--A003, A005 measured; A004 recombined--unconstrained	Amelin et al. 2010	isochron age
inclusions (Ca-Al)	Sm-Nd	4.80	0.07	Coarse-grained, melilite and pyroxene separates	Papanastassiou, Ngo, and Wasserburg 1987	isochron age (4 point)
inclusions (Ca-Al)	Sm-Nd	4.80	0.18	Coarse-grained, melilite and pyroxene separates	Papanastassiou, Ngo, and Wasserburg 1987	isochron age (2 point)
inclusions (Ca-Al)	Sm-Nd	4.53	0.09	Coarse-grained, melilite and pyroxene separates	Papanastassiou, Ngo, and Wasserburg 1987	isochron age (2 point)
chondrule	Sm-Nd	4.588	0.1	One sample plotted with 33 other samples from 8 other meteorites	Amelin and Rotenberg 2004	isochron age
Calibrated by Pb-Pb Ages						
inclusions (Ca-Al)	Al-Mg	4.5671	0.0004	Six unleached fractions of a Ca-Al inclusion, relative to D'O E60 Pb-Pb age	Bouvier, Vervoort, and Patchett 2008	isochron age
inclusions (Ca-Al)	Al-Mg	4.5692	0.0003	Six unleached fractions of a Ca-Al inclusion, relative to D'O Pb-Pb age	Bouvier, Vervoort, and Patchett 2008	isochron age
inclusions (Ca-Al)	Hf-W	4.5678	0.0022	Six separates of Ca-Al inclusions relative to St. Marguerite	Kleine et al. 2005	isochron age
inclusions (Ca-Al)	Hf-W	4.4678	0.0022	Six separates from MS-1	Kleine et al. 2005	isochron age
inclusions (Ca-Al)	Hf-W	4.5683	0.0007	Numerous mineral separates from Ca-Al inclusions, relative to Pb-Pb age of D'O, Sah & NWA	Burkhardt et al. 2008	isochron age
inclusions	I-Xe	4.5670	0.0002	Dark	Hohenburg et al. 2001	isochron age
inclusions	I-Xe	4.5678	0.0002	Dark	Hohenburg et al. 2001	isochron age
bulk sample	Mn-Cr	4.5681	0.0009	One bulk sample plotted with five other carbonacious chondrites	Shukolyukov and Lugmair 2006	isochron age
fractions (9)	Mn-Cr	4.5625	0.0016	Nine fractions including CAI, whole rock, and chondrule	Trinquier et al. 2008	isochron age
chondrules	Mn-Cr	4.56791	0.00076	Relative to the Pb-Pb age of D'Orbigny	Yin et al. 2009	isochron age
chondrules	Mn-Cr	4.56742	0.00083	Relative to the Pb-Pb age of LEW 86010	Yin et al. 2009	isochron age

Table 2. Model ages for chondrules in the Allende CV3 carbonaceous chondrite meteorite, with the details and literature sources.

Sample	Method	Age	Error +/-	Notes	Source	Type
β-Decayers						
chondrule(s)	^{40}Ar-^{39}Ar	4.56	0.05	Sample 5, Fine barred	Jessberger et al. 1980	plateau age
ferromagnesian chondrule-A	K-Ar	4.63	0.01	Sample 3915	Herzog et al. 1980	total fusion model age
ferromagnesian chondrule-A	K-Ar	4.36	0.01	Sample 3915	Herzog et al. 1980	total fusion model age
ferromagnesian chondrule-A	K-Ar	4.44	0.01	Sample 3915	Herzog et al. 1980	total fusion model age
ferromagnesian chondrule-A rim	K-Ar	4.76	0.02	Sample 3915	Herzog et al. 1980	total fusion model age
ferromagnesian chondrule-B	K-Ar	3.97	0.01	Sample 3915	Herzog et al. 1980	total fusion model age
ferromagnesian chondrule-B	K-Ar	4.08	0.01	Sample 3915	Herzog et al. 1980	total fusion model age
ferromagnesian chondrule-C	K-Ar	4.43	0.02	Sample 3915	Herzog et al. 1980	total fusion model age
ferromagnesian chondrule-C	K-Ar	4.40	0.02	Sample 3915	Herzog et al. 1980	total fusion model age
chondrule	K-Ar	4.62	0.07	Sample 3, Monosomatic	Jessberger et al. 1980	model age
chondrule	K-Ar	4.63	0.07	Sample 4, Barred	Jessberger et al. 1980	model age
chondrule	K-Ar	4.26	0.16	Sample 5, Fine barred	Jessberger et al. 1980	model age
chondrule	K-Ar	4.53	0.06	Sample 6, Granular	Jessberger et al. 1980	model age
chondrule	K-Ar	4.51	0.07	Sample 7, Granular	Jessberger et al. 1980	model age
chondrule	K-Ar	4.56	0.03	Sample 8, Black	Jessberger et al. 1980	model age

olivine condrule	Rb-Sr	4.33	0.04	B17	Gray, Papanastassiou, and Wasserburg 1973	model age
olivine condrule	Rb-Sr	4.59	0.03	B12	Gray, Papanastassiou, and Wasserburg 1973	model age
olivine condrule	Rb-Sr	4.28	0.02	B22	Gray, Papanastassiou, and Wasserburg 1973	model age
pyroxene condrule	Rb-Sr	4.33	0.02	A5	Gray, Papanastassiou, and Wasserburg 1973	model age
pyroxene condrule	Rb-Sr	4.53	0.02	D4	Gray, Papanastassiou, and Wasserburg 1973	model age
pyroxene condrule	Rb-Sr	4.23	0.02	B19	Gray, Papanastassiou, and Wasserburg 1973	model age
pyroxene condrule	Rb-Sr	4.49	0.02	E1 s2	Gray, Papanastassiou, and Wasserburg 1973	model age
pyroxene condrule	Rb-Sr	4.5	0.02	E1 s3	Gray, Papanastassiou, and Wasserburg 1973	model age
chondrule	Rb-Sr	4.08		Ca-Al-rich	Tatsumoto, Unruh, and Desborough 1976	model age
chondrule	Rb-Sr	4.17		Ca-Al-rich	Tatsumoto, Unruh, and Desborough 1976	model age
chondrule	Rb-Sr	4.34		Mg-rich	Tatsumoto, Unruh, and Desborough 1976	model age
chondrule	Rb-Sr	4.36		Mg-rich	Tatsumoto, Unruh, and Desborough 1976	model age
chondrule	Rb-Sr	4.36		Mg-rich	Tatsumoto, Unruh, and Desborough 1976	model age
chondrule	Rb-Sr	2.64		Mg-rich	Tatsumoto, Unruh, and Desborough 1976	model age
chondrule	Rb-Sr	4.49		Mg-rich	Tatsumoto, Unruh, and Desborough 1976	model age
chondrule	Rb-Sr	4.03		Mg-rich	Tatsumoto, Unruh, and Desborough 1976	model age
chondrule	Rb-Sr	4.38		Mg-rich	Tatsumoto, Unruh, and Desborough 1976	model age
chondrule	Rb-Sr	4.17		Mg-rich	Tatsumoto, Unruh, and Desborough 1976	model age
chondrule	Rb-Sr	4.10		Mg-rich	Tatsumoto, Unruh, and Desborough 1976	model age
chondrule	Rb-Sr	4.17		Mg-rich	Tatsumoto, Unruh, and Desborough 1976	model age
chondrule	Rb-Sr	4.35		Mg-rich	Tatsumoto, Unruh, and Desborough 1976	model age
chondrule	Rb-Sr	4.19		Mg-rich	Tatsumoto, Unruh, and Desborough 1976	model age
chondrule	Rb-Sr	4.22		Mg-rich	Tatsumoto, Unruh, and Desborough 1976	model age
chondrule	Rb-Sr	4.08		Mg-rich	Tatsumoto, Unruh, and Desborough 1976	model age
chondrule	Rb-Sr	4.37		H-5	Shimoda et al. 2005	model age
chondrule	Rb-Sr	9.24		H-293 inner	Shimoda et al. 2005	model age
chondrule	Rb-Sr	4.04		H-293 outer	Shimoda et al. 2005	model age
chondrule	Rb-Sr	3.54		H-343	Shimoda et al. 2005	model age
chondrule	Rb-Sr	1.78		H-344	Shimoda et al. 2005	model age
chondrule	Rb-Sr	4.40		H-356 inner	Shimoda et al. 2005	model age
chondrule	Rb-Sr	1.96		H-356 outer	Shimoda et al. 2005	model age
chondrule	Rb-Sr	4.29		H-350	Shimoda et al. 2005	model age
chondrule	Rb-Sr	4.31		H-353	Shimoda et al. 2005	model age
chondrule	Rb-Sr	4.13		H-355	Shimoda et al. 2005	model age
chondrule	Rb-Sr	4.45		H-4	Shimoda et al. 2005	model age
chondrule	Rb-Sr	4.22		H-13	Shimoda et al. 2005	model age
chondrule	Rb-Sr	4.28		H-18	Shimoda et al. 2005	model age
chondrule	Rb-Sr	4.12		H-44	Shimoda et al. 2005	model age
chondrule	Rb-Sr	3.99		H-280	Shimoda et al. 2005	model age

chondrule	Rb-Sr	4.08		H-297	Shimoda et al. 2005	model age
chondrule	Rb-Sr	4.00		H-298	Shimoda et al. 2005	model age
chondrule	Rb-Sr	4.34		H-305	Shimoda et al. 2005	model age
chondrule	Rb-Sr	4.22		H-336	Shimoda et al. 2005	model age
chondrule	Rb-Sr	4.71		H-347	Shimoda et al. 2005	model age
chondrule	Rb-Sr	4.80		H-351	Shimoda et al. 2005	model age
chondrule	Rb-Sr	4.70		H-357	Shimoda et al. 2005	model age
chondrule	Rb-Sr	4.80		NH-3	Shimoda et al. 2005	model age
chondrule	Rb-Sr	3.89		H-349	Shimoda et al. 2005	model age
α-Decayers						
chondrule	^{207}Pb-^{206}Pb	4.573			Chen and Tilton 1976	model age
chondrule	^{207}Pb-^{206}Pb	4.583			Chen and Tilton 1976	model age
chondrule	^{207}Pb-^{206}Pb	4.533			Chen and Tilton 1976	model age
chondrule	^{207}Pb-^{206}Pb	4.568			Chen and Tilton 1976	model age
chondrule N1	^{207}Pb-^{206}Pb	4.552			Tatsumoto, Unruh, and Desborough 1976	model age
chondrule N1	^{207}Pb-^{206}Pb	4.569			Tatsumoto, Unruh, and Desborough 1976	model age
chondrule N2	^{207}Pb-^{206}Pb	4.567			Tatsumoto, Unruh, and Desborough 1976	model age
chondrule N2	^{207}Pb-^{206}Pb	4.544			Tatsumoto, Unruh, and Desborough 1976	model age
chondrule N3	^{207}Pb-^{206}Pb	4.553			Tatsumoto, Unruh, and Desborough 1976	model age
chondrule N3	^{207}Pb-^{206}Pb	4.540			Tatsumoto, Unruh, and Desborough 1976	model age
chondrule N17	^{207}Pb-^{206}Pb	4.503			Tatsumoto, Unruh, and Desborough 1976	model age
chondrule N17	^{207}Pb-^{206}Pb	4.488			Tatsumoto, Unruh, and Desborough 1976	model age
chondrule N18	^{207}Pb-^{206}Pb	4.546			Tatsumoto, Unruh, and Desborough 1976	model age
chondrule N18	^{207}Pb-^{206}Pb	4.528			Tatsumoto, Unruh, and Desborough 1976	model age
chondrule N19	^{207}Pb-^{206}Pb	4.554			Tatsumoto, Unruh, and Desborough 1976	model age
chondrule N19	^{207}Pb-^{206}Pb	4.554			Tatsumoto, Unruh, and Desborough 1976	model age
chondrule N20	^{207}Pb-^{206}Pb	4.518			Tatsumoto, Unruh, and Desborough 1976	model age
chondrule N20	^{207}Pb-^{206}Pb	4.568			Tatsumoto, Unruh, and Desborough 1976	model age
chondrule N34	^{207}Pb-^{206}Pb	4.533			Tatsumoto, Unruh, and Desborough 1976	model age
chondrule N40	^{207}Pb-^{206}Pb	4.521			Tatsumoto, Unruh, and Desborough 1976	model age
chondrule N41	^{207}Pb-^{206}Pb	4.538			Tatsumoto, Unruh, and Desborough 1976	model age
chondrule	^{207}Pb-^{206}Pb	4.5705	0.0032	Residue 1	Amelin and Krot 2007	model age
chondrule	^{207}Pb-^{206}Pb	4.57	0.0036	Residue 2	Amelin and Krot 2007	model age
chondrule	^{207}Pb-^{206}Pb	4.5702	0.004	Residue 3	Amelin and Krot 2007	model age
chondrule	^{207}Pb-^{206}Pb	4.5635	0.0037	Residue 4	Amelin and Krot 2007	model age
chondrule	^{207}Pb-^{206}Pb	4.568	0.0019	Residue 5	Amelin and Krot 2007	model age
chondrule	^{207}Pb-^{206}Pb	4.5554	0.0037	Residue 6	Amelin and Krot 2007	model age
chondrule	^{207}Pb-^{206}Pb	4.5602	0.0021	Residue 7	Amelin and Krot 2007	model age
chondrule	^{207}Pb-^{206}Pb	4.5503	0.0095	Residue 8	Amelin and Krot 2007	model age
chondrule	^{207}Pb-^{206}Pb	4.5512	0.0071	Residue 9	Amelin and Krot 2007	model age
chondrule	^{207}Pb-^{206}Pb	4.5616	0.0018	Residue 10	Amelin and Krot 2007	model age
chondrules (2)	^{207}Pb-^{206}Pb	4.565	0.0065	Residue 11	Amelin and Krot 2007	model age
chondrule	^{207}Pb-^{206}Pb	4.5653	0.0011	Residue 12	Amelin and Krot 2007	model age
chondrules (2)	^{207}Pb-^{206}Pb	4.5645	0.0016	Residue 13	Amelin and Krot 2007	model age
chondrules (2)	^{207}Pb-^{206}Pb	4.5671	0.0017	Residue 14	Amelin and Krot 2007	model age

chondrules (6)	^{207}Pb-^{206}Pb	4.5627	0.0026	Residue 15	Amelin and Krot 2007	model age
chondrules (4)	^{207}Pb-^{206}Pb	4.5625	0.0018	Residue 16	Amelin and Krot 2007	model age
chondrules (4)	^{207}Pb-^{206}Pb	4.561	0.0024	Residue 17	Amelin and Krot 2007	model age
chondrules (multiple 1)	^{207}Pb-^{206}Pb	4.5662	0.0036	Residue 18	Amelin and Krot 2007	model age
chondrules (multiple 2)	^{207}Pb-^{206}Pb	4.5736	0.0031	Residue 19	Amelin and Krot 2007	model age
chondrules (multiple 3)	^{207}Pb-^{206}Pb	4.5681	0.0031	Residue 20a	Amelin and Krot 2007	model age
chondrules (multiple 4)	^{207}Pb-^{206}Pb	4.5694	0.0076	Residue 20c	Amelin and Krot 2007	model age
chondrules (12)	^{207}Pb-^{206}Pb	4.5656	0.0033	Residue 21	Amelin and Krot 2007	model age
chondrules (8)	^{207}Pb-^{206}Pb	4.5661	0.0045	Residue 22	Amelin and Krot 2007	model age
chondrules (19)	^{207}Pb-^{206}Pb	4.5681	0.0034	Residue 23	Amelin and Krot 2007	model age
chondrules (21)	^{207}Pb-^{206}Pb	4.5641	0.0023	Residue 24	Amelin and Krot 2007	model age
chondrules (16)	^{207}Pb-^{206}Pb	4.5673	0.0024	Residue 25	Amelin and Krot 2007	model age
chondrules (9)	^{207}Pb-^{206}Pb	4.5663	0.0018	Residue 26	Amelin and Krot 2007	model age
chondrules (14)	^{207}Pb-^{206}Pb	4.5659	0.002	Residue 27	Amelin and Krot 2007	model age
chondrules (20)	^{207}Pb-^{206}Pb	4.5656	0.0017	Residue 28	Amelin and Krot 2007	model age
chondrules (multiple)	^{207}Pb-^{206}Pb	4.5631	0.0017	Residue 29	Amelin and Krot 2007	model age
chondrules (multiple)	^{207}Pb-^{206}Pb	4.5613	0.002	Residue 30	Amelin and Krot 2007	model age
chondrules (multiple)	^{207}Pb-^{206}Pb	4.565	0.0028	Residue 31	Amelin and Krot 2007	model age
chondrules (multiple)	^{207}Pb-^{206}Pb	4.5646	0.003	Residue 32	Amelin and Krot 2007	model age
chondrules (multiple)	^{207}Pb-^{206}Pb	4.5635	0.0022	Residue 33	Amelin and Krot 2007	model age
chondrules (multiple)	^{207}Pb-^{206}Pb	4.5659	0.0017	Residue 35	Amelin and Krot 2007	model age
chondrules (12)	^{207}Pb-^{206}Pb	4.5423	0.013	Acid leachate 21 HNO_3	Amelin and Krot 2007	model age
chondrules (12)	^{207}Pb-^{206}Pb	4.5677	0.0073	Acid leachate 21 HCl	Amelin and Krot 2007	model age
chondrules (8)	^{207}Pb-^{206}Pb	4.5318	0.0073	Acid leachate 21 HNO_3	Amelin and Krot 2007	model age
chondrules (8)	^{207}Pb-^{206}Pb	4.3609	0.0098	Acid leachate 21 HCl	Amelin and Krot 2007	model age
chondrules (19)	^{207}Pb-^{206}Pb	4.5577	0.0049	Acid leachate 21 HNO_3	Amelin and Krot 2007	model age
chondrules (19)	^{207}Pb-^{206}Pb	4.5677	0.011	Acid leachate 21 HCl	Amelin and Krot 2007	model age
chondrules (21)	^{207}Pb-^{206}Pb	4.559	0.009	Acid leachate 21 HNO_3	Amelin and Krot 2007	model age
chondrules (21)	^{207}Pb-^{206}Pb	4.5871	0.0356	Acid leachate 21 HCl	Amelin and Krot 2007	model age
chondrules (16)	^{207}Pb-^{206}Pb	4.5629	0.0082	Acid leachate 21 HNO_3	Amelin and Krot 2007	model age
chondrules (16)	^{207}Pb-^{206}Pb	4.5767	0.0201	Acid leachate 21 HCl	Amelin and Krot 2007	model age
chondrules (9)	^{207}Pb-^{206}Pb	4.5529	0.0065	Acid leachate 21 HNO_3	Amelin and Krot 2007	model age
chondrules (9)	^{207}Pb-^{206}Pb	4.5671	0.0065	Acid leachate 21 HCl	Amelin and Krot 2007	model age
chondrules (14)	^{207}Pb-^{206}Pb	4.5653	0.0054	Acid leachate 21 HNO_3	Amelin and Krot 2007	model age
chondrules (14)	^{207}Pb-^{206}Pb	4.5748	0.0132	Acid leachate 21 HCl	Amelin and Krot 2007	model age
chondrules (20)	^{207}Pb-^{206}Pb	4.5112	0.2005	Acid leachate 21 HNO_3	Amelin and Krot 2007	model age
chondrules (20)	^{207}Pb-^{206}Pb	4.5684	0.0074	Acid leachate 21 HNO_3	Amelin and Krot 2007	model age
chondrules	^{207}Pb-^{206}Pb	4.5309	0.0019		Connelly et al. 2008	model age
chondrules	^{207}Pb-^{206}Pb	4.5275	0.0031		Connelly et al. 2008	model age
chondrules	^{207}Pb-^{206}Pb	4.5575	0.0034		Connelly et al. 2008	model age
chondrules	^{207}Pb-^{206}Pb	4.5637	0.0018		Connelly et al. 2008	model age
chondrules	^{207}Pb-^{206}Pb	4.5642	0.0062		Connelly et al. 2008	model age
chondrules	^{207}Pb-^{206}Pb	4.5625	0.0016		Connelly et al. 2008	model age
chondrules	^{207}Pb-^{206}Pb	4.5652	0.0012		Connelly et al. 2008	model age
chondrules	^{207}Pb-^{206}Pb	4.5642	0.0015		Connelly et al. 2008	model age
chondrules	^{207}Pb-^{206}Pb	4.5436	0.0036		Connelly et al. 2008	model age
chondrules	Pb-Pb	4.5666	0.001	Average of Amelin and Krot (2007) chondrule data—7 sets of 2 washes and 1 residue	Connelly and Bizzarro 2009	model age
chondrules	Pb-Pb	4.5659	0.0008	Average of eight residues' model ages in Amelin and Krot (2007) chondrule data	Connelly and Bizzarro 2009	model age
chondrule	^{232}Th-^{208}Pb	3.328			Chen and Tilton 1976	model age
chondrule	^{232}Th-^{208}Pb	4.622			Chen and Tilton 1976	model age
chondrule	^{232}Th-^{208}Pb	3.271			Chen and Tilton 1976	model age
chondrule	^{232}Th-^{208}Pb	3.862			Chen and Tilton 1976	model age
chondrule N1	^{232}Th-^{208}Pb	11.7			Tatsumoto, Unruh, and Desborough 1976	model age

chondrule N2	^{232}Th-^{208}Pb	10.40			Tatsumoto, Unruh, and Desborough 1976	model age
chondrule N3	^{232}Th-^{208}Pb	9.55			Tatsumoto, Unruh, and Desborough 1976	model age
chondrule N17	^{232}Th-^{208}Pb	7.52			Tatsumoto, Unruh, and Desborough 1976	model age
chondrule N18	^{232}Th-^{208}Pb	5.35			Tatsumoto, Unruh, and Desborough 1976	model age
chondrule N19	^{232}Th-^{208}Pb	6.99			Tatsumoto, Unruh, and Desborough 1976	model age
chondrule N20	^{232}Th-^{208}Pb	6.40			Tatsumoto, Unruh, and Desborough 1976	model age
chondrule	^{238}U-^{206}Pb	5.104			Chen and Tilton 1976	model age
chondrule	^{238}U-^{206}Pb	4.688			Chen and Tilton 1976	model age
chondrule	^{238}U-^{206}Pb	3.312			Chen and Tilton 1976	model age
chondrule	^{238}U-^{206}Pb	4.410			Chen and Tilton 1976	model age
chondrule N1	^{238}U-^{206}Pb	5.34			Tatsumoto, Unruh, and Desborough 1976	model age
chondrule N1	^{238}U-^{206}Pb	5.44			Tatsumoto, Unruh, and Desborough 1976	model age
chondrule N2	^{238}U-^{206}Pb	4.40			Tatsumoto, Unruh, and Desborough 1976	model age
chondrule N2	^{238}U-^{206}Pb	4.54			Tatsumoto, Unruh, and Desborough 1976	model age
chondrule N3	^{238}U-^{206}Pb	5.04			Tatsumoto, Unruh, and Desborough 1976	model age
chondrule N3	^{238}U-^{206}Pb	5.07			Tatsumoto, Unruh, and Desborough 1976	model age
chondrule N17	^{238}U-^{206}Pb	6.50			Tatsumoto, Unruh, and Desborough 1976	model age
chondrule N17	^{238}U-^{206}Pb	6.50			Tatsumoto, Unruh, and Desborough 1976	model age
chondrule N18	^{238}U-^{206}Pb	4.26			Tatsumoto, Unruh, and Desborough 1976	model age
chondrule N18	^{238}U-^{206}Pb	3.91			Tatsumoto, Unruh, and Desborough 1976	model age
chondrule N19	^{238}U-^{206}Pb	5.02			Tatsumoto, Unruh, and Desborough 1976	model age
chondrule N19	^{238}U-^{206}Pb	5.01			Tatsumoto, Unruh, and Desborough 1976	model age
chondrule N20	^{238}U-^{206}Pb	5.73			Tatsumoto, Unruh, and Desborough 1976	model age
chondrule N20	^{238}U-^{206}Pb	5.69			Tatsumoto, Unruh, and Desborough 1976	model age
chondrule N34	^{238}U-^{206}Pb	6.05			Tatsumoto, Unruh, and Desborough 1976	model age
chondrule N40	^{238}U-^{206}Pb	6.66			Tatsumoto, Unruh, and Desborough 1976	model age
chondrule N41	^{238}U-^{206}Pb	6.35			Tatsumoto, Unruh, and Desborough 1976	model age
chondrule	^{238}U-^{206}Pb	4.536		Residue 1	Amelin and Krot 2007	model age
chondrule	^{238}U-^{206}Pb	4.423		Residue 2	Amelin and Krot 2007	model age
chondrule	^{238}U-^{206}Pb	4.536		Residue 3	Amelin and Krot 2007	model age
chondrule	^{238}U-^{206}Pb	4.483		Residue 4	Amelin and Krot 2007	model age
chondrule	^{238}U-^{206}Pb	4.614		Residue 5	Amelin and Krot 2007	model age
chondrule	^{238}U-^{206}Pb	4.659		Residue 6	Amelin and Krot 2007	model age
chondrule	^{238}U-^{206}Pb	4.569		Residue 7	Amelin and Krot 2007	model age
chondrule	^{238}U-^{206}Pb	5.526		Residue 8	Amelin and Krot 2007	model age
chondrule	^{238}U-^{206}Pb	5.147		Residue 9	Amelin and Krot 2007	model age
chondrule	^{238}U-^{206}Pb	4.791		Residue 10	Amelin and Krot 2007	model age
chondrules (2)	^{238}U-^{206}Pb	5.18		Residue 11	Amelin and Krot 2007	model age
chondrule	^{238}U-^{206}Pb	4.733		Residue 12	Amelin and Krot 2007	model age

chondrules (2)	^{238}U-^{206}Pb	4.875		Residue 13	Amelin and Krot 2007	model age
chondrules (2)	^{238}U-^{206}Pb	4.59		Residue 14	Amelin and Krot 2007	model age
chondrules (6)	^{238}U-^{206}Pb	4.824		Residue 15	Amelin and Krot 2007	model age
chondrules (4)	^{238}U-^{206}Pb	4.798		Residue 16	Amelin and Krot 2007	model age
chondrules (4)	^{238}U-^{206}Pb	4.85		Residue 17	Amelin and Krot 2007	model age
chondrules (12)	^{238}U-^{206}Pb	5.369		Residue 21	Amelin and Krot 2007	model age
chondrules (20)	^{238}U-^{206}Pb	5.956		Residue 28	Amelin and Krot 2007	model age
chondrules (8)	^{238}U-^{206}Pb	4.879		Residue 22	Amelin and Krot 2007	model age
chondrules (19)	^{238}U-^{206}Pb	5.462		Residue 23	Amelin and Krot 2007	model age
chondrules (21)	^{238}U-^{206}Pb	5.345		Residue 24	Amelin and Krot 2007	model age
chondrules (16)	^{238}U-^{206}Pb	5.336		Residue 25	Amelin and Krot 2007	model age
chondrules (9)	^{238}U-^{206}Pb	6.945		Residue 26	Amelin and Krot 2007	model age
chondrules (14)	^{238}U-^{206}Pb	5.604		Residue 27	Amelin and Krot 2007	model age
chondrules (12)	^{238}U-^{206}Pb	4.525		Acid leachate 21 HNO_3	Amelin and Krot 2007	model age
chondrules (12)	^{238}U-^{206}Pb	4.281		Acid leachate 21 HCl	Amelin and Krot 2007	model age
chondrules (8)	^{238}U-^{206}Pb	4.95		Acid leachate 21 HNO_3	Amelin and Krot 2007	model age
chondrules (8)	^{238}U-^{206}Pb	10.066		Acid leachate 21 HCl	Amelin and Krot 2007	model age
chondrules (19)	^{238}U-^{206}Pb	4.151		Acid leachate 21 HNO_3	Amelin and Krot 2007	model age
chondrules (19)	^{238}U-^{206}Pb	4.842		Acid leachate 21 HCl	Amelin and Krot 2007	model age
chondrules (21)	^{238}U-^{206}Pb	4.399		Acid leachate 21 HNO_3	Amelin and Krot 2007	model age
chondrules (21)	^{238}U-^{206}Pb	3.926		Acid leachate 21 HCl	Amelin and Krot 2007	model age
chondrules (16)	^{238}U-^{206}Pb	4.092		Acid leachate 21 HNO_3	Amelin and Krot 2007	model age
chondrules (16)	^{238}U-^{206}Pb	4.756		Acid leachate 21 HCl	Amelin and Krot 2007	model age
chondrules (9)	^{238}U-^{206}Pb	3.855		Acid leachate 21 HNO_3	Amelin and Krot 2007	model age
chondrules (9)	^{238}U-^{206}Pb	4.175		Acid leachate 21 HCl	Amelin and Krot 2007	model age
chondrules (14)	^{238}U-^{206}Pb	4.125		Acid leachate 21 HNO_3	Amelin and Krot 2007	model age
chondrules (14)	^{238}U-^{206}Pb	4.208		Acid leachate 21 HCl	Amelin and Krot 2007	model age
chondrules (20)	^{238}U-^{206}Pb	1.799		Acid leachate 21 HNO_3	Amelin and Krot 2007	model age
chondrules (20)	^{238}U-^{206}Pb	3.986		Acid leachate 21 HNO_3	Amelin and Krot 2007	model age
chondrule	^{235}U-^{207}Pb	4.730			Chen and Tilton 1976	model age
chondrule	^{235}U-^{207}Pb	4.615			Chen and Tilton 1976	model age
chondrule	^{235}U-^{207}Pb	4.114			Chen and Tilton 1976	model age
chondrule	^{235}U-^{207}Pb	4.519			Chen and Tilton 1976	model age
chondrule N1	^{235}U-^{207}Pb	4.78			Tatsumoto, Unruh, and Desborough 1976	model age
chondrule N1	^{235}U-^{207}Pb	4.82			Tatsumoto, Unruh, and Desborough 1976	model age
chondrule N2	^{235}U-^{207}Pb	4.51			Tatsumoto, Unruh, and Desborough 1976	model age
chondrule N2	^{235}U-^{207}Pb	4.54			Tatsumoto, Unruh, and Desborough 1976	model age
chondrule N3	^{235}U-^{207}Pb	4.70			Tatsumoto, Unruh, and Desborough 1976	model age
chondrule N3	^{235}U-^{207}Pb	4.70			Tatsumoto, Unruh, and Desborough 1976	model age
chondrule N17	^{235}U-^{207}Pb	5.05			Tatsumoto, Unruh, and Desborough 1976	model age
chondrule N17	^{235}U-^{207}Pb	5.04			Tatsumoto, Unruh, and Desborough 1976	model age
chondrule N18	^{235}U-^{207}Pb	4.46			Tatsumoto, Unruh, and Desborough 1976	model age
chondrule N18	^{235}U-^{207}Pb	4.33			Tatsumoto, Unruh, and Desborough 1976	model age
chondrule N19	^{235}U-^{207}Pb	4.69			Tatsumoto, Unruh, and Desborough 1976	model age
chondrule N19	^{235}U-^{207}Pb	4.69			Tatsumoto, Unruh, and Desborough 1976	model age
chondrule N20	^{235}U-^{207}Pb	4.86			Tatsumoto, Unruh, and Desborough 1976	model age
chondrule N20	^{235}U-^{207}Pb	4.89			Tatsumoto, Unruh, and Desborough 1976	model age

chondrule N34	^{235}U-^{207}Pb	4.96			Tatsumoto, Unruh, and Desborough 1976	model age
chondrule N40	^{235}U-^{207}Pb	5.10			Tatsumoto, Unruh, and Desborough 1976	model age
chondrule N41	^{235}U-^{207}Pb	5.04			Tatsumoto, Unruh, and Desborough 1976	model age

Table 3. Model ages for Ca-Al inclusions (CAIs) in the Allende CV3 carbonaceous chondrite meteorite, with the details and literature sources.

Sample	Method	Age	Error +/-	Notes	Source	Type
β-Decayers						
inclusion	^{40}Ar-^{39}Ar	4.397	0.015	#15 white center	Dominik et al. 1978	total apparent age
inclusion	^{40}Ar-^{39}Ar	4.232	0.009	#16 rim fragment	Dominik et al. 1978	total apparent age
inclusion	^{40}Ar-^{39}Ar	4.517	0.025	#14 gray core	Dominik et al. 1978	plateau age
inclusion	^{40}Ar-^{39}Ar	4.529	0.018	#15 white pocket	Dominik et al. 1978	plateau age
inclusion	^{40}Ar-^{39}Ar	4.476	0.023	#16 white rim	Dominik et al. 1978	plateau age
inclusion	^{40}Ar-^{39}Ar	4.98	0.06	Sample 17	Jessberger and Dominik 1979a, b	plateau age
inclusion	^{40}Ar-^{39}Ar	4.89	0.03	Sample 18	Jessberger and Dominik 1979a, b	plateau age
inclusion	^{40}Ar-^{39}Ar	5.43	0.04	Sample 17	Jessberger and Dominik 1979a	total fusion age
inclusion	^{40}Ar-^{39}Ar	5.37	0.10	Sample 18	Jessberger and Dominik 1979a	total fusion age
inclusion	^{40}Ar-^{39}Ar	4.68	0.12	Sample 19	Jessberger and Dominik 1979a	total fusion age
inclusion	^{40}Ar-^{39}Ar	5.27	0.18	Sample 20	Jessberger and Dominik 1979a	total fusion age
inclusion	^{40}Ar-^{39}Ar	4.62	0.10	Sample 21	Jessberger and Dominik 1979a	total fusion age
inclusion	^{40}Ar-^{39}Ar	4.47	0.01	Sample 10, White fine	Jessberger et al. 1980	plateau age
inclusion	^{40}Ar-^{39}Ar	4.55	0.03	Sample 11, White fluffy	Jessberger et al. 1980	plateau age
inclusion	^{40}Ar-^{39}Ar	4.50	0.02	Sample 13, White coarse	Jessberger et al. 1980	plateau age
inclusion	^{40}Ar-^{39}Ar	4.98	0.06	Sample 17, White coarse	Jessberger et al. 1980	plateau age
inclusion	^{40}Ar-^{39}Ar	5.43	0.04	Sample 17, White coarse	Jessberger et al. 1980	plateau age
inclusion	^{40}Ar-^{39}Ar	4.92	0.03	Sample 18, White coarse	Jessberger et al. 1980	plateau age
inclusion	^{40}Ar-^{39}Ar	5.37	0.10	Sample 18, White coarse	Jessberger et al. 1980	plateau age
inclusion	^{40}Ar-^{39}Ar	4.68	0.12	Sample 19, White coarse	Jessberger et al. 1980	plateau age
inclusion	^{40}Ar-^{39}Ar	5.27	0.18	Sample 20, White coarse	Jessberger et al. 1980	plateau age
inclusion	^{40}Ar-^{39}Ar	4.62	0.10	Sample 21, White coarse	Jessberger et al. 1980	plateau age
inclusion	K-Ar	4.20	0.13	#14 gray core	Dominik et al 1978	model age
inclusion	K-Ar	4.40	0.11	#15 white pocket	Dominik et al 1978	model age
inclusion	K-Ar	4.23	0.10	#16 white rim	Dominik et al 1978	model age
inclusion	K-Ar	5.12	0.03	Sample 17	Jessberger and Dominik 1979a, b	model age
inclusion	K-Ar	5.08	0.08	Sample 18	Jessberger and Dominik 1979a, b	model age
inclusion	K-Ar	4.92	0.11	Sample 19	Jessberger and Dominik 1979a	model age
inclusion	K-Ar	5.54	0.09	Sample 20	Jessberger and Dominik 1979a	model age
inclusion	K-Ar	5.26	0.10	Sample 21	Jessberger and Dominik 1979a	model age
inclusion	K-Ar	4.57	0.41	Sample 23	Jessberger and Dominik 1979a	model age
inclusion Ca-Al	K-Ar	5.11	0.2	Sample 3839 fine-grained	Herzog et al. 1980	total fusion model age
inclusion Ca-Al	K-Ar	5.09	0.1	Sample 3839 fine-grained	Herzog et al. 1980	total fusion model age
inclusion Ca-Al	K-Ar	4.68	0.01	Sample 3839 fine-grained	Herzog et al. 1980	total fusion model age
inclusion Ca-Al	K-Ar	4.80	0.02	Sample 3839 fine-grained	Herzog et al. 1980	total fusion model age
inclusion Ca-Al	K-Ar	4.34	0.10	Sample 3839 fine-grained	Herzog et al. 1980	total fusion model age
inclusion Ca-Al	K-Ar	4.25	0.12	Sample 3839 fine-grained	Herzog et al. 1980	total fusion model age
inclusion	K-Ar	4.28	0.01	Sample 3915	Herzog et al. 1980	total fusion model age
inclusion	K-Ar	4.52	0.07	Sample 9, White fine	Jessberger et al. 1980	model age
inclusion	K-Ar	4.33	0.08	Sample 10, White fine	Jessberger et al.1980	model age
inclusion	K-Ar	4.44	0.07	Sample 11, White fluffy	Jessberger et al. 1980	model age
inclusion	K-Ar	4.82	0.06	Sample 12, White comp. of coarse	Jessberger et al. 1980	model age
inclusion	K-Ar	4.49	0.03	Sample 13, White coarse	Jessberger et al. 1980	model age
Ca-Al aggregates-low Rb	Rb-Sr	4.18	0.15	D2	Gray, Papanastassiou, and Wasserburg 1973	model age
Ca-Al aggregates-low Rb	Rb-Sr	3.93	0.26	A8	Gray, Papanastassiou, and Wasserburg 1973	model age

Ca-Al aggregates-low Rb	Rb-Sr	3.97	0.05	A4	Gray, Papanastassiou, and Wasserburg 1973	model age
Ca-Al aggregates-low Rb	Rb-Sr	4.21	0.07	B30 a	Gray, Papanastassiou, and Wasserburg 1973	model age
Ca-Al aggregates-low Rb	Rb-Sr	4.39	0.06	B30 b	Gray, Papanastassiou, and Wasserburg 1973	model age
Ca-Al aggregates-high Rb	Rb-Sr	4.58	0.02	D3	Gray, Papanastassiou, and Wasserburg 1973	model age
Ca-Al aggregates-high Rb	Rb-Sr	4.29	0.02	B29 a	Gray, Papanastassiou, and Wasserburg 1973	model age
Ca-Al aggregates-high Rb	Rb-Sr	4.55	0.02	B29 b	Gray, Papanastassiou, and Wasserburg 1973	model age
Ca-Al aggregates-high Rb	Rb-Sr	4.63	0.03	B29 c	Gray, Papanastassiou, and Wasserburg 1973	model age
Ca-Al aggregates-high Rb	Rb-Sr	3.69	0.02	B29 d	Gray, Papanastassiou, and Wasserburg 1973	model age
Ca-Al aggregates-high Rb	Rb-Sr	3.65	0.02	B29 e	Gray, Papanastassiou, and Wasserburg 1973	model age
Ca-Al aggregates-high Rb	Rb-Sr	4.35	0.02	B32	Gray, Papanastassiou, and Wasserburg 1973	model age
Ca-Al aggregates-high Rb	Rb-Sr	4.3	0.02	B31 s1	Gray, Papanastassiou, and Wasserburg 1973	model age
Ca-Al aggregates-high Rb	Rb-Sr	4.27	0.02	B31 s2	Gray, Papanastassiou, and Wasserburg 1973	model age
Ca-Al aggregates-high Rb	Rb-Sr	4.32	0.02	B31 s3	Gray, Papanastassiou, and Wasserburg 1973	model age
Ca-Al aggregates-high Rb	Rb-Sr	4.56	0.03	B31 m1	Gray, Papanastassiou, and Wasserburg 1973	model age
Ca-Al aggregates-high Rb	Rb-Sr	4.36	0.02	A10	Gray, Papanastassiou, and Wasserburg 1973	model age
Ca-Al aggregates-high Rb	Rb-Sr	3.59	0.02	B33 s1	Gray, Papanastassiou, and Wasserburg 1973	model age
Ca-Al aggregates-high Rb	Rb-Sr	3.59	0.02	B33 s2	Gray, Papanastassiou, and Wasserburg 1973	model age
Ca-Al aggregates-high Rb	Rb-Sr	4.49	0.03	A1	Gray, Papanastassiou, and Wasserburg 1973	model age
Ca-Al aggregates-high Rb	Rb-Sr	4.16	0.02	A9	Gray, Papanastassiou, and Wasserburg 1973	model age
α-Decayers						
inclusion	^{207}Pb-^{206}Pb	4.555		White	Chen and Tilton 1976	model age
inclusion	^{207}Pb-^{206}Pb	4.556		Pink	Chen and Tilton 1976	model age
inclusion	^{207}Pb-^{206}Pb	4.564		Coarse-grained	Chen and Wasserburg 1981	model age
inclusion	^{207}Pb-^{206}Pb	4.561		Coarse-grained	Chen and Wasserburg 1981	model age
inclusion	^{207}Pb-^{206}Pb	4.544		Coarse-grained	Chen and Wasserburg 1981	model age
inclusion	^{207}Pb-^{206}Pb	4.557		Coarse-grained	Chen and Wasserburg 1981	model age
inclusion	^{207}Pb-^{206}Pb	4.498		Fine-grained	Chen and Wasserburg 1981	model age
inclusion	^{207}Pb-^{206}Pb	4.490		Fine-grained	Chen and Wasserburg 1981	model age
inclusion	^{207}Pb-^{206}Pb	4.565		Coarse-grained	Chen and Wasserburg 1981	model age
inclusion	^{207}Pb-^{206}Pb	4.561		Coarse-grained	Chen and Wasserburg 1981	model age
inclusion	^{207}Pb-^{206}Pb	4.408		Coarse-grained	Chen and Wasserburg 1981	model age
inclusion	^{207}Pb-^{206}Pb	4.422		Fine-grained	Chen and Wasserburg 1981	model age
inclusion	^{207}Pb-^{206}Pb	4.471		Fine-grained	Chen and Wasserburg 1981	model age
CaAl inclusion G2/6	Pb-Pb	4.5657	0.0026		Manhes, Gopel, and Allègre 1988	model age
CaAl inclusion Br9/6	Pb-Pb	4.5683	0.0031		Manhes, Gopel, and Allègre 1988	model age
CaAl inclusion 48C/7	Pb-Pb	4.566	0.0007		Manhes, Gopel, and Allègre 1988	model age
CaAl inclusion A1/7	Pb-Pb	4.5651	0.0009		Manhes, Gopel, and Allègre 1988	model age
inclusion	^{207}Pb-^{206}Pb	4.5657	0.0026		Allègre, Manhes, and Gopel 1995	model age
inclusion	^{207}Pb-^{206}Pb	4.5683	0.0031		Allègre, Manhes, and Gopel 1995	model age
inclusion	^{207}Pb-^{206}Pb	4.5660	0.0007		Allègre, Manhes, and Gopel 1995	model age
inclusion	^{207}Pb-^{206}Pb	4.5651	0.0009		Allègre, Manhes, and Gopel 1995	model age

CAI F2, Type B2, >3.15	Pb-Pb	4.567	0.0007	Assuming primordial Pb	Amelin et al. 2002	model age
CAI TS32, Type CTA, >3.15	Pb-Pb	4.5669	0.0008	Assuming primordial Pb	Amelin et al. 2002	model age
CAI TS33, Type B1, >3.15	Pb-Pb	4.5676	0.0009	Assuming primordial Pb	Amelin et al. 2002	model age
CAI F2, Type B2, 2.85-3.15	Pb-Pb	4.5663	0.0008	Assuming primordial Pb	Amelin et al. 2002	model age
CAI TS32, Type CTA, 2.85-3.15	Pb-Pb	4.5678	0.0008	Assuming primordial Pb	Amelin et al. 2002	model age
CAI TS33, Type B1, 2.85-3.15	Pb-Pb	4.5667	0.0007	Assuming primordial Pb	Amelin et al. 2002	model age
CAI F2, Type B2, >3.15	Pb-Pb	4.5675	0.001	Assuming common Pb	Amelin et al. 2002	model age
CAI TS32, Type CTA, >3.15	Pb-Pb	4.5679	0.0017	Assuming common Pb	Amelin et al. 2002	model age
CAI TS33, Type B1, >3.15	Pb-Pb	4.5686	0.0018	Assuming common Pb	Amelin et al. 2002	model age
CAI F2, Type B2, 2.85-3.15	Pb-Pb	4.5671	0.0015	Assuming common Pb	Amelin et al. 2002	model age
CAI TS32, Type CTA, 2.85-3.15	Pb-Pb	4.5682	0.001	Assuming common Pb	Amelin et al. 2002	model age
CAI TS33, Type B1, 2.85-3.15	Pb-Pb	4.5678	0.0019	Assuming common Pb	Amelin et al. 2002	model age
inclusions (Ca-Al)	^{207}Pb-^{206}Pb	4.5679	0.0005	Mean of six ages on three inclusions with Canyon Diablo troilite	Amelin et al 2002	model age
inclusions	^{207}Pb-^{206}Pb	4.5336	0.0011	F2 plagioclase rich	Connelly et al. 2008	model age
inclusions	^{207}Pb-^{206}Pb	4.5664	0.0008	F2 melilite rich	Connelly et al. 2008	model age
inclusions	^{207}Pb-^{206}Pb	4.5664	0.0008	F2 pyroxene rich	Connelly et al. 2008	model age
inclusions	^{207}Pb-^{206}Pb	4.5663	0.0016	TS32 plagioclase rich	Connelly et al. 2008	model age
inclusions	^{207}Pb-^{206}Pb	4.5678	0.0008	TS32 melilite rich	Connelly et al. 2008	model age
inclusions	^{207}Pb-^{206}Pb	4.5669	0.0008	TS32 pyroxene rich	Connelly et al. 2008	model age
inclusions	^{207}Pb-^{206}Pb	4.5580	0.0020	TS33 plagioclase rich	Connelly et al. 2008	model age
inclusions	^{207}Pb-^{206}Pb	4.5668	0.0007	TS33 melilite rich	Connelly et al. 2008	model age
inclusions	^{207}Pb-^{206}Pb	4.5676	0.0009	TS33 pyroxene rich	Connelly et al. 2008	model age
inclusion (Ca-Al)	^{207}Pb-^{206}Pb	4.56759	0.0001	Acid-leached residues (3) + leachate	Bouvier, Vervoort, and Patchett 2008	model age
inclusion (Ca-Al)	^{207}Pb-^{206}Pb	4.5668	0.0004	AJEF Pyroxene	Jacobsen et al. 2008	model age
inclusion (Ca-Al)	^{207}Pb-^{206}Pb	4566.6	0.0007	AJEF Metilite coarse	Jacobsen et al. 2008	model age
inclusion (Ca-Al)	^{207}Pb-^{206}Pb	4.5677	0.0006	AJEF 1.8 A m + nm medium-coarse	Jacobsen et al. 2008	model age
inclusion (Ca-Al)	^{207}Pb-^{206}Pb	4.5696	0.0009	AJEF Pyroxene first wash	Jacobsen et al. 2008	model age
inclusion (Ca-Al)	^{207}Pb-^{206}Pb	4.5659	0.001	AJEF Pyroxene second wash	Jacobsen et al. 2008	model age
inclusion (Ca-Al)	^{207}Pb-^{206}Pb	4.5667	0.0004	A43 Pyroxene from 0.4-1.1 A	Jacobsen et al. 2008	model age
inclusion (Ca-Al)	^{207}Pb-^{206}Pb	4.5682	0.0039	A43 0.4-1.1 A mag med-coarse	Jacobsen et al. 2008	model age
inclusion (Ca-Al)	^{207}Pb-^{206}Pb	4.5656	0.0027	A43 0.4-1.1 A mag med-fine	Jacobsen et al. 2008	model age
inclusion (Ca-Al)	^{207}Pb-^{206}Pb	4.5659	0.0014	A43 0.4-1.1 A mag	Jacobsen et al. 2008	model age
inclusions (Ca-Al)	^{207}Pb-^{206}Pb	4.568	0.003	MNHN-A residue with Canyon Diablo troilite	Bouvier, Vervoort, and Patchett 2008	model age
inclusions (Ca-Al)	^{207}Pb-^{206}Pb	4.5715	0.0005	MNHN-A residue with leachate 1	Bouvier, Vervoort, and Patchett 2008	model age
inclusions (Ca-Al)	^{207}Pb-^{206}Pb	4.5482	0.0005	MNHN-A residue with leachate 2	Bouvier, Vervoort, and Patchett 2008	model age
inclusions (Ca-Al)	^{207}Pb-^{206}Pb	4.5222	0.003	MNHN-B residue with Canyon Diablo troilite	Bouvier, Vervoort, and Patchett 2008	model age
inclusions (Ca-Al)	^{207}Pb-^{206}Pb	4.5188	0.029	MNHN-B residue with leachate 1	Bouvier, Vervoort, and Patchett 2008	model age
inclusions (Ca-Al)	^{207}Pb-^{206}Pb	4.4914	0.0046	MNHN-B residue with leachate 2	Bouvier, Vervoort, and Patchett 2008	model age
inclusions (Ca-Al)	^{207}Pb-^{206}Pb	4.5657	0.0023	UCLA-A residue with Canyon Diablo troilite	Bouvier, Vervoort, and Patchett 2008	model age

inclusions (Ca-Al)	^{207}Pb-^{206}Pb	4.566	0.0023	UCLA-A residue with leachate 1	Bouvier, Vervoort, and Patchett 2008	model age
inclusions (Ca-Al)	^{207}Pb-^{206}Pb	4.5603	0.0033	UCLA-A residue with leachate 2	Bouvier, Vervoort, and Patchett 2008	model age
inclusions (Ca-Al)	^{207}Pb-^{206}Pb	4.5655	0.0023	UCLA-B residue with Canyon Diablo troilite	Bouvier, Vervoort, and Patchett 2008	model age
inclusions (Ca-Al)	^{207}Pb-^{206}Pb	4.5659	0.0023	UCLA-B residue with leachate 1	Bouvier, Vervoort, and Patchett 2008	model age
inclusions (Ca-Al)	^{207}Pb-^{206}Pb	4.57	0.0036	UCLA-B residue with leachate 2	Bouvier, Vervoort, and Patchett 2008	model age
inclusions (Ca-Al)	^{207}Pb-^{206}Pb	4.5646	0.0029	UCLA-C residue with Canyon Diablo troilite	Bouvier, Vervoort, and Patchett 2008	model age
inclusions (Ca-Al)	^{207}Pb-^{206}Pb	4.5653	0.003	UCLA-C residue with leachate 1	Bouvier, Vervoort, and Patchett 2008	model age
inclusions (Ca-Al)	^{207}Pb-^{206}Pb	4.5685	0.0042	UCLA-C residue with leachate 2	Bouvier, Vervoort, and Patchett 2008	model age
inclusions	Pb-Pb	4.56857	0.00087	Mean of A004 third washes	Amelin et al. 2010	model age
inclusions	Pb-Pb	4.56702	0.00022	Mean of A003 and A005 residues	Amelin et al. 2010	model age
inclusions	Pb-Pb	4.56664	0.00033	Mean of A004 residues	Amelin et al. 2010	model age
inclusion	^{232}Th-^{208}Pb	3.773		White	Chen and Tilton 1976	model age
inclusion	^{232}Th-^{208}Pb	4.063		Pink	Chen and Tilton 1976	model age
inclusion	^{238}U-^{206}Pb	4.023		White	Chen and Tilton 1976	model age
inclusion	^{238}U-^{206}Pb	4.644		Pink	Chen and Tilton 1976	model age
inclusion	^{238}U-^{206}Pb	4.73		Coarse-grained	Chen and Wasserburg 1981	model age
inclusion	^{238}U-^{206}Pb	5.31		Coarse-grained	Chen and Wasserburg 1981	model age
inclusion	^{238}U-^{206}Pb	4.83		Coarse-grained	Chen and Wasserburg 1981	model age
inclusion	^{238}U-^{206}Pb	13.0		Fine-grained	Chen and Wasserburg 1981	model age
inclusion	^{238}U-^{206}Pb	5.0		Fine-grained	Chen and Wasserburg 1981	model age
inclusion	^{238}U-^{206}Pb	4.56		Coarse-grained	Chen and Wasserburg 1981	model age
inclusion	^{238}U-^{206}Pb	4.59		Coarse-grained	Chen and Wasserburg 1981	model age
inclusion	^{238}U-^{206}Pb	16.7		Fine-grained	Chen and Wasserburg 1981	model age
inclusion (Ca-Al)	^{238}U-^{206}Pb	4.301		AJEF Pyroxene first wash	Jacobsen et al. 2008	model age
inclusion (Ca-Al)	^{238}U-^{206}Pb	4.34		AJEF Pyroxene second wash	Jacobsen et al. 2008	model age
inclusion (Ca-Al)	^{238}U-^{206}Pb	4.761		AJEF 1.8 A m + nm medium-coarse	Jacobsen et al. 2008	model age
inclusion (Ca-Al)	^{238}U-^{206}Pb	4.827		A43 Pyroxene from 0.4-1.1 A	Jacobsen et al. 2008	model age
inclusion (Ca-Al)	^{238}U-^{206}Pb	4.741		A43 0.4-1.1 A mag med-coarse	Jacobsen et al. 2008	model age
inclusion (Ca-Al)	^{238}U-^{206}Pb	4.663		A43 0.4-1.1 A mag med-fine	Jacobsen et al. 2008	model age
inclusion (Ca-Al)	^{238}U-^{206}Pb	4.858		A43 0.4-1.1 A mag	Jacobsen et al. 2008	model age
inclusion	^{235}U-^{207}Pb	4.385		White	Chen and Tilton 1976	model age
inclusion	^{235}U-^{207}Pb	4.583		Pink	Chen and Tilton 1976	model age
CAI F2, Type B2, >3.15	U-Pb	4.564	0.029		Amelin et al. 2002	model age
CAI TS32, Type CTA, >3.15	U-Pb	4.604	0.01		Amelin et al. 2002	model age
CAI TS33, Type B1, >3.15	U-Pb	4.67	0.016		Amelin et al. 2002	model age
CAI F2, Type B2, 2.85-3.15	U-Pb	4.762	0.038		Amelin et al. 2002	model age
CAI TS32, Type CTA, 2.85-3.15	U-Pb	4.573	0.009		Amelin et al. 2002	model age
CAI TS33, Type B1, 2.85-3.15	U-Pb	4.716	0.02		Amelin et al. 2002	model age
inclusions (Ca-Al)	U-Pb	4.5666	0.0013	CAIs AJEF & A43 residues & px second washes	Jacobsen et al. 2008	concordia age (upper intercept)
inclusions (Ca-Al)	U-Pb	4.5675	0.0012	CAIs AJEF & A43 residues & px second washes	Jacobsen et al. 2008	concordia age (upper intercept)
Calibrated by Pb-Pb Ages						
dark inclusions	I-Xe	4.5645	0.0001	Relative to Shallowater absolute I-Xe age	Pravdivtseva et al. 2003	model age
dark inclusions	I-Xe	4.5649	0.0002	Relative to Shallowater absolute I-Xe age	Pravdivtseva et al. 2003	model age
dark inclusions	I-Xe	4.5641	0.0002	Relative to Shallowater absolute I-Xe age	Pravdivtseva et al. 2003	model age

dark inclusions	I-Xe	4.5652	0.0003	Relative to Shallowater absolute I-Xe age	Pravdivtseva et al. 2003	model age
inclusions (Ca-Al)	I-Xe	4.5629	0.0002	Relative to Shallowater absolute I-Xe age	Pravdivtseva et al. 2003	model age
inclusions (Ca-Al)	I-Xe	4.563	0.0002	Relative to Shallowater absolute I-Xe age	Pravdivtseva et al. 2003	model age
inclusions (Ca-Al)	I-Xe	4.5623	0.0002	Relative to Shallowater absolute I-Xe age	Pravdivtseva et al. 2003	model age

Table 4. Model ages for whole-rock, matrix and other samples of the Allende CV3 carbonaceous chondrite meteorite, with the details and literature sources.

Sample	Method	Age	Error +/-	Notes	Source	Type
β-Decayers						
whole rock	^{40}Ar-^{39}Ar	4.57	0.03	Sample 2	Jessberger et al. 1980	plateau age
whole rock	K-Ar	4.43	0.10	Fine-grained	Dominik and Jessberger 1979	model age
matrix	K-Ar	3.34	0.02	Sample 3915	Herzog et al. 1980	total fusion model age
matrix	K-Ar	3.58	0.02	Sample 3915	Herzog et al. 1980	total fusion model age
matrix	K-Ar	3.43	0.04	Sample 3915	Herzog et al. 1980	total fusion model age
matrix	K-Ar	3.63	0.05	Sample 3915	Herzog et al. 1980	total fusion model age
matrix	K-Ar	3.99	0.01	Sample 3915	Herzog et al. 1980	total fusion model age
granular material	K-Ar	6.29	0.01	Sample 3915	Herzog et al. 1980	total fusion model age
granular material	K-Ar	4.11	0.02	Sample 3915	Herzog et al. 1980	total fusion model age
anorthite	K-Ar	14.2	1.3	Sample 3529Z	Herzog et al. 1980	total fusion model age
anorthite	K-Ar	8.5	1.3	Sample 3529Z	Herzog et al. 1980	total fusion model age
anorthite	K-Ar	6.2	1.1	Sample 3529Z	Herzog et al. 1980	total fusion model age
anorthite	K-Ar	14.5	1.3	Sample 3529Z	Herzog et al. 1980	total fusion model age
pyroxene	K-Ar	8.5	1.3	Sample 3529Z	Herzog et al. 1980	total fusion model age
pyroxene	K-Ar	5.3	0.9	Sample 3529Z	Herzog et al. 1980	total fusion model age
pyroxene	K-Ar	8.2	1.3	Sample 3529Z	Herzog et al. 1980	total fusion model age
melilite	K-Ar	6.0	1.3	Sample 3529Z	Herzog et al. 1980	total fusion model age
melilite	K-Ar	5.4	1.3	Sample 3529Z	Herzog et al. 1980	total fusion model age
fine-grained material	K-Ar	8.8	1.3	Sample 3529Z	Herzog et al. 1980	total fusion model age
fine-grained material	K-Ar	6.8	0.9	Sample 3529Z	Herzog et al. 1980	total fusion model age
fine-grained material	K-Ar	7.6	0.9	Sample 3529Z	Herzog et al. 1980	total fusion model age
vein	K-Ar	7.97	0.6	Sample 3655A	Herzog et al. 1980	total fusion model age
vein	K-Ar	5.10	0.17	Sample 3655A	Herzog et al. 1980	total fusion model age
vein	K-Ar	4.30	0.03	Sample 3655A	Herzog et al. 1980	total fusion model age
vein	K-Ar	4.86	0.04	Sample 3655A	Herzog et al. 1980	total fusion model age
vein	K-Ar	7.12	0.9	Sample 3655A	Herzog et al. 1980	total fusion model age
spinel	K-Ar	6.46	0.6	Sample 3655A	Herzog et al. 1980	total fusion model age
spinel	K-Ar	7.33	1.2	Sample 3655A	Herzog et al. 1980	total fusion model age
spinel	K-Ar	6.13	0.46	Sample 3655A	Herzog et al. 1980	total fusion model age
spinel	K-Ar	9.37	1	Sample 3655A	Herzog et al. 1980	total fusion model age
melilite	K-Ar	10.90	1.3	Sample 3655A	Herzog et al. 1980	total fusion model age
melilite	K-Ar	16.24	1.3	Sample 3655A	Herzog et al. 1980	total fusion model age
melilite	K-Ar	10.07	1.34	Sample 3655A	Herzog et al. 1980	total fusion model age
melilite	K-Ar	14.80	1.34	Sample 3655A	Herzog et al. 1980	total fusion model age
pyroxene	K-Ar	13.50	1.3	Sample 3655A	Herzog et al. 1980	total fusion model age
pyroxene	K-Ar	9.3	1.3	Sample 3655A	Herzog et al. 1980	total fusion model age
pyroxene	K-Ar	8.87	1.34	Sample 3655A	Herzog et al. 1980	total fusion model age
rim	K-Ar	4.09	0.02	Sample 3655A	Herzog et al. 1980	total fusion model age
rim	K-Ar	4.01	0.02	Sample 3655A	Herzog et al. 1980	total fusion model age
rim	K-Ar	4.18	0.01	Sample 3655A	Herzog et al. 1980	total fusion model age
inner part of vein	K-Ar	16.83	1.34	Sample 3655A	Herzog et al. 1980	total fusion model age
fine-grained material	K-Ar	9.18	1.32	Sample 3655A	Herzog et al. 1980	total fusion model age
matrix	K-Ar	3.80	0.09	Sample 1	Jessberger et al. 1980	model age
whole rock	K-Ar	4.43	0.09	Sample 2	Jessberger et al. 1980	model age
total meteorite	Rb-Sr	4.52	0.04	A6 a	Gray, Papanastassiou, and Wasserburg 1973	model age

total meteorite	Rb-Sr	4.55	0.04	A6 b	Gray, Papanastassiou, and Wasserburg 1973	model age
total meteorite	Rb-Sr	4.56	0.03	A6 s1	Gray, Papanastassiou, and Wasserburg 1973	model age
total meteorite	Rb-Sr	4.59	0.03	A6 s2	Gray, Papanastassiou, and Wasserburg 1973	model age
total meteorite	Rb-Sr	4.56	0.04	A6 s3	Gray, Papanastassiou, and Wasserburg 1973	model age
whole rock	Rb-Sr	4.48			Tatsumoto, Unruh, and Desborough1976	model age
whole rock	Rb-Sr	4.49			Tatsumoto, Unruh, and Desborough1976	model age
matrix	Rb-Sr	4.84			Tatsumoto, Unruh, and Desborough1976	model age
matrix	Rb-Sr	4.60			Tatsumoto, Unruh, and Desborough1976	model age
aggregate	Rb-Sr	3.33		White	Tatsumoto, Unruh, and Desborough1976	model age
aggregate	Rb-Sr	4.41		Pinkish-white	Tatsumoto, Unruh, and Desborough1976	model age
whole rock	Rb-Sr	4.56		WR1	Shimoda et al. 2005	model age
whole rock	Rb-Sr	4.58		WR2	Shimoda et al. 2005	model age
α-Decayers						
whole rock	^{207}Pb-^{206}Pb	4.528	0.04		Huey and Kohman 1973	model age
whole rock	^{207}Pb-^{206}Pb	4.496	0.01		Tatsumoto, Knight, and Allègre 1973	model age
whole rock	^{207}Pb-^{206}Pb	4.51			Tilton 1973	model age
whole rock	^{207}Pb-^{206}Pb	4.52			Tilton 1973	model age
aggregate	^{207}Pb-^{206}Pb	4.562		White	Chen and Tilton 1976	model age
whole rock	^{207}Pb-^{206}Pb	4.496			Tatsumoto, Unruh, and Desborough1976	model age
matrix	^{207}Pb-^{206}Pb	4.494			Tatsumoto, Unruh, and Desborough1976	model age
matrix	^{207}Pb-^{206}Pb	4.481			Tatsumoto, Unruh, and Desborough1976	model age
matrix	^{207}Pb-^{206}Pb	4.489			Tatsumoto, Unruh, and Desborough1976	model age
matrix	^{207}Pb-^{206}Pb	4.506			Tatsumoto, Unruh, and Desborough1976	model age
matrix	^{207}Pb-^{206}Pb	4.524			Tatsumoto, Unruh, and Desborough1976	model age
magnetic	^{207}Pb-^{206}Pb	4.467			Tatsumoto, Unruh, and Desborough1976	model age
magnetic	^{207}Pb-^{206}Pb	4.492			Tatsumoto, Unruh, and Desborough1976	model age
magnetic	^{207}Pb-^{206}Pb	4.483			Tatsumoto, Unruh, and Desborough1976	model age
aggregate	^{207}Pb-^{206}Pb	4.557		White	Tatsumoto, Unruh, and Desborough1976	model age
aggregate	^{207}Pb-^{206}Pb	4.562		White	Tatsumoto, Unruh, and Desborough1976	model age
aggregate	^{207}Pb-^{206}Pb	4.547		Pinkish	Tatsumoto, Unruh, and Desborough1976	model age
aggregate	^{207}Pb-^{206}Pb	4.533		Pinkish	Tatsumoto, Unruh, and Desborough1976	model age
matrix	^{207}Pb-^{206}Pb	4.49		C3 same sample	Tatsumoto, Unruh, and Desborough1976	model age
matrix	^{207}Pb-^{206}Pb	4.52		C3 same sample	Tatsumoto, Unruh, and Desborough1976	model age
A003 1W1	^{207}Pb-^{206}Pb	4.54569	0.0027	Assuming primordial isotopic composition of initial Pb	Amelin et al. 2010	model age
A003 1W1 + extra HBr	^{207}Pb-^{206}Pb	4.54968	0.00186	Assuming primordial isotopic composition of initial Pb	Amelin et al. 2010	model age
A004 2W1	^{207}Pb-^{206}Pb	4.55967	0.00861	Assuming primordial isotopic composition of initial Pb	Amelin et al. 2010	model age
A004 3W1	^{207}Pb-^{206}Pb	4.55548	0.00507	Assuming primordial isotopic composition of initial Pb	Amelin et al. 2010	model age
A004 4W1	^{207}Pb-^{206}Pb	4.54045	0.00276	Assuming primordial isotopic composition of initial Pb	Amelin et al. 2010	model age
A004 5W1	^{207}Pb-^{206}Pb	4.53429	0.00209	Assuming primordial isotopic composition of initial Pb	Amelin et al. 2010	model age
A005 6W1	^{207}Pb-^{206}Pb	4.55282	0.00555	Assuming primordial isotopic composition of initial Pb	Amelin et al. 2010	model age
A005 7W1	^{207}Pb-^{206}Pb	4.55808	0.00235	Assuming primordial isotopic composition of initial Pb	Amelin et al. 2010	model age
A005 8W1	^{207}Pb-^{206}Pb	4.53446	0.00244	Assuming primordial isotopic composition of initial Pb	Amelin et al. 2010	model age

A005 9W1	^{207}Pb-^{206}Pb	4.55494	0.00164	Assuming primordial isotopic composition of initial Pb	Amelin et al. 2010	model age
A003 1W2	^{207}Pb-^{206}Pb	4.56563	0.00143	Assuming primordial isotopic composition of initial Pb	Amelin et al. 2010	model age
A003 1W2 + extra HBr	^{207}Pb-^{206}Pb	4.56748	0.00159	Assuming primordial isotopic composition of initial Pb	Amelin et al. 2010	model age
A004 2W2	^{207}Pb-^{206}Pb	4.56847	0.00114	Assuming primordial isotopic composition of initial Pb	Amelin et al. 2010	model age
A004 4W2	^{207}Pb-^{206}Pb	4.56926	0.00187	Assuming primordial isotopic composition of initial Pb	Amelin et al. 2010	model age
A004 5W2	^{207}Pb-^{206}Pb	4.56756	0.00101	Assuming primordial isotopic composition of initial Pb	Amelin et al. 2010	model age
A005 6W2	^{207}Pb-^{206}Pb	4.50331	0.00358	Assuming primordial isotopic composition of initial Pb	Amelin et al. 2010	model age
A005 7W2	^{207}Pb-^{206}Pb	4.56954	0.00137	Assuming primordial isotopic composition of initial Pb	Amelin et al. 2010	model age
A005 8W2	^{207}Pb-^{206}Pb	4.56872	0.00206	Assuming primordial isotopic composition of initial Pb	Amelin et al. 2010	model age
A005 9W2	^{207}Pb-^{206}Pb	4.57021	0.00101	Assuming primordial isotopic composition of initial Pb	Amelin et al. 2010	model age
A004 2W3	^{207}Pb-^{206}Pb	4.57036	0.00175	Assuming primordial isotopic composition of initial Pb	Amelin et al. 2010	model age
A004 3W3	^{207}Pb-^{206}Pb	4.56837	0.00033	Assuming primordial isotopic composition of initial Pb	Amelin et al. 2010	model age
A004 4W3	^{207}Pb-^{206}Pb	4.56905	0.00047	Assuming primordial isotopic composition of initial Pb	Amelin et al. 2010	model age
A004 5W3	^{207}Pb-^{206}Pb	4.56758	0.00103	Assuming primordial isotopic composition of initial Pb	Amelin et al. 2010	model age
A003 1R Medium-fine “whole rock”	^{207}Pb-^{206}Pb	4.56679	0.00025	Assuming primordial isotopic composition of initial Pb	Amelin et al. 2010	model age
A003 1R+ (aliquot 2 + extra HBr)	^{207}Pb-^{206}Pb	4.56697	0.00024	Assuming primordial isotopic composition of initial Pb	Amelin et al. 2010	model age
A004 2R Coarse pyroxene-rich	^{207}Pb-^{206}Pb	4.56697	0.00029	Assuming primordial isotopic composition of initial Pb	Amelin et al. 2010	model age
A004 3R Coarse melilite and feldspar-rich	^{207}Pb-^{206}Pb	4.56643	0.00017	Assuming primordial isotopic composition of initial Pb	Amelin et al. 2010	model age
A004 4R Coarse “whole rock”	^{207}Pb-^{206}Pb	4.5667	0.00018	Assuming primordial isotopic composition of initial Pb	Amelin et al. 2010	model age
A004 5R Medium-fine “whole rock”	^{207}Pb-^{206}Pb	4.56671	0.00023	Assuming primordial isotopic composition of initial Pb	Amelin et al. 2010	model age
A005 6R Medium-fine dark	^{207}Pb-^{206}Pb	4.56781	0.00044	Assuming primordial isotopic composition of initial Pb	Amelin et al. 2010	model age
A005 7R Medium-fine light	^{207}Pb-^{206}Pb	4.56712	0.0003	Assuming primordial isotopic composition of initial Pb	Amelin et al. 2010	model age

A005 8R Fine “whole rock”	^{207}Pb-^{206}Pb	4.56714	0.00028	Assuming primordial isotopic composition of initial Pb	Amelin et al. 2010	model age
A005 9R Very fine “whole rock”	^{207}Pb-^{206}Pb	4.56725	0.00033	Assuming primordial isotopic composition of initial Pb	Amelin et al. 2010	model age
A004 2R+W3 recombined	^{207}Pb-^{206}Pb	4.56787	0.00068	Assuming primordial isotopic composition of initial Pb	Amelin et al. 2010	model age
A004 3R+W3 recombined	^{207}Pb-^{206}Pb	4.56701	0.00021	Assuming primordial isotopic composition of initial Pb	Amelin et al. 2010	model age
A004 4R+W3 recombined	^{207}Pb-^{206}Pb	4.5673	0.00025	Assuming primordial isotopic composition of initial Pb	Amelin et al. 2010	model age
A004 5R+W3 recombined	^{207}Pb-^{206}Pb	4.56699	0.00049	Assuming primordial isotopic composition of initial Pb	Amelin et al. 2010	model age
A003 Frac.1 recombined	^{207}Pb-^{206}Pb	4.56314	0.00077	Assuming primordial isotopic composition of initial Pb	Amelin et al. 2010	model age
A003 Frac.1+ recombined	^{207}Pb-^{206}Pb	4.56413	0.00064	Assuming primordial isotopic composition of initial Pb	Amelin et al. 2010	model age
A004 Frac.2 recombined	^{207}Pb-^{206}Pb	4.56717	0.0015	Assuming primordial isotopic composition of initial Pb	Amelin et al. 2010	model age
A004 Frac.3 recombined	^{207}Pb-^{206}Pb	4.56595	0.00066	Assuming primordial isotopic composition of initial Pb	Amelin et al. 2010	model age
A004 Frac.4 recombined	^{207}Pb-^{206}Pb	4.56453	0.00077	Assuming primordial isotopic composition of initial Pb	Amelin et al. 2010	model age
A004 Frac.5 recombined	^{207}Pb-^{206}Pb	4.56047	0.00088	Assuming primordial isotopic composition of initial Pb	Amelin et al. 2010	model age
A005 Frac.6 recombined	^{207}Pb-^{206}Pb	4.5297	0.00287	Assuming primordial isotopic composition of initial Pb	Amelin et al. 2010	model age
A005 Frac.7 recombined	^{207}Pb-^{206}Pb	4.56594	0.00079	Assuming primordial isotopic composition of initial Pb	Amelin et al. 2010	model age
A005 Frac.8 recombined	^{207}Pb-^{206}Pb	4.56079	0.00094	Assuming primordial isotopic composition of initial Pb	Amelin et al. 2010	model age
A005 Frac.9 recombined	^{207}Pb-^{206}Pb	4.56455	0.00077	Assuming primordial isotopic composition of initial Pb	Amelin et al. 2010	model age
A004 3W1	^{207}Pb-^{206}Pb	4.75219	0.00657	Assuming primordial isotopic composition of initial Pb	Amelin et al. 2010	model age
A004 5W1	^{207}Pb-^{206}Pb	6.14348	0.07377	Assuming primordial isotopic composition of initial Pb	Amelin et al. 2010	model age
A005 7W1	^{207}Pb-^{206}Pb	4.80634	0.00291	Assuming primordial isotopic composition of initial Pb	Amelin et al. 2010	model age
A005 9W1	^{207}Pb-^{206}Pb	4.87254	0.00258	Assuming primordial isotopic composition of initial Pb	Amelin et al. 2010	model age
A003 1W2	^{207}Pb-^{206}Pb	4.65712	0.00142	Assuming primordial isotopic composition of initial Pb	Amelin et al. 2010	model age
A003 1W2 + extra HBr	^{207}Pb-^{206}Pb	4.65956	0.00195	Assuming primordial isotopic composition of initial Pb	Amelin et al. 2010	model age

A004 2W2	^{207}Pb-^{206}Pb	4.61145	0.00096	Assuming primordial isotopic composition of initial Pb	Amelin et al. 2010	model age
A004 4W2	^{207}Pb-^{206}Pb	4.69912	0.00217	Assuming primordial isotopic composition of initial Pb	Amelin et al. 2010	model age
A004 5W2	^{207}Pb-^{206}Pb	4.59785	0.00082	Assuming primordial isotopic composition of initial Pb	Amelin et al. 2010	model age
A005 6W2	^{207}Pb-^{206}Pb	5.41676	0.04032	Assuming primordial isotopic composition of initial Pb	Amelin et al. 2010	model age
A005 7W2	^{207}Pb-^{206}Pb	4.61215	0.00121	Assuming primordial isotopic composition of initial Pb	Amelin et al. 2010	model age
A005 8W2	^{207}Pb-^{206}Pb	4.59428	0.00184	Assuming primordial isotopic composition of initial Pb	Amelin et al. 2010	model age
A005 9W2	^{207}Pb-^{206}Pb	4.59091	0.00073	Assuming primordial isotopic composition of initial Pb	Amelin et al. 2010	model age
A004 2W3	^{207}Pb-^{206}Pb	4.57146	0.00155	Assuming primordial isotopic composition of initial Pb	Amelin et al. 2010	model age
A004 3W3	^{207}Pb-^{206}Pb	4.56929	0.0003	Assuming primordial isotopic composition of initial Pb	Amelin et al. 2010	model age
A004 4W3	^{207}Pb-^{206}Pb	4.57121	0.00044	Assuming primordial isotopic composition of initial Pb	Amelin et al. 2010	model age
A004 5W3	^{207}Pb-^{206}Pb	4.56825	0.00101	Assuming primordial isotopic composition of initial Pb	Amelin et al. 2010	model age
A003 1R Medium-fine “whole rock”	^{207}Pb-^{206}Pb	4.56755	0.00022	Assuming primordial isotopic composition of initial Pb	Amelin et al. 2010	model age
A003 1R+ (aliquot 2 + extra HBr)	^{207}Pb-^{206}Pb	4.5677	0.00021	Assuming primordial isotopic composition of initial Pb	Amelin et al. 2010	model age
A004 2R Coarse pyroxene-rich	^{207}Pb-^{206}Pb	4.56751	0.00022	Assuming primordial isotopic composition of initial Pb	Amelin et al. 2010	model age
A004 3R Coarse melilite and feldspar-rich	^{207}Pb-^{206}Pb	4.56669	0.0001	Assuming primordial isotopic composition of initial Pb	Amelin et al. 2010	model age
A004 4R Coarse “whole rock”	^{207}Pb-^{206}Pb	4.56722	0.00014	Assuming primordial isotopic composition of initial Pb	Amelin et al. 2010	model age
A004 5R Medium-fine “whole rock”	^{207}Pb-^{206}Pb	4.56708	0.00013	Assuming primordial isotopic composition of initial Pb	Amelin et al. 2010	model age
A005 6R Medium-fine dark	^{207}Pb-^{206}Pb	4.56822	0.00019	Assuming primordial isotopic composition of initial Pb	Amelin et al. 2010	model age
A005 7R Medium-fine light	^{207}Pb-^{206}Pb	4.56733	0.00021	Assuming primordial isotopic composition of initial Pb	Amelin et al. 2010	model age
A005 8R Fine “whole rock”	^{207}Pb-^{206}Pb	4.56733	0.00013	Assuming primordial isotopic composition of initial Pb	Amelin et al. 2010	model age
A005 9R Very fine “whole rock”	^{207}Pb-^{206}Pb	4.56754	0.0002	Assuming primordial isotopic composition of initial Pb	Amelin et al. 2010	model age
A004 2R+W3 recombined	^{207}Pb-^{206}Pb	4.56856	0.00058	Assuming primordial isotopic composition of initial Pb	Amelin et al. 2010	model age

A004 3R+W3 recombined	^{207}Pb-^{206}Pb	4.56747	0.00016	Assuming primordial isotopic composition of initial Pb	Amelin et al. 2010	model age
A004 4R+W3 recombined	^{207}Pb-^{206}Pb	4.56823	0.00022	Assuming primordial isotopic composition of initial Pb	Amelin et al. 2010	model age
A004 5R+W3 recombined	^{207}Pb-^{206}Pb	4.56746	0.00041	Assuming primordial isotopic composition of initial Pb	Amelin et al. 2010	model age
A003 Frac.1 recombined	^{207}Pb-^{206}Pb	3.81054	0.0003	Assuming primordial isotopic composition of initial Pb	Amelin et al. 2010	model age
A003 Frac.1+ recombined	^{207}Pb-^{206}Pb	3.81241	0.00034	Assuming primordial isotopic composition of initial Pb	Amelin et al. 2010	model age
A004 Frac.2 recombined	^{207}Pb-^{206}Pb	4.13562	0.00058	Assuming primordial isotopic composition of initial Pb	Amelin et al. 2010	model age
A004 Frac.3 recombined	^{207}Pb-^{206}Pb	4.5844	0.00075	Assuming primordial isotopic composition of initial Pb	Amelin et al. 2010	model age
A004 Frac.4 recombined	^{207}Pb-^{206}Pb	4.0668	0.00048	Assuming primordial isotopic composition of initial Pb	Amelin et al. 2010	model age
A004 Frac.5 recombined	^{207}Pb-^{206}Pb	4.8893	0.01526	Assuming primordial isotopic composition of initial Pb	Amelin et al. 2010	model age
A005 Frac.6 recombined	^{207}Pb-^{206}Pb	4.44588	0.02266	Assuming primordial isotopic composition of initial Pb	Amelin et al. 2010	model age
A005 Frac.7 recombined	^{207}Pb-^{206}Pb	4.61371	0.0008	Assuming primordial isotopic composition of initial Pb	Amelin et al. 2010	model age
A005 Frac.8 recombined	^{207}Pb-^{206}Pb	3.65461	0.00033	Assuming primordial isotopic composition of initial Pb	Amelin et al. 2010	model age
A005 Frac.9 recombined	^{207}Pb-^{206}Pb	4.64884	0.00089	Assuming primordial isotopic composition of initial Pb	Amelin et al .2010	model age
aggregate	^{232}Th-^{208}Pb	4.391		White	Chen and Tilton 1976	model age
whole rock	^{232}Th-^{208}Pb	10.40			Tatsumoto, Unruh, and Desborough 1976	model age
matrix	^{232}Th-^{208}Pb	9.86			Tatsumoto, Unruh, and Desborough 1976	model age
matrix	^{232}Th-^{208}Pb	16.49			Tatsumoto, Unruh, and Desborough 1976	model age
matrix	^{232}Th-^{208}Pb	9.15			Tatsumoto, Unruh, and Desborough 1976	model age
magnetic	^{232}Th-^{208}Pb	4.81			Tatsumoto, Unruh, and Desborough 1976	model age
magnetic	^{232}Th-^{208}Pb	10.1			Tatsumoto, Unruh, and Desborough 1976	model age
aggregate	^{232}Th-^{208}Pb	5.15		White	Tatsumoto, Unruh, and Desborough 1976	model age
aggregate	^{232}Th-^{208}Pb	5.44		Pinkish	Tatsumoto, Unruh, and Desborough 1976	model age
aggregate	^{238}U-^{206}Pb	4.349		White	Chen and Tilton 1976	model age
whole rock	^{238}U-^{206}Pb	8.82			Tatsumoto, Unruh, and Desborough 1976	model age
matrix	^{238}U-^{206}Pb	6.44			Tatsumoto, Unruh, and Desborough 1976	model age
matrix	^{238}U-^{206}Pb	6.33			Tatsumoto, Unruh, and Desborough 1976	model age
matrix	^{238}U-^{206}Pb	6.42			Tatsumoto, Unruh, and Desborough 1976	model age
matrix	^{238}U-^{206}Pb	7.80			Tatsumoto, Unruh, and Desborough 1976	model age
matrix	^{238}U-^{206}Pb	5.45			Tatsumoto, Unruh, and Desborough 1976	model age
magnetic	^{238}U-^{206}Pb	4.41			Tatsumoto, Unruh, and Desborough 1976	model age
magnetic	^{238}U-^{206}Pb	7.75			Tatsumoto, Unruh, and Desborough 1976	model age
magnetic	^{238}U-^{206}Pb	7.82			Tatsumoto, Unruh, and Desborough 1976	model age
aggregate	^{238}U-^{206}Pb	4.96		White	Tatsumoto, Unruh, and Desborough 1976	model age
aggregate	^{238}U-^{206}Pb	4.92		White	Tatsumoto, Unruh, and Desborough 1976	model age
aggregate	^{238}U-^{206}Pb	5.73		Pinkish	Tatsumoto, Unruh, and Desborough 1976	model age
aggregate	^{238}U-^{206}Pb	5.50		Pinkish	Tatsumoto, Unruh, and Desborough 1976	model age
A003 1W1	^{238}U-^{206}Pb	4.2287			Amelin et al. 2010	model age

A003 1W1 + extra HBr	^{238}U-^{206}Pb	4.2333			Amelin et al. 2010	model age
A004 2W1	^{238}U-^{206}Pb	5.0618			Amelin et al. 2010	model age
A004 3W1	^{238}U-^{206}Pb	3.5471			Amelin et al. 2010	model age
A004 4W1	^{238}U-^{206}Pb	4.1125			Amelin et al. 2010	model age
A004 5W1	^{238}U-^{206}Pb	4.6855			Amelin et al. 2010	model age
A005 6W1	^{238}U-^{206}Pb	4.1773			Amelin et al. 2010	model age
A005 7W1	^{238}U-^{206}Pb	4.029			Amelin et al. 2010	model age
A005 8W1	^{238}U-^{206}Pb	4.4346			Amelin et al. 2010	model age
A005 9W1	^{238}U-^{206}Pb	4.1142			Amelin et al. 2010	model age
A003 1W2	^{238}U-^{206}Pb	3.634			Amelin et al. 2010	model age
A003 1W2 + extra HBr	^{238}U-^{206}Pb	3.6411			Amelin et al. 2010	model age
A004 2W2	^{238}U-^{206}Pb	3.7778			Amelin et al. 2010	model age
A004 4W2	^{238}U-^{206}Pb	3.8166			Amelin et al. 2010	model age
A004 5W2	^{238}U-^{206}Pb	3.9313			Amelin et al. 2010	model age
A005 6W2	^{238}U-^{206}Pb	11.6247			Amelin et al. 2010	model age
A005 7W2	^{238}U-^{206}Pb	4.1284			Amelin et al. 2010	model age
A005 8W2	^{238}U-^{206}Pb	3.8734			Amelin et al. 2010	model age
A005 9W2	^{238}U-^{206}Pb	4.0317			Amelin et al. 2010	model age
A004 2W3	^{238}U-^{206}Pb	4.3613			Amelin et al. 2010	model age
A004 3W3	^{238}U-^{206}Pb	4.3663			Amelin et al. 2010	model age
A004 4W3	^{238}U-^{206}Pb	4.316			Amelin et al. 2010	model age
A004 5W3	^{238}U-^{206}Pb	4.3897			Amelin et al. 2010	model age
A003 1R Medium-fine "whole rock"	^{238}U-^{206}Pb	4.772			Amelin et al. 2010	model age
A003 1R+ (aliquot 2 + extra HBr)	^{238}U-^{206}Pb	4.7727			Amelin et al. 2010	model age
A004 2R Coarse pyroxene-rich	^{238}U-^{206}Pb	4.9657			Amelin et al. 2010	model age
A004 3R Coarse melilite and feldspar-rich	^{238}U-^{206}Pb	5.0338			Amelin et al. 2010	model age
A004 4R Coarse "whole rock"	^{238}U-^{206}Pb	4.963			Amelin et al. 2010	model age
A004 5R Medium-fine "whole rock"	^{238}U-^{206}Pb	5.0656			Amelin et al. 2010	model age
A005 6R Medium-fine dark	^{238}U-^{206}Pb	4.7688			Amelin et al. 2010	model age
A005 7R Medium-fine light	^{238}U-^{206}Pb	4.7881			Amelin et al. 2010	model age
A005 8R Fine "whole rock"	^{238}U-^{206}Pb	4.8041			Amelin et al. 2010	model age
A005 9R Very fine "whole rock"	^{238}U-^{206}Pb	4.8472			Amelin et al. 2010	model age
A004 2R+W3 recombined	^{238}U-^{206}Pb	4.8047			Amelin et al. 2010	model age
A004 3R+W3 recombined	^{238}U-^{206}Pb	4.834			Amelin et al. 2010	model age
A004 4R+W3 recombined	^{238}U-^{206}Pb	4.7986			Amelin et al. 2010	model age
A004 5R+W3 recombined	^{238}U-^{206}Pb	4.8475			Amelin et al. 2010	model age
A003 Frac.1 recombined	^{238}U-^{206}Pb	4.5705			Amelin et al. 2010	model age
A003 Frac.1+ recombined	^{238}U-^{206}Pb	4.5727			Amelin et al. 2010	model age
A004 Frac.2 recombined	^{238}U-^{206}Pb	4.6835			Amelin et al. 2010	model age
A004 Frac.3 recombined	^{238}U-^{206}Pb	4.716			Amelin et al. 2010	model age
A004 Frac.4 recombined	^{238}U-^{206}Pb	4.5766			Amelin et al. 2010	model age
A004 Frac.5 recombined	^{238}U-^{206}Pb	4.6935			Amelin et al. 2010	model age
A005 Frac.6 recombined	^{238}U-^{206}Pb	8.5341			Amelin et al. 2010	model age
A005 Frac.7 recombined	^{238}U-^{206}Pb	4.5683			Amelin et al. 2010	model age
A005 Frac.8 recombined	^{238}U-^{206}Pb	4.6101			Amelin et al. 2010	model age
A005 Frac.9 recombined	^{238}U-^{206}Pb	4.5388			Amelin et al. 2010	model age
aggregate	^{235}U-^{207}Pb	4.496		White	Chen and Tilton 1976	model age
whole rock	^{235}U-^{207}Pb	5.57			Tatsumoto, Unruh, and Desborough 1976	model age
matrix	^{235}U-^{207}Pb	5.03			Tatsumoto, Unruh, and Desborough 1976	model age
matrix	^{235}U-^{207}Pb	4.99			Tatsumoto, Unruh, and Desborough 1976	model age
matrix	^{235}U-^{207}Pb	5.02			Tatsumoto, Unruh, and Desborough 1976	model age
matrix	^{235}U-^{207}Pb	5.36			Tatsumoto, Unruh, and Desborough 1976	model age
matrix	^{235}U-^{207}Pb	4.79			Tatsumoto, Unruh, and Desborough 1976	model age
magnetic	^{235}U-^{207}Pb	4.45			Tatsumoto, Unruh, and Desborough 1976	model age
magnetic	^{235}U-^{207}Pb	5.34			Tatsumoto, Unruh, and Desborough 1976	model age
magnetic	^{235}U-^{207}Pb	5.34			Tatsumoto, Unruh, and Desborough 1976	model age

aggregate	^{235}U-^{207}Pb	4.68		White	Tatsumoto, Unruh, and Desborough 1976	model age
aggregate	^{235}U-^{207}Pb	4.67		White	Tatsumoto, Unruh, and Desborough 1976	model age
aggregate	^{235}U-^{207}Pb	4.88		Pinkish	Tatsumoto, Unruh, and Desborough 1976	model age
aggregate	^{235}U-^{207}Pb	4.81		Pinkish	Tatsumoto, Unruh, and Desborough 1976	model age
A003 1W1	^{235}U-^{207}Pb	4.446			Amelin et al. 2010	model age
A003 1W1 + extra HBr	^{235}U-^{207}Pb	4.450			Amelin et al. 2010	model age
A004 2W1	^{235}U-^{207}Pb	4.709			Amelin et al. 2010	model age
A004 3W1	^{235}U-^{207}Pb	4.218			Amelin et al. 2010	model age
A004 4W1	^{235}U-^{207}Pb	4.404			Amelin et al. 2010	model age
A004 5W1	^{235}U-^{207}Pb	4.580			Amelin et al. 2010	model age
A005 6W1	^{235}U-^{207}Pb	4.434			Amelin et al. 2010	model age
A005 7W1	^{235}U-^{207}Pb	4.389			Amelin et al. 2010	model age
A005 8W1	^{235}U-^{207}Pb	4.503			Amelin et al. 2010	model age
A005 9W1	^{235}U-^{207}Pb	4.415			Amelin et al. 2010	model age
A003 1W2	^{235}U-^{207}Pb	4.257			Amelin et al. 2010	model age
A003 1W2 + extra HBr	^{235}U-^{207}Pb	4.261			Amelin et al. 2010	model age
A004 2W2	^{235}U-^{207}Pb	4.310			Amelin et al. 2010	model age
A004 4W2	^{235}U-^{207}Pb	4.324			Amelin et al. 2010	model age
A004 5W2	^{235}U-^{207}Pb	4.362			Amelin et al. 2010	model age
A005 6W2	^{235}U-^{207}Pb	6.131			Amelin et al. 2010	model age
A005 7W2	^{235}U-^{207}Pb	4.430			Amelin et al. 2010	model age
A005 8W2	^{235}U-^{207}Pb	4.343			Amelin et al. 2010	model age
A005 9W2	^{235}U-^{207}Pb	4.398			Amelin et al. 2010	model age
A004 2W3	^{235}U-^{207}Pb	4.505			Amelin et al. 2010	model age
A004 3W3	^{235}U-^{207}Pb	4.505			Amelin et al. 2010	model age
A004 4W3	^{235}U-^{207}Pb	4.490			Amelin et al. 2010	model age
A004 5W3	^{235}U-^{207}Pb	4.512			Amelin et al. 2010	model age
A003 1R Medium-fine “whole rock”	^{235}U-^{207}Pb	4.629			Amelin et al. 2010	model age
A003 1R+ (aliquot 2 + extra HBr)	^{235}U-^{207}Pb	4.629			Amelin et al. 2010	model age
A004 2R Coarse pyroxene-rich	^{235}U-^{207}Pb	4.686			Amelin et al. 2010	model age
A004 3R Coarse melilite and feldspar-rich	^{235}U-^{207}Pb	4.705			Amelin et al. 2010	model age
A004 4R Coarse “whole rock”	^{235}U-^{207}Pb	4.685			Amelin et al. 2010	model age
A004 5R Medium-fine “whole rock”	^{235}U-^{207}Pb	4.715			Amelin et al. 2010	model age
A005 6R Medium-fine dark	^{235}U-^{207}Pb	4.629			Amelin et al. 2010	model age
A005 7R Medium-fine light	^{235}U-^{207}Pb	4.634			Amelin et al. 2010	model age
A005 8R Fine “whole rock”	^{235}U-^{207}Pb	4.639			Amelin et al. 2010	model age
A005 9R Very fine “whole rock”	^{235}U-^{207}Pb	4.651			Amelin et al. 2010	model age
A004 2R+W3 recombined	^{235}U-^{207}Pb	4.638			Amelin et al. 2010	model age
A004 3R+W3 recombined	^{235}U-^{207}Pb	4.645			Amelin et al. 2010	model age
A004 4R+W3 recombined	^{235}U-^{207}Pb	4.635			Amelin et al. 2010	model age
A004 5R+W3 recombined	^{235}U-^{207}Pb	4.649			Amelin et al. 2010	model age
A003 Frac.1 recombined	^{235}U-^{207}Pb	4.562			Amelin et al. 2010	model age
A003 Frac.1+ recombined	^{235}U-^{207}Pb	4.563			Amelin et al. 2010	model age
A004 Frac.2 recombined	^{235}U-^{207}Pb	4.598			Amelin et al. 2010	model age
A004 Frac.3 recombined	^{235}U-^{207}Pb	4.606			Amelin et al. 2010	model age
A004 Frac.4 recombined	^{235}U-^{207}Pb	4.563			Amelin et al. 2010	model age
A004 Frac.5 recombined	^{235}U-^{207}Pb	4.597			Amelin et al. 2010	model age
A005 Frac.6 recombined	^{235}U-^{207}Pb	5.445			Amelin et al. 2010	model age
A005 Frac.7 recombined	^{235}U-^{207}Pb	4.564			Amelin et al. 2010	model age
A005 Frac.8 recombined	^{235}U-^{207}Pb	4.573			Amelin et al. 2010	model age
A005 Frac.9 recombined	^{235}U-^{207}Pb	4.553			Amelin et al. 2010	model age

focus on compiling the copious radioisotope data on meteorites to examine the claimed concordance of the isochron ages for them, especially since the meteorite radioisotope data could be relevant to the question of just how much apparent accelerated radioisotope decay may have occurred during the earth's history.

Morris (2007) also highlighted the significance of meteorites in the determination of the age of the earth, and then focused on Allende as an example of a well-studied meteorite analyzed by many radioisotope dating methods. However, he only discussed the radioisotope dating results from one, older paper (Tatsumoto, Unruh, and Desborough 1976). In that discussion he focused on the U-Th-Pb model ages published in that paper to report that they are very discordant (which has been well-documented in the literature for some time), and therefore to demonstrate that such dating methods are unreliable. He also stated that "no isochron was possible." In so saying he completely ignored the excellent Pb-Pb isochron age of 4.553±0.004 Ga based on some twenty isotopic analyses of the matrix, magnetic separates, aggregates and chondrules reported in the same paper (fig. 16), as well as the U-Pb concordia isochron age of 4.548±0.025 Ga based on those same samples.

Therefore, in order to thoroughly investigate the radioisotope dating of the Allende CV3 carbonaceous chondrite meteorite all the relevant literature was searched. When papers containing radioisotope dating results for the Allende meteorite were found, the reference lists were scanned to find further relevant papers. In this way a comprehensive set of papers, articles, and abstracts on the radioisotope dating of Allende was collected. While it cannot be claimed that all the papers, articles, and abstracts which have ever been published containing radioisotope dating results for Allende have thus been obtained, the cross-checking undertaken between these publications does indicate the data set obtained is very comprehensive.

All the radioisotope dating results from these papers, articles and abstracts were then compiled and tabulated. Because of the huge number of radioisotope dates, and because of the various portions of the Allende CV3 chondrite which have been analyzed, the results were tabulated in four categories—isochron ages for some or all components (table 1), model ages for chondrules (table 2), model ages for CAIs (table 3), and model ages for whole-rock, matrix and other samples (table 4).

The data in these tables were then plotted on frequency versus age histogram diagrams, with the same color coding being used to show the ages obtained by the different radioisotope dating methods—the isochron ages for some or all components (fig. 18), the model ages for chondrules (fig. 19), the model ages for CAIs (fig. 20), and the model ages for whole-rock, matrix and other samples (fig. 21).

Discussion

In all instances the investigators took extreme care in the preparation of whole-rock samples and the separation of components for subsequent radioisotope analyses. Fusion crusts were removed before crushing whole-rock samples, and often components were then hand picked. If components were separated by density differences in heavy liquids and/or by their magnetic properties, care was always taken to inspect under a microscope the purity of the final products before proceeding with the radioisotope analyses.

In whole-rock analyses the complete samples were digested and therefore the components were homogenized in solution before the target radioisotopes were extracted. Whether it was component minerals or constituents such as chondrules or CAIs that were separated, they too were similarly digested and homogenized in solution. In the literature the suitability and integrity for radioisotope analyses of components such as chondrules and CAIs has never been questioned. This is because such components have been found from microscope study to be distinct entities within the overall fabric of meteorites, independent from other components and therefore "self-contained" units suitable for radioisotope analyses on their own. Furthermore, the fairly uniform mineralogical composition of chondrules and CAIs insures that bulk samples of such separated components from individual meteorites will be representative. Therefore, the integrity and quality of the tabulated radioisotope dates has been carefully maintained.

The two most obvious observations from a quick glance at Figs. 18–21 are that:

1. In spite of some outlying scattered data, the bulk of the results strongly cluster so that the mode in all four frequency diagrams lies in the range 4.56–4.57 Ga, which would appear to convincingly suggest the Allende CV3 chondrite has an apparent age of between 4.56 and 4.57 Ga. However, this mode disappears entirely if the Pb-Pb ages (and the radioisotope systems calibrated to them) are omitted. The "some outlying scattered data" refers to >90% of the non-Pb-Pb and non-Pb-Pb-calibrated data. Consequently, the only dating method that shows strong clustering is Pb-Pb, and that clustering occurs between 4.56 and 4.57 Ga, although the wide scatter in the results from the other dating methods does seem to roughly group around an apparent age of 4.56 and 4.57 Ga.

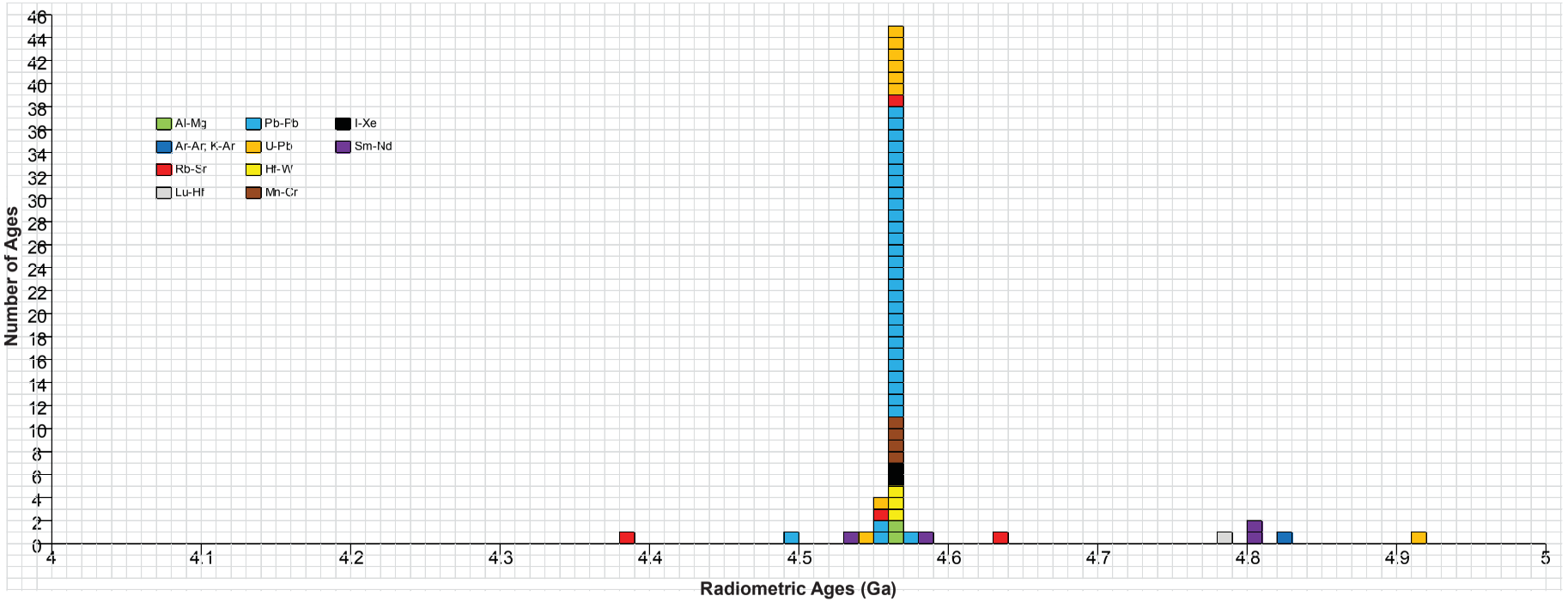

Fig. 18. Frequency versus radioisotope ages histogram diagram for the isochron ages for some or all components of the Allende CV3 carbonaceous chondrite meteorite, with color coding being used to show the ages obtained by the different radioisotope dating methods.

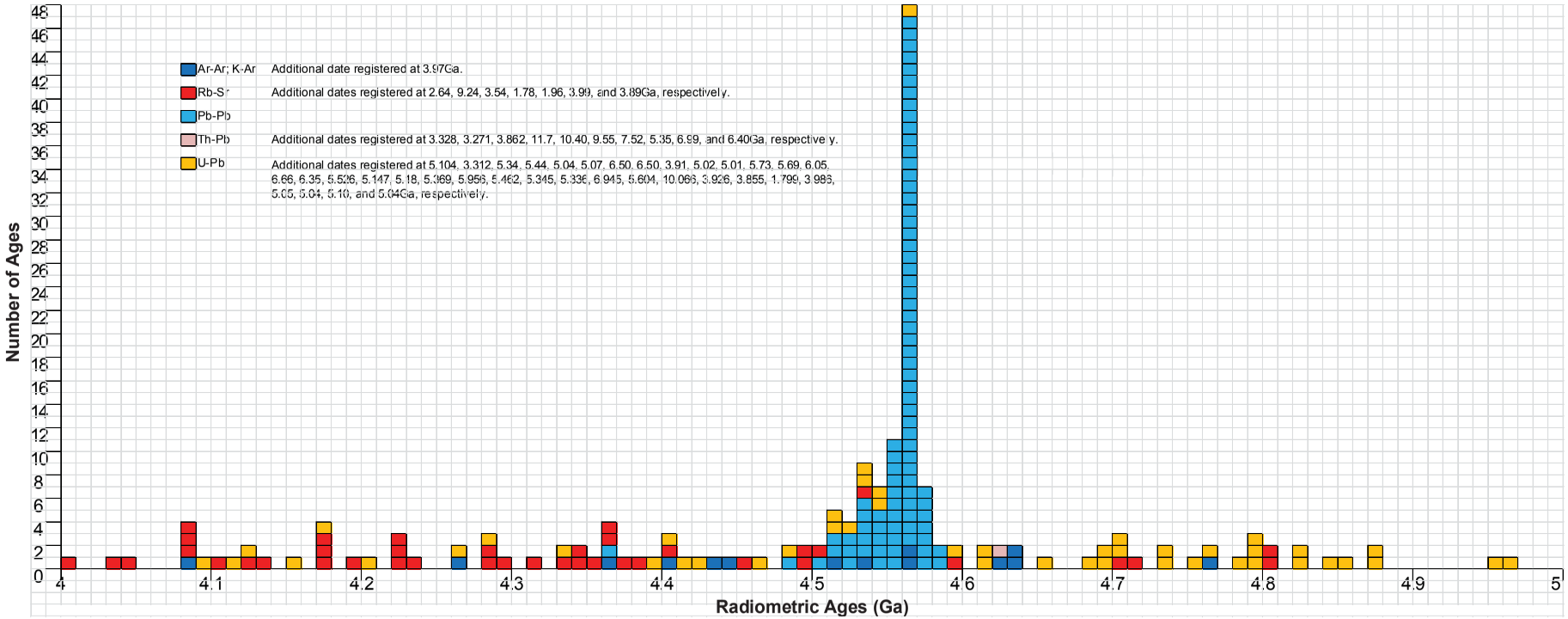

Fig. 19. Frequency versus radioisotope ages histogram diagram for the model ages for chondrules in the Allende CV3 carbonaceous chondrite meteorite, with color coding being used to show the ages obtained by the different radioisotope dating methods.

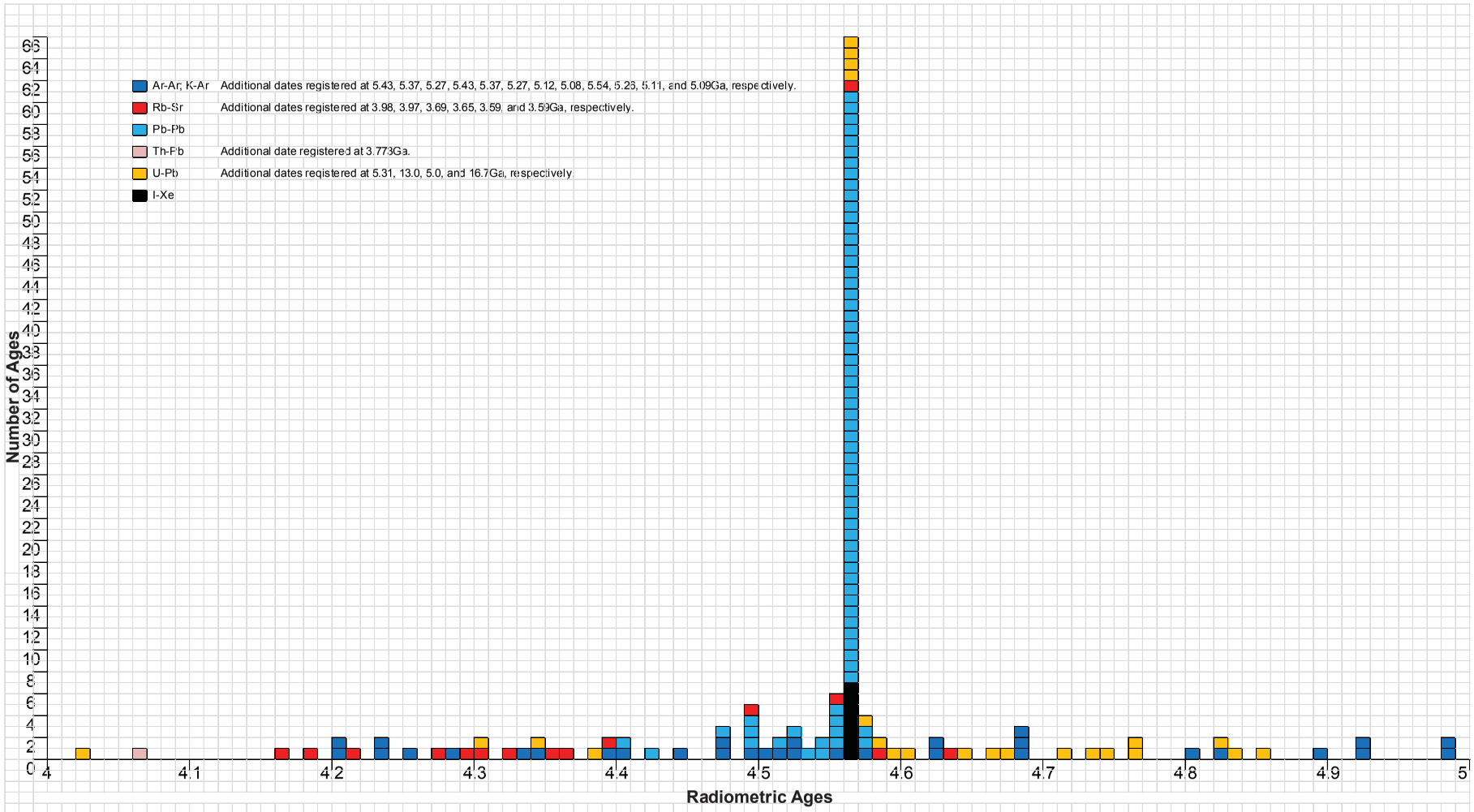

Fig. 20. Frequency versus radioisotope ages histogram diagram for the model ages for Ca-Al inclusions (CAIs) in the Allende CV3 carbonaceous chondrite meteorite, with color coding being used to show the ages obtained by the different radioisotope dating methods.

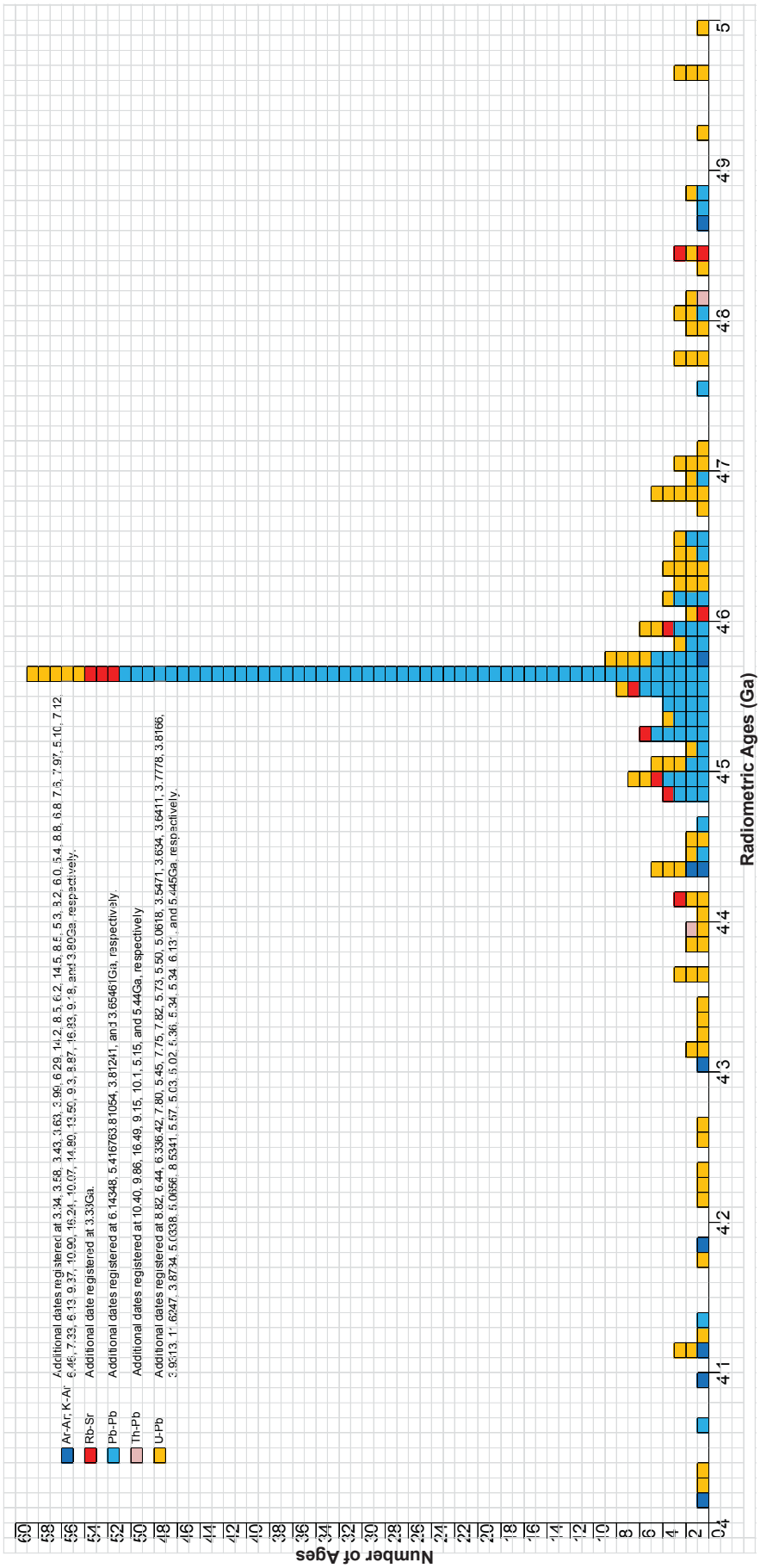

Fig. 21. Frequency versus radioisotope ages histogram diagram for the model ages for whole-rock, matrix and other samples of the Allende CV3 carbonaceous chondrite meteorite, with color coding being used to show the ages obtained by the different radioisotope dating methods.

2. As already noted the dominant radioisotope system used to obtain this apparent age is Pb-Pb, via both isochron (multi-sample) and model (single sample) methods. Indeed, if the Pb-Pb and ages calibrated with the Pb-Pb ages are ignored, there is no strong clustering at all.

Furthermore, a perusal of Tables 1–4 readily reveals that

1. In spite of improvements in the technology and greater sophistication in the techniques to measure the Pb-Pb isotope ratios even more precisely over the decades during which the listed studies were undertaken, there has really been no substantial change in the estimated age for the Allende CV3 chondrite. Indeed, Tatsumoto, Unruh, and Desborough in 1976 determined the first Pb-Pb isochron age of 4.553±0.004 Ga (fig. 16), and yet 34 years later Amelin et al in 2010 reported the most recently determined Pb-Pb isochron age of 4.56718±0.0002 Ga (fig. 17), a mere difference between these two determinations of only 0.01418 billion years, or 14.18 million years!
2. The Pb-Pb model ages on the Allende whole-rock samples, chondrules, Ca-Al inclusions (CAIs), and its matrix **all** essentially cluster strongly around the same 4.56–4.57 Ga mark, giving the uniformitarians much certainty that they have successfully and firmly dated the Allende CV3 chondrite as 4.567 Ga old.
3. The same pattern apparent in the Pb-Pb isochron ages is also apparent in the Pb-Pb model ages, namely, that in spite of improvements in the technology and greater sophistication in the techniques to measure the Pb-Pb isotope ratios even more precisely over the decades during which the listed studies were undertaken, there has really been no substantial change in the estimated age for the Allende CV3 chondrite. For example:
   (a) Huey and Kohman in 1973 obtained a Pb-Pb model age for an Allende whole-rock sample of 4.528±0.04 Ga, yet 37 years later Amelin et al in 2010 determined a Pb-Pb model age of 4.56755±0.0002 Ga, a mere difference between these two determinations of only 0.03955 billion years, or 39.55 million years!
   (b) Similarly, Chen and Tilton in 1976 determined Pb-Pb model ages for Allende chondrules of 4.568 Ga and 4.573 Ga, yet 33 years later Connelly and Bizzarro in 2009 obtained Pb-Pb model ages of 4.5659±0.0004 Ga and 4.5666±0.001 Ga, again only meager differences between these determinations of 0.0021 billion years or 2.1 million years and 0.0064 billion years or 6.4 million years respectively!
   (c) And again, Chen and Tilton in 1976 determined Pb-Pb model ages for Allende Ca-Al inclusions of 4.555 Ga and 4.556 Ga, yet 34 years later Amelin et al in 2010 obtained Pb-Pb model ages of 4.56664±0.0003 Ga and 4.56702±0.0002 Ga, again only small differences between these determinations of 0.01164 billion years or 11.64 million years and 0.01102 billion years or 11.02 million years respectively!

But what of the other radioisotope dating methods? As to be expected, the U-Pb isochron method also yielded similar ages to those obtained by the Pb-Pb isochron method, because both methods involve the radioisotope decay of U to Pb. However, the Rb-Sr and Sm-Nd isochron methods yielded some results within the 4.56–4.57 Ga mode, but also results within 0.3 billion years either side of that mode (fig. 18). Not only are the Rb-Sr isochron ages on either side of the mode of Pb-Pb isochron ages, but so are the model Rb-Sr ages generally in Figs. 19–21. In contrast, the Sm-Nd isochron ages are greater than the Pb-Pb isochron ages (fig. 18).

The other "successful" radioisotope methods are not really independent and thus objective, because they are calibrated against the Pb-Pb method (see table 1) and therefore are automatically guaranteed to give ages identical to those obtained by the Pb-Pb isochron method. Specifically, the Al-Mg method is calibrated against the Pb-Pb isochron age for the D'Orbigny achondrite meteorite (Bouvier, Vervoort, and Patchett 2008), the Hf-W method is calibrated against the Pb-Pb isochron age for the St. Marguerite chondrite meteorite (Kleine et al. 2005) and the D'Orbigny achondrite meteorite (Burkhardt et al. 2008), the Mn-Cr method is calibrated against the Pb-Pb isochron age for the St. Marguerite chondrite meteorite (Trinquier et al. 2008), and the D'Orbigny and LEW 86010 achondrite meteorites (Yin et al. 2009), and the I-Xe method is calibrated against the I-Xe age of the Shallowater achondrite meteorite (Hohenberg et al. 2001), which is calibrated against the Pb-Pb isochron age for the St. Marguerite chondrite meteorite (Brazzle et al. 1999). Thus, as to be expected, all the dates obtained by these methods which are calibrated against these Pb-Pb isochron ages all plot in the 4.56–4.57 Ga mode with the clustered Pb-Pb dates (figs 18 and 20).

This strong clustering around the mode of 4.56–4.57 Ga is thus an example of high precision (versus accuracy), with only the Pb-Pb (and calibrated methods) shows precision in ages. So in the eyes of uniformitarians the Pb-Pb isochron dating method stands supreme as the ultimate, most reliable tool for determining the age of the Allende CV3 carbonaceous chondrite meteorite.

The same is also true for the model ages obtained for Allende (figs. 19–21 and tables 2–4). Whether it

is chondrules, Ca-Al inclusions (CAIs), or whole-rock samples, the Pb-Pb model ages have proven to be the most precise, the overwhelming numbers of analyses consistently clustering around the 4.56–4.57Ga mark. Model ages obtained via the U-Pb, Rb-Sr, and Ar-Ar methods occasionally confirm the Pb-Pb model ages, but they along with the Th-Pb method are also the major contributors to the many scattered model ages among the data.

So having established the superior precision of the Pb-Pb radioisotope dating method, now we need to explore whether there are any other patterns in all these isochron and model ages for the Allende CV3 carbonaceous chondrite meteorite that might provide us with clues about the meaning and significance of these isochron and model ages within the biblical framework for the history of the earth and the solar system.

The major conclusion of the 1997–2005 RATE (radioisotopes and the age of the earth) project was that radioisotope decay rates have not necessarily been constant throughout earth history, because there is evidence that there have been one or more episodes of accelerated rates of radioisotope decay, particularly during the Flood only about 4350 years ago (Vardiman, Snelling, and Chaffin 2005). While there were several lines of documented evidence that confirmed this conclusion, the principal evidence was different isochron ages obtained from the same samples from the same rock units by the different radioisotope dating methods (Snelling 2005; Vardiman, Snelling, and Chaffin 2005).

Furthermore, there was a consistent pattern to the isochron ages from the different methods that indicated that there was an underlying systematic cause of these age differences, namely, an episode of accelerated radioisotope decay (Snelling 2005; Vardiman, Snelling, and Chaffin 2005). For example, it was found that the α-decaying radioisotopes U and Sm always gave older ages than the β-decaying K and Rb. And then between the β-decayers, K with the shorter half-life (more rapid decay today) and the lighter atomic weight, always yielded younger ages than the slower decaying and heavier Rb. While exactly the same pattern was not confirmed among the α-decaying U and Sm, both the half-lives and the atomic weights were still believed to be the factors at work.

An example will best illustrate how this pattern of different isochron ages obtained from the same samples from the same rock units by the different radioisotope dating methods provides evidence of the proposed accelerated radioisotope decay event. Snelling, Austin, and Hoesch (2003) used the same samples from the Precambrian Bass Rapids diabase sill in the Grand Canyon to obtain isochron dates for this rock unit of 841.5±164Ma (K-Ar), 1060±24Ma (Rb-Sr), 1250±130Ma (Pb-Pb), and 1379±140Ma (Sm-Nd). Thus it was argued that if all the radioisotope "clocks" were set to zero when the diabase sill crystallized and cooled, then the only way to reconcile these discordant radioisotope dates is if the different parent radioisotopes then decayed over the same real time period from formation of the sill until today at different faster rates than their rates today. It was also suggested that the parent radioisotopes decaying at different accelerated rates was caused by their different atomic weights and abilities to decay (their half-lives) (Snelling, 2005; Vardiman, Snelling, and Chaffin 2005).

The mechanism proposed for this past episode of accelerated radioisotope decay was small changes to the binding forces in the nuclei of the parent radioisotopes (Vardiman, Snelling, and Chaffin 2005). These changes would thus have to have affected every atom making up the earth, and by logical extension every atom of the universe at the same time, because God appears to have created the physical laws governing the universe to operate consistently through time and space, though of course He Himself is not bound by those physical laws which He can change at any time anywhere or everywhere. Therefore, we should expect that this past episode of accelerated radioisotope decay had affected the asteroids from where many meteorites have come, and that the meteorites may thus today yield the same pattern of different radioisotope ages from the different radioisotope dating methods.

However, looking over Figs. 18–21 again, there appears to be no identical systematic pattern of different radioisotope ages from the different radioisotope dating methods, whether isochron or even model ages. This is more easily seen in Figs. 22 and 23, which are plots of the isochron ages versus the atomic weights and half-lives respectively, based on the data in Table 1 in which the data has been grouped according to the mode of decay of the parent radioisotope. The sole K-Ar isochron age is greater than any of the Rb-Sr isochron ages, and it is also greater than the sole Lu-Hf isochron age, although the latter has a very broad error margin (see table 1). Yet this is the opposite of what should be expected, because K has the shortest half-life today and has the lightest atomic weight among these three β-decayers. At least the sole Lu-Hf isochron age is predictably older than all the Rb-Sr isochron ages, expected because the β-decaying Lu has a longer half-life today and has a heavier atomic weight than Rb. But the Sm-Nd isochron ages are both older and younger than, and similar to, the Pb-Pb and U-Pb isochron ages (figs. 22 and 23). And among all the model ages (tables 2–4)

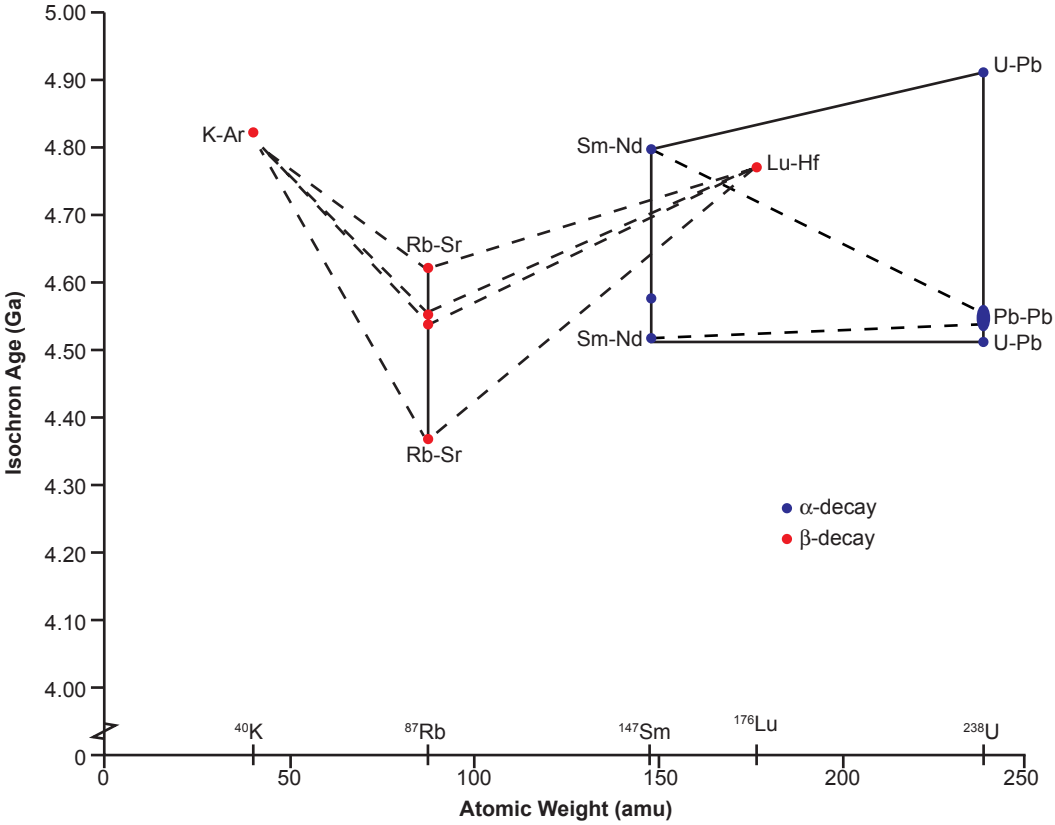

Fig, 22. The isochron age yielded by five radioisotope systems in samples of some or all components from the Allende CV3 carbonaceous chondrite meteorite plotted against the atomic weights of the parent radioisotopes according to their mode of decay.

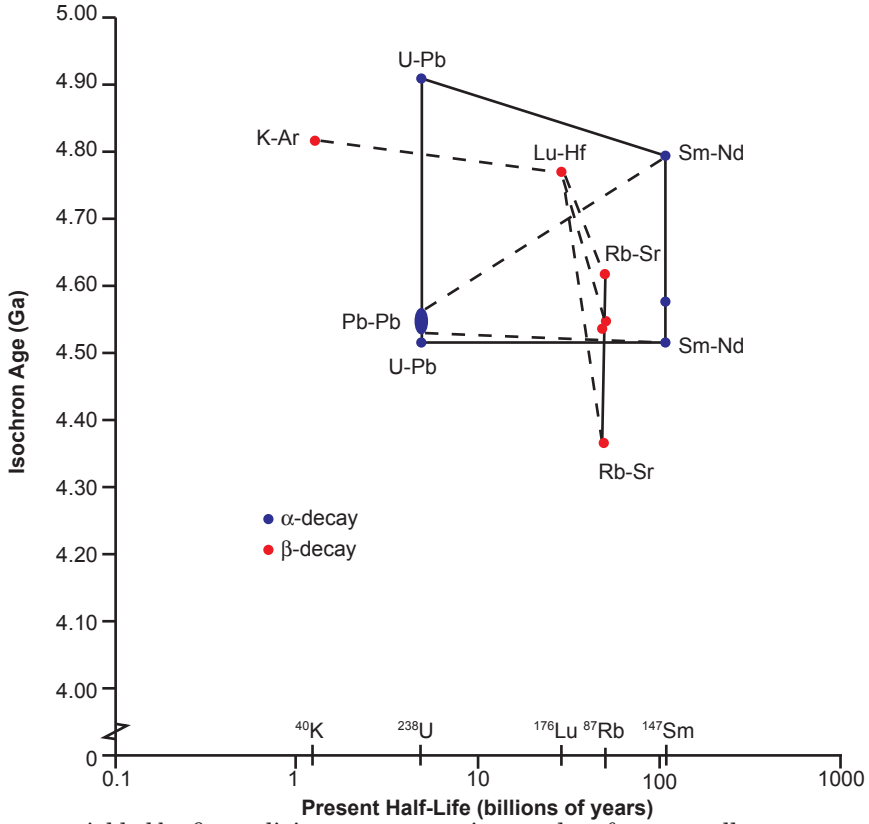

Fig. 23. The isochron ages yielded by five radioisotope systems in samples of some or all components from the Allende CV3 carbonaceous chondrite meteorite plotted against the present half-lives of the parent radioisotopes according to their mode of decay.

there is so much scatter no discernible systematic pattern is evident. In any case, model ages were not determined and compared during the RATE project, primarily because model ages are dependent on, and thus subject to, the assumptions and deficiencies of the models used to derive them. This is well-documented in the literature, and is why model ages generally, apart from Pb-Pb model ages, are regarded as unreliable (Faure and Mensing 2005). Of course, it is premature to draw too firm a conclusion from these observations, because this is just one set of radioisotope ages for one meteorite. More sets of such data from more meteorites are needed, and subsequent papers in preparation will supply these, enabling firmer conclusions to be drawn.

What is also clear is that even for earth-bound rock units there are not yet enough data sets of discordant radioisotope ages derived by different radioisotope dating methods. Those we so far have are primarily for Precambrian rock units, and even for those the pattern of discordance and the amount of discordance are not uniform or the same (Snelling 2005). For example, Austin and Snelling (1998) reported their radioisotope dating study of the Precambrian Cardenas Basalt in the Grand Canyon. The same samples yielded isochron ages of 516±30 Ma (K-Ar), 1111±81 Ma (Rb-Sr) and 1588±170 Ma (Sm-Nd). No Pb-Pb isochron age could be derived from the U-Pb isotopic analytical results. Now while these ages follow the same discordance pattern as those for the Precambrian Bass Rapids diabase sill listed earlier, the amount of discordance is even greater, since the Rb-Sr isochron age is more than twice as large as the K-Ar isochron age, and the Sm-Nd isochron age is more than three times as large as the K-Ar isochron age. These two Precambrian rock units are about the same 1060–1111 Ma Rb-Sr isochron age, are found in the same Grand Canyon region, and within the biblical framework of earth history are generally regarded as pre-Flood. One would have thought that these two Precambrian rock units would have thus both equally suffered from the same accelerated radioisotope decay episode during the Flood year about 4350 years ago, and therefore their radioisotope ages should be discordant by about the same amount.

Similarly, the discordance between the isochron ages of 1240±84 Ma (Rb-Sr), 1655±40 Ma (Sm-Nd), and 1883±53 Ma (Pb-Pb) for the Precambrian Brahma amphibolites in the Grand Canyon is different again (Snelling 2005, 2008). Not only is the amount of discordance between the isochron ages different to the discordances between the isochron ages for the other two Grand Canyon Precambrian rock units, but the pattern is also different. For the Bass Rapids diabase sill the Sm-Nd isochron age is older than the Pb-Pb isochron age, whereas for the Brahma amphibolites the Sm-Nd isochron age is younger than the Pb-Pb isochron age. So again, we need many more sets of discordant radioisotope ages data for many more rock units spanning more of the geologic record before any further conclusions can be drawn.

However, there is still the issue of why the isochron and model ages for the Allende CV3 carbonaceous chondrite meteorite so definitely cluster around an apparent radioisotope age of 4.56–4.57 Ga, with the current best Pb-Pb isochron and model ages of 4.56718±0.0002 Ga (fig. 17) and 4.56702±0.0002 Ga respectively (Amelin et al. 2010). Of course, it is premature to come to any firm conclusions just based on this set of radioisotope dating data for this one meteorite, but it is nevertheless worthwhile to begin considering possibilities, which can then be discussed in the light of more data sets in future papers.

Faulkner (1999) suggested that when God created the planets and satellites on Day Four of the Creation Week He may have formed them from material He had already created in His creative act of Genesis 1:1. In further developing this proposal, Faulkner (2013) pointed out that the Hebrew word *ʿāśâ* meaning "to do" and "to make" is used specifically of the creation of the astronomical bodies in Genesis 1:16, rather than the Hebrew word *bārāʾ* meaning "to create" as used in Genesis 1:1 in reference to the creation of the universe generally. Indeed, the Hebrew word *bārāʾ* appears only with God as its agent (cf. Koehler and Baumgartner 2001, p. 153). Similarly, the Hebrew word *ʿāśâ* is used in Genesis 1:26 when God took already-existing material, which in Genesis 2:7 we are told was "the dust of the ground," to make man's body, before breathing "into his nostrils the breath of life" to make man "a living soul" (Genesis 2:7). Faulkner (2013) goes on to say:

> Granted, such is not always the intended meaning, even with respect to the astronomical bodies (for example, compare Genesis 1:1 with 2 Kings 19:15; Isaiah 37:16; 66:22; Jeremiah 32:17). However, the use of *ʿāśâ* in the Day Four creation record *apart from any contextual clues to suggest that it must bear the sense of creation out of nothing* suggests that there is a distinct possibility that the making of the astronomical bodies was instead a matter of fashioning them from material previously created on Day One. Just as the description of the earth in Genesis 1:2 is of something unfinished that God returned (to) over the next several days to shape and prepare, perhaps the matter that would become the astronomical bodies was created on Day One but was shaped on Day Four. (p. 298, emphasis his)

Furthermore, though Jesus took already existing water to make it into wine at the wedding feast in Cana (John 2:1–11), it was nonetheless a similar act of creation, because He was taking water molecules and adding to them carbon atoms as He instantaneously fashioned it all into the complex organic molecules of wine.

Therefore, it seems entirely possible to read Genesis 1:16 as saying God used already-existing "primordial material" which He had created out of nothing at the beginning of Day One of the Creation Week (Genesis 1:1) to then fashion it into the other planets, their satellites and the stars. Most meteorites are believed have been derived from asteroids via collisions between them breaking off fragments that then hurtled towards the earth. So to be consistent, if the asteroids were also made on Day Four from this Day One primordial material left over from the making of the planets and their satellites in the solar system, then this would imply the meteorites could represent samples of this same "primordial material." Similarly, this would have to also mean that at the beginning of Day One the earth was also fashioned out of the same "primordial material." Thus the 4.56–4.57 Ga Pb isotopic composition of both this Allende meteorite and the bulk earth (as plotted on the geochron) may represent a geochemical signature from this "primordial material" created by God "in the beginning."

This raises the obvious question about another aspect of the radioisotope dating technique. The evidence of past accelerated radioisotope decay (non-constant radioisotope decay rates), that is, the inconsistent radioisotope age data in earth rocks (Vardiman, Snelling, and Chaffin 2005), would appear to negate the assumption of constant decay rates that enables the radioisotope "clocks" to be "reading" 4.56–4.57 Ga for the supposed elapsed real time since the formation of the meteorites and the earth. However, another assumption necessary for these radioisotope "clocks" to work is that all the daughter isotopes were only derived by radioisotope decay from the parent isotopes. But what if God made all the isotopes at the beginning in the "primordial material", including isotopes that subsequently formed by radioisotope decay as daughter isotopes from parent isotopes? In other words, when God made the "primordial material" did He include in it ^{206}Pb, ^{207}Pb, and ^{208}Pb atoms along with ^{238}U, ^{235}U, and ^{232}Th atoms? It may be reasonable to posit that He did, given that when created the "primordial material" had to have some initial isotopic ratios. Even the conventional scientific community have assumed the initial material of the solar system had the "primeval" Pb isotopic ratios as measured in the troilite (iron sulfide) in the Canyon Diablo iron meteorite (Faure and Mensing 2005). So if He did, then the Pb isotopes we measure today are not all the product of radioisotope decay, and they therefore cannot be measuring the elapsed real time since God created the earth and the universe at the beginning only about 6000 real-time years ago.

Following from this is one final consideration. How many atoms of the Pb isotopes did God create in the "primordial material"? And if the 4.56–4.57 Ga "age" for this meteorite is a geochemical signature of the "primordial material" God created with some of the Pb isotopes we measure today already in it, then how many of the atoms of the measured-today Pb isotopes are due to past accelerated radioisotope decay? Was it most of them, or only some of them? So far we don't know. What we do know is that here on the earth we don't find rocks that still have the 4.56–4.57 Ga Pb isotopic signature in them, though most rocks that date back to the continental foundations laid down during Creation Week still contain various large amounts of Pb isotopes in them and therefore yield an array of multi-Ga "ages." Significantly, the earth sample that plotted on Patterson's 1956 geochron (fig. 1) was a modern ocean sediment sample whose Pb isotopic signature had been acquired by mixing and integration from many earth rocks over time. This may point to a third possible process responsible for the Pb isotopic compositions in earth rocks, namely, inheritance and mixing in the earth's mantle and crust subsequent to the creation of the original earth on Day One of the Creation Week, as previously proposed by Snelling (2000, 2005), primarily during the catastrophic geologic processes of the Day Three Upheaval when the dry land was formed and during the Flood (Snelling 2009).

The resultant conclusion from all these considerations and deliberations, based on the assumptions made, is that the 4.56718±0.0002 Ga "age" for the Allende CV3 carbonaceous chondrite meteorite obtained by Pb-Pb radioisotope isochron dating of one of its Ca-Al inclusions (CAIs) (Amelin et al. 2010) is likely not its true real-time age. The assumptions on which the radioisotope dating methods are based are simply unprovable, and in the light of the evidence for possible past accelerated radioisotope decay in earth rocks and the possibility of an inherited primordial geochemical signature, these assumptions are unreasonable. However, we are still left without a coherent explanation of what these radioisotope compositions really mean within our biblical young-age Creation-Flood framework for earth and universe history. We have some possible clues already, and a clearer picture may yet emerge from continued investigations now in progress, for example, of the radioisotope dating of many other meteorites.

Conclusions

There is no doubt that after decades of numerous careful radioisotope dating investigations of the Allende CV3 carbonaceous chondrite meteorite that its Pb-Pb isochron age of 4.56718±0.0002 Ga has been well established. This date for Allende is supported by a very strong clustering of other Pb-Pb isochron and model ages in the 4.56–4.57 Ga range, as well as being confirmed by Pb-Pb model ages and by both isochron and model age results by the U-Pb, and to a lesser extent, the Rb-Sr and Sm-Nd methods. The Al-Mg, Hf-W, Mn-Cr, and I-Xe methods are all calibrated against the Pb-Pb isochron method, so their results are not objectively independent. Thus the Pb-Pb isochron dating method stands supreme as the ultimate, most precise tool for determining the age of the Allende CV3 carbonaceous chondrite meteorite.

There is no other discernible systematic pattern in the isochron and model ages for Allende, apart from scatter of the U-Pb, Th-Pb, Rb-Sr, and Ar-Ar model ages particularly. The Allende ages do not follow the systematic pattern found in Grand Canyon Precambrian rock units during the RATE project, where the β-decay ages are younger than the α-decay ages according to the lengths of the half-lives and the atomic weights of the parent radioisotopes. Thus there appears to be no evidence in the Allende CV3 carbonaceous chondrite meteorite similar to the evidence found in earth rocks of past accelerated radioisotope decay.

Any explanation for the 4.56718±0.0002 Ga age for this Allende meteorite needs to consider the origin of meteorites. Most meteorites appear to be fragments derived from asteroids via collisions, but even in the naturalistic paradigm the asteroids, and thus the meteorites, are regarded as primordial material left over from the formation of the solar system. Similarly, the Hebrew text of Genesis suggests God made primordial material on Day One of the Creation Week from which He made the non-earth portion of the solar system on Day Four, so today's measured radioisotope composition of the Allende meteorite may reflect a geochemical signature of that primordial material, which included atoms of all elemental isotopes created by God. Thus if some of the daughter isotopes were "inherited" by the Allende meteorite when it was formed from that primordial material, and the parent isotopes in the meteorite were also subject to subsequent accelerated radioisotope decay, then the 4.56718±0.0002 Ga Pb-Pb isochron "age" for the Allende CV3 carbonaceous chondrite meteorite cannot be its true real-time age, which according to the biblical paradigm is only about 6000 real-time years.

However, these conclusions and the suggested explanation can at best be regarded as tentative and interim while their confirmation or adjustment awaits the examination of more radioisotope dating data from many more meteorites. Such studies are already in progress.

Acknowledgments

At the outset of this project Joe Farris, at the time a student at Patrick Henry College, Purcellville, Virginia, in collaboration assisted in finding some of the relevant papers and compiling the radioisotope dating data from them as part of a class assignment set by Dr. Neal Doran. The subsequent invaluable help of my research assistant Lee Anderson, Jr. in compiling the eventual voluminous radioisotope dating data into the tables and then plotting the data in the color coded age versus frequency histogram diagrams is also acknowledged.

References

Allègre, C.-J., G. Manhes, and C. Gopel. 1995. The age of the earth. *Geochimica et Cosmochimica Acta* 59:1445–1456.

Amelin, Y., L. Grossman, A. Krot, T. Pestaj, S.B. Simon, and A.A. Ulyanov. 2002. U-Pb age of refractory inclusions from the CV carbonaceous chondrites Allende and Efremovka. *Lunar and Planetary Science Conference* XXXIII, #1151.

Amelin, Y., and E. Rotenberg. 2004. Sm-Nd systematics of chondrites. *Earth and Planetary Science Letters* 223: 267–282.

Amelin, Y., and A.N. Krot. 2007. Pb isotopic age of the Allende chondrules. *Meteoritics and Planetary Science* 42: 1321–1335.

Amelin, Y., J. Connelly, R.E. Zartman, J.H. Chen, C. Gopel, and L.A. Neymark. 2009. Modern U-Pb chronometry of meteorites: Advancing to higher time resolution reveals new problems. *Geochimica et Cosmochimica Acta* 73:5212–5223.

Amelin, Y. A., Kaltenbach, T. Iizuka, C.H. Stirling, T.R. Ireland, M. Petaev, and S.B. Jacobsen. 2010. U-Pb chronology of the Solar system's oldest solids with variable $^{238}U/^{235}U$. *Earth and Planetary Science Letters* 300:343–350.

Austin, S.A. and A.A. Snelling. 1998. Discordant potassium-argon model and isochron "ages" for Cardenas Basalt (Middle Proterozoic) and associated diabase of eastern Grand Canyon, Arizona. In *Proceedings of the Fourth International Conference on Creationism*, ed. R.E. Walsh, pp.35–51. Pittsburgh, Pennsylvania: Creation Science Fellowship.

Bouvier, A., J. Blichert-Toft, F. Moynier, J.D. Vervoort, and F. Albarede. 2007. Pb-Pb dating constraints on the accretion and cooling history of chondrites. *Geochimica et Cosmochimica Acta* 71:1583–1604.

Bouvier, A., J.D. Vervoort, and P.J. Patchett. 2008. The Lu-Hf and Sm-Nd isotopic composition of CHUR: Constraints from unequilibrated chondrites and implications for the bulk composition of terrestrial planets. *Earth and Planetary Science Letters* 273:48–57.

Brazzle, R.H., O.V. Pravdivtseva, A.P. Meshik, and C.M. Hohenberg. 1999. Verification and interpretation of the I-Xe chronometer. *Geochimica et Cosmochimica Acta* 63:739–760.

Burkhardt, C., T. Kleine, B. Bourdon, H. Palme, J. Zipfel, J.M. Friedrich, and D.S. Ebel. 2008. Hf-W mineral isochron for Ca Al-rich inclusions: Age of the solar system and the timing of core formation in planetesimals. *Geochimica et Cosmochimica Acta* 72:6177–6197.

Chen, J.H., and G.R. Tilton. 1976. Isotopic lead investigations on the Allende carbonaceous chondrite. *Geochimica et Cosmochimica Acta* 40:635–643.

Chen, J.H., and G.J. Wasserburg. 1981. The isotopic composition of uranium and lead in Allende inclusions and meteoritic phosphates. *Earth and Planetary Science Letters* 52:1–15.

Clarke, R.S. Jr., E. Jarosewich, B. Mason, J. Nelen, M. Gomez, and J.R. Hyde. 1970. The Allende, Mexico, meteorite shower. *Smithsonian contributions to the earth sciences* 5:1–53. Washington DC: Smithsonian Institution Press.

Connelly, J.N., and M. Bizzarro. 2009. Pb-Pb dating of chondrules from CV chondrites by progressive dissolution. *Chemical Geology* 259:143–151.

Connelly, J.N., Y. Amelin, A.N. Krot, and M. Bizzarro. 2008. Chronology of the solar system's oldest solids. *The Astrophysical Journal* 675:L121–L124.

Cronin, J.R., S. Pizzarello, and D.P. Cruikshank. 1988. Organic matter in carbonaceous chondrites, planetary satellites, asteroids and comets. In *Meteorites and the early solar system*, eds. J.F. Kerridge and M.S. Matthews, pp.819–857. Tucson, Arizona: University of Arizona Press.

Dalrymple, G.B. 1991. *The age of the earth*. Stanford, California: Stanford University Press.

Dalrymple, G.B. 2004. *Ancient earth, ancient skies.* Stanford, California: Stanford University Press.

Dominik, B. and E.K. Jessberger. 1979. ^{40}Ar-^{39}Ar dating of Murchison, Allende and Leadville. *Lunar and Planetary Science Conference* X:306–308.

Dominik, B., E.K. Jessberger, T. Staudacher, K. Nagel, and A. El Gorsey. 1978. A new type of white inclusion in Allende: Petrography, mineral chemistry, ^{40}Ar-^{39}Ar ages, and genetic implications. *Lunar and Planetary Science Conference* IX:1249–1266.

Faulkner, D.R. 1999. A biblically-based cratering theory. *Creation Ex Nihilo Technical Journal* 13.1:100–104.

Faulkner, D.R. 2013. A proposal for a new solution to the light travel time problem. *Answers Research Journal* 6:2 95–300. Retrieved from http://www.answersingenesis.org/articles/arj/v6/n1/light-travel-time-problem.

Faure, G., and T.M. Mensing. 2005. *Isotopes: Principles and applications*. 3rd ed. Hoboken, New Jersey: John Wiley & Sons.

Gray, C.M., D.A. Papanastassiou, and G.J. Wasserburg. 1973. The identification of early condensates from the solar nebula. *Icarus* 20:213–239.

Hans, U., T. Kleine, and B. Bourdon. 2013. Rb-Sr chronology of volatile depletion in differentiated protoplanets: BABI, ADOR and ALL revisited. *Earth and Planetary Science Letters* 374:204–214.

Herzog, G.F., A.E. Bence, J. Bender, G. Eichhorn, H. Maluski, and O.E. Schaeffer. 1980. ^{39}Ar/^{40}Ar systematics of Allende inclusions. *Lunar and Planetary Science Conference* XI:959–976.

Hohenburg, C.M., A.P. Meshik, O.V. Pravdivtseva, and A.N Krot. 2001. I-Xe dating: Dark inclusions from Allende CV3. *Meteoritics and Planetary Science* 36:A83.

Huey, J.M. and T.P. Kohman. 1973. ^{207}Pb-^{206}Pb isochron and age of chondrites. *Journal of Geophysical Research* 78:3227–3244.

Jacobsen, B., Q.-Z. Yin, F. Moynier, Y. Amelin, A.N. Krot, K. Nagashima, I.D. Hutcheon, and H. Palme. 2008. ^{26}Al-^{26}Mg and ^{207}Pb-^{206}Pb systematics of Allende CAIs: Canonical solar initial ^{26}Al/^{27}Al ratio reinstated. *Earth and Planetary Science Letters* 272:353–364.

Jessberger, E.K. and B. Dominik. 1979a. Further K-Ar ages of Allende inclusions. *Lunar and Planetary Science Conference* X:628–630.

Jessberger, E.K. and B. Dominik. 1979b. Gerontology of the Allende meteorite. *Nature* 277:554–556.

Jessberger, E.K., B. Dominik, T. Staudacher, and G.F. Herzog. 1980. ^{40}Ar/^{39}Ar ages of Allende. *Icarus* 42: 380–405.

Kleine, T., K. Mezger, H. Palme, E. Scherer, and C. Munker. 2005. Early core formation in asteroids and late accretion of chondrite parent bodies: Evidence from ^{182}Hf-^{182}W in CAIs, metal-rich chondrites, and iron meteorites. *Geochimica et Cosmochimica Acta* 69:5805–5818.

Koehler, L. and W. Baumgartner. 2001. *The Hebrew and Aramaic Lexicon of the Old Testament*. Vol. 1. Rev. ed. Trans. and ed. M.E.J. Richardson. Leiden, Netherlands: Brill.

Krot, A.N., K. Keil, C.A. Goodrich, E.R.D. Scott, and M.K. Weisberg. 2005. Classification of meteorites. In *Meteorites, comets, and planets*, ed. A.M. Davis, *Treatise on Geochemistry*, vol.1, pp.83–128. Amsterdam, Netherlands: Elsevier.

Krot, A.N., Y. Amelin, P. Bland, F.J. Ciesla, J.N. Connelly, A.M. Davis, G.R. Huss, I.D. Hutcheon, K. Makide, K. Nagashima, L.E. Nyquist, et al. 2009. Origin and chronology of chondritic components: A review. *Geochimica et Cosmochimica Acta* 73:4963–4997.

Manhes, G., C. Gopel, and C.-J. Allègre. 1988. Systematique U-Pb dans les inclusions réfractaires d'Allende: le plus vieux matériau solaire. *Comptes Rendus de l'ATP Planetologie*, pp.323–327.

MacPherson, G.J. 2005. Calcium-aluminum-rich inclusions in chondritic meteorites. In *Meteorites, comets, and planets*, ed. A.M. Davis, *Treatise on Geochemistry*, vol.1, pp.201–246. Amsterdam, Netherlands: Elsevier.

Morris, J.D. 2007. *The young earth*. Rev. ed., pp.59–61. Green Forest, Arkansas: Master Books.

Norton, O.R. 2002. *The Cambridge encyclopedia of meteorites*. Cambridge, United Kingdom: Cambridge University Press.

Papanastassiou, D.A., H.H. Ngo, and G.J. Wasserburg. 1987. Sm-Nd systematics in coarse-grained refractory inclusions from Allende. *Lunar and Planetary Science Conference* XVIII:760–761.

Patchett, P.J., J.D. Vervoort, U. Sunderlund, and V.J.M. Salters. 2004. Lu–Hf and Sm–Nd isotopic systematics in chondrites and their constraints on the Lu–Hf properties of the earth. *Earth and Planetary Science Letters* 222: 29–41.

Patterson, C. 1956. Age of meteorites and the earth. *Geochimica et Cosmochimica Acta* 10:230–237.

Podosek, F.A., E.K. Zinner, G.J. MacPherson, L.L. Lundberg, J.C. Brannon, and A.J. Fahey. 1991. Correlated study of initial $^{87}Sr/^{86}Sr$ and Al-Mg isotopic systematics and petrologic properties in a suite of refractory inclusions from Allende meteorite. *Geochimica et Cosmochimica Acta* 55:1083–1110.

Pravdivtseva, O.V., A.N. Krot, C.M. Hohenberg, A.P. Meshik, M.K. Weisberg, and K. Keil. 2003. The I-Xe record of alteration in the Allende CV chondrite. *Geochimica et Cosmochimica Acta* 67:5011–5026.

Scott, E.R.D., and A.N. Krot. 2005. Chondrites and their components. In *Meteorites, comets, and planets*, ed. A.M. Davis, *Treatise on Geochemistry*, vol.1, pp.143–200. Amsterdam, Netherlands: Elsevier.

Sears D.W.G., F.A. Hasan, J.D. Batchelor, and J. Lu. 1991. Chemical and physical studies of type 3 chondrites: XI. Metamorphism, pairing, and brecciation of ordinary chondrites. *Proceedings of the Lunar and Planetary Science Conferences* 21:493–512.

Shimoda, G., N. Nakamura, M. Kimura, T. Kani, S. Nohda, and K. Yamamoto. 2005. Evidence from the Rb-Sr system for 4.4Ga alteration of chondrules in the Allende (CV3) parent body. *Meteoritics and Planetary Science* 40: 1059–1072.

Shukolyukov, A. and G.W. Lugmair 2006. Manganese-chromium isotope systematics of carbonaceous chondrites. *Earth and Planetary Science Letters* 250:200–213.

Snelling, A.A. 2000. Geochemical processes in the mantle and crust. In *Radioisotopes and the age of the earth: A young-earth creationist research initiative*, ed. L. Vardiman, A.A. Snelling, and E.F. Chaffin, pp.123–304. El Cajon, California: Institute for Creation Research, and St. Joseph, Missouri: Creation Research Society.

Snelling, A.A., S.A. Austin, and W.A. Hoesch. 2003. Radioisotopes in the diabase sill (upper Precambrian) at Bass Rapids, Grand Canyon, Arizona: An application and test of the isochron dating method. In *Proceedings of the Fifth International Conference on Creationism*, ed. R.L. Ivey, pp.269–284. Pittsburgh, Pennsylvania: Creation Science Fellowship.

Snelling, A.A. 2005. Isochron discordances and the role of inheritance and mixing of radioisotopes in the mantle and crust. In *Radioisotopes and the age of the earth: Results of a young-earth creationist research initiative*, ed. L. Vardiman, A.A. Snelling, and E.F. Chaffin, pp.393–524. El Cajon, California: Institute for Creation Research, and Chino Valley, Arizona: Creation Research Society.

Snelling, A.A. 2008. Significance of highly discordant radioisotope dates for Precambrian amphibolites in Grand Canyon, USA. In *Proceedings of the Sixth International Conference on Creationism*, ed. A.A. Snelling, pp.407–424. Pittsburgh, Pennsylvania: Creation Science Fellowship, and Dallas, Texas: Institute for Creation Research.

Snelling, A.A. 2009. *Earth's catastrophic past: Geology, Creation and the Flood*. Dallas, Texas: Institute for Creation Research.

Tatsumoto, M., R.J. Knight, and C.-J. Allègre. 1973. Time differences in the formation of meteorites as determined from the ratio of lead-207 to lead-206. *Science* 180: 1279–1283.

Tatsumoto, M., D.M. Unruh, and G.A. Desborough. 1976. U-Th-Pb and Rb-Sr systematics of Allende and U-Th-Pb of Orgueil. *Geochimica et Cosmochimica Acta* 40:617–634.

Tilton, G.R. 1973. Isotopic lead ages of chondritic meteorites. *Earth and Planetary Science Letters* 19:321–329.

Trinquier, A., J.-L. Birck, C.-J. Allègre, C. Gopel, and D. Ulfbeck. 2008. ^{53}Mn-^{53}Cr systematics of the early Solar system revisited. *Geochimica et Cosmochimica Acta* 72:5146–5163.

Van Schmus, W.R. and J.A. Wood. 1967. A chemical-petrologic classification for the chondritic meteorites. *Geochimica et Cosmochimica Acta* 31:747–765.

Vardiman, L., A.A. Snelling, and E.F. Chaffin, eds. 2005. *Radioisotopes and the age of the earth: Results of a young-earth creationist research initiative*. El Cajon, California: Institute for Creation Research, and Chino Valley, Arizona: Creation Research Society.

Wood, J.A. 1967. Chondrites: Their metallic minerals, thermal histories, and parent planets. *Icarus* 6:1–49.

Woodmorappe, J. 1999. *The mythology of modern dating methods*. El Cajon, California: Institute for Creation Research.

Yin, Q.-Z., K. Yamashita, A. Yamakawa, R. Tanaka, B. Jacobsen, D. Ebel, I.D. Hutcheon, and E. Nakamura. 2009. ^{53}Mn-^{53}Cr systematics of Allende chondrules and $\varepsilon^{54}Cr$-$\Delta^{17}O$ correlation in bulk carbonaceous chondrites. *Lunar and Planetary Science Conference* XL: #2006.